The Location of the Cytochrome *c* Binding Site on Flavocytochrome b_2

Duncan M. Short

THESIS PRESENTED FOR THE DEGREE OF DOCTOR OF PHILOSOPHY

THE UNIVERSITY OF EDINBURGH

NOVEMBER 1996

To my family.

'Mountains should be climbed with as little effort as possible and without desire. The reality of your own nature should determine the speed. If you become restless, speed up. If you become winded, slow down. You climb the mountain in an equilibrium between restlessness and exhaustion. Then, when you're no longer thinking ahead, each footstep isn't a means to an end but a unique event in itself. *This* leaf has jagged edges. *This* rock looks loose. From *this* place the snow is less visible, even though closer. These are things you should notice anyway. To live only for some future goal is shallow. It's the sides of the mountain that sustain life, not the top. Here's where things grow.'

Zen and the Art of Motorcycle Maintenance.
Robert M. Pirsig.

Acknowledgements

I would like to thank my two supervisors Prof. Stephen K. Chapman and Dr. Graeme A. Reid for their excellent scientific supervision throughout my PhD. My thanks go to the 'biologists' who helped me to produce the mutant-enzymes that I worked on in my third year: Mr. Euan Gordon, Mr. Rosli Illias, Miss Rhona Sinclair, Mr. Lars Ostergaard; and the 'chemists', for providing all kinds of advice when it was needed: Dr. Simon Daff, Dr. Alexis Balme, Mr. Cameron Bell, Mr. Andrew Pike, Mr. Fraser Welsh. My thanks also go to the ex-members of the Chapman-Reid coalition: Dr. Forbes Manson, Dr. Trish Dunlop, Dr. Eryl Sharp. All the above people provided a stimulating atmosphere that encouraged good humour and hard work. Last, but not least, I have to thank my family, my fiancée, and Benji, for all their support.

Abstract

Flavocytochrome b_2 is a L-lactate dehydrogenase found in the intermembrane space of certain yeasts. Its physiological partner is cytochrome *c*. The enzyme exists as a homotetramer with each subunit consisting of two domains, a flavodehydrogenase domain and a cytochrome domain. The cytochrome domain is homologous with the extensively studied cytochrome b_5. The two domains are joined by an inter-domain hinge. A computer model of how a complex may be formed between flavocytochrome b_2 and cytochrome *c* was produced in 1993, and predicted several residues to be important for molecular recognition. In accordance with other simulated models of protein complexes, the negative aspartates and glutamates of flavocytochrome b_2 were aligned with the positive arginines and lysines of cytochrome *c*. The haems were found to be parallel, with an iron-iron separation of 25.6Å. An electron-transfer pathway was also proposed between the two haems. This involved the side-chain of isoleucine 50, which is in contact with the flavocytohrome b_2 haem, the backbone of lysine 51, and the aromatic ring of phenylalanine 52, which was reported to be in van der Waal's contact with the haem of cytochrome *c*. The model predicted a key residue for complex formation on flavocytochrome b_2, glutamate 91. The construction of a mutant-enzyme, with glutamate 91 mutated to a lysine, produced a second-order rate constant for the reduction of cytochrome *c* of 37.7 $\mu M^{-1}s^{-1}$, within the value for the wild-type enzyme of 34.8 $\mu M^{-1}s^{-1}$ (pH 7.5, $I = 0.1M$, 25°C). The haem redox potential for the mutant-enzyme was -13mV, a value again within error of the wild-type enzyme, -17mV. These data, along with data from two other mutant-enzymes, showed that the hypothetical complex was not a realistic model of how cytochrome *c* binds to flavocytochrome b_2. However, with the aid of molecular graphics and the sequence homology conserved within the 'cytochrome b_5 fold', several residues were postulated to form a binding site for cytochrome *c*, and the subsequent kinetic analysis on the mutant-enzymes confirmed two of these residues to be essential for molecular recognition and complex formation. The individual mutations of glutamate 63, and aspartate 72 of flavocytochrome b_2 to positive lysine residues led to a decrease in the second-order rate constant, for the reduction of cytochrome *c*, from 34.8 $\mu M^{-1}s^{-1}$, to 13.0 $\mu M^{-1}s^{-1}$ and 24.3 $\mu M^{-1}s^{-1}$ (pH

7.5,I = 0.1M,25°C) respectively. The construction of a double mutation led to a maximum decrease in the second-order rate constant to $6\mu M^{-1}s^{-1}$. The redox potentials of the haem domain in all three mutant-enzymes were all measured to be ~20mV greater than the wild-type enzyme. This will not affect the reaction as the redox potential difference between the two proteins is still 1/4V, and the rate-limiting step is the formation of the complex and not the electron transfer itself. These results have now been used to create a computer model of what the complex may look like. The model predicts that a third residue, located in the flavin domain, is also involved in the formation of the complex, glutamate 237. The two haems are approximately orthogonal and are separated by a distance of 13.1Å. An electron-transfer pathway has been proposed: The pathway extends from histidine 66, the axial ligand to the flavocytochrome b_2 haem, through the backbone of alanine 67, and on to proline 68. There is then a 3Å through-space jump to the cytochrome *c* haem. Four cytochromes *c* can be accommodated on the tetramer, each cytochrome *c* binds to just one subunit.

ABBREVIATIONS AND UNITS

Amino acids

	Code	Symbol
Alanine	Ala	A
Arginine	Arg	R
Asparagine	Asn	N
Aspartic acid	Asp	D
Cysteine	Cys	C
Glutamic acid	Glu	E
Glutamine	Gln	Q
Glycine	Gly	G
Histidine	His	H
Isoleucine	Ile	I
Leucine	Leu	L
Lysine	Lys	K
Methionine	Met	M
Phenylalanine	Phe	F
Proline	Pro	P
Serine	Ser	S
Threonine	Thr	T
Tryptophan	Trp	W
Tyrosine	Tyr	Y
Valine	Val	V

Oligonucleotides

	Symbol
Adenine	A
Guanine	G
Cytosine	C
Thymine	T

Mutations

Mutant-enzymes are identified by specifying the wild-type amino acid, the location of the residue on the polypeptide chain, and the amino acid that replaces it. The replacement of aspartate 72 with a lysine is represented by Asp72Lys, or D72K.

Kinetic Parameters

K_m	Michaelis constant
k_{cat}	Rate constant at saturation
K_d	Dissociation constant
k	Rate constant

Standard Units

m	metre
g	gram
s	second
l	litre
^oC	Degree celsius
M	Molar
V	Volt
Å	Angstrom

Textual abbreviations

Abs	Absorbance
Da	Daltons
DNA	Deoxyribonucleic acid
E. coli	*Escherichia coli*
EDTA	Ethylenediaminetetraacetic acid
FMN	Flavin mononucleotide
ΔG	Free energy change
H. anomala	*Hansenula anomala*
I	Ionic strength
M_r	Molecular weight
PAGE	Polyacrylamide gel electrophoresis
SDS	Sodium dodecyl sulphate
TEMED	N,N,N',N'- Tetramethylethylene amine
Tris	Tris(hydroxymethyl)aminomethane
UV	Ultraviolet
Vis	Visible
nmr	nuclear magnetic resonance

CONTENTS

		PAGE
1	**GENERAL INTRODUCTION**	1
1.1	**ELECTRON TRANSFER**	2
1.1.1	**Introduction**	2
1.1.2	**Theory**	2
1.2	**PROTEIN-PROTEIN ASSOCIATIONS**	
1.2.1	**Cytochrome b_5:Cytochrome *c***	9
1.2.2	**Cytochrome *c* Peroxidase:Cytochrome *c***	10
1.2.3	**The Blue Copper Proteins: Plastocyanin and Amicyanin**	15
1.2.4	**The nature of the association**	20
1.3	**FLAVOCYTOCHROME b_2 (from *Saccharromyces cerevisiae*)**	
1.3.1	**The physiological role of flavocytochrome b_2**	23
1.3.2	**The structure of flavocytochrome b_2**	23
1.3.3	**Comparison of S.cerevisiae and H.anomala flavocytochromes b_2**	25
1.3.4	**The active site**	27
1.3.5	**The catalytic cycle** *Flavin to haem electron transfer*	28
1.3.6	**The interaction with cytochrome *c***	33

2 MATERIALS AND METHODS 35

2.1 GROWTH AND MAINTENANCE OF STOCKS 36

Bacterial stocks; E.coli growth; Storage of cultures

2.2 SOLUTIONS 37

2.2.1 DNA manipulation 37

TE;10xTBE; 10xloading buffer; DNA sequencing gel

2.2.2 Protein purification 38

0.1M purification buffer; 10mM Tris/HCl buffer.

2.3 SUPPLIERS 38

Enzymes; General laboratory chemicals.

2.4 DNA MANIPULATION 38

2.4.1 Plasmids 38

2.4.2 Oligonucleotide primers 39

2.4.3 Transformation and selection procedures 40

Preparation of competent cells; Transformation of E.coli

2.4.4 Preparation and isolation of *E.coli* 41

Isolation of plasmid DNA from E.coli; Preparation of single stranded DNA; Isolation of single stranded DNA.

2.4.5 Gel electrophoresis of DNA 42

Agarose gel electrophoresis of DNA; Recovery of DNA from agarose gels

2.4.6 Digestion and ligation 43

Cleavage of DNA with restriction enzymes; Ligation of DNA ends.

2.4.7 Site-directed mutagenesis 43

Mutagenesis; Extension/ligation.

2.4.8 Sequencing of single-stranded DNA 45

2.5 PURIFICATION OF FLAVOCYTOCHROME b_2 46

Growth and harvesting of E.coli cells over-expressing flavocytochrome b_2; Cell lysis; Ammonium sulphate fractionation; Dialysis; Column chromatography.

2.6 STEADY-STATE KINETIC ANALYSIS

Ferricyanide; Cytochrome c; Flavocytochrome b_2 51

2.7 STOPPED-FLOW KINETIC ANALYSIS 52

'Super-steady-state' reduction of cytochrome c; Oxidation of L-lactate; Pre-steady-state reduction of cytochrome c.

2.8 REDOX POTENTIOMETRY 56

Preparation of redox standard solutions; Calibrating the electrode; Redox solutions; Measurement of the haem redox mid-point potential.

3 THE CYTOCHROME *c* INTERACTION WITH FLAVOCYTOCHROME b_2 59

3.1 INTRODUCTION 60

3.1.1 The stoichiometry of the interaction *of Saccharromyces cerevisiae* flavocytochrome b_2 and cytochrome *c* 60

3.1.2 The stoichiometry of the interaction of Hansenula anomala flavocytochrome b_2 and cytochrome *c* 61

3.1.3 The effect of electrostatics on the interaction 61

3.2 RESULTS 66

3.3 DISCUSSION 71

4. LOCATION OF A CYTOCHROME *c* BINDING SITE ON THE FLAVOCYTOCHROME b_2 STRUCTURE 74

4.1 INTRODUCTION 75

4.2 RESULTS 76

4.2.1 Construction and description of the model 78

4.3 DISCUSSION

4.3.1 Kinetics of the association 84

4.3.2 The model of the complex 86

4.4 CONCLUSION 89

FIGURES

		PAGE
1.1.2.1	Reaction profile for non-adiabatic electron transfer.	3
1.1.2.2	Energy diagrams for normal, activationless and inverted non-adiabatic electron-transfer reactions.	7
1.1.2.3	The Marcus inverted region.	8
1.2.1.1	The positive residues surrounding the exposed haem edge of cytochrome *c*.	11
1.2.1.2	Salemme's original hypothetical model of the cytochrome b_5:cytochrome *c* complex.	12
1.2.2.1	The interface of the co-crystals of cytochrome *c* peroxidase:cytochrome *c* complex.	14
1.2.3.1	The two interaction areas proposed for plastocyanin and its interaction with photosystem I and cytochrome *f*.	17
1.2.3.2	The two interaction areas proposed for amicyanin and its interaction with cytochrome c551i and methylamine dehydrogenase.	18
1.2.3.3	Model for the electron-transfer reactions between amicyanin and cytochrome *c*551i.	19
1.3.1.1	The location of flavocytochrome b_2 in relation to the intermembrane space of yeast mitochondria	24
1.3.2.1	The structure of flavocytochrome b_2	26
1.3.4.1	The active site of flavocytochrome b_2.	29
1.3.4.2	The two possible mechanisms of L-lactate dehydrogenation as catalysed by flavocytochrome b_2.	30
1.3.5.1	The catalytic cycle	31

2.5.1	The oxidised/reduced spectra of flavocytochrome b_2.	50
2.7.1	Michaelis curve derived from the 'Super-steady-state' reduction of cytochrome *c*.	55
2.8.1	Redox potentiometry combination electrode.	57
3.1.4.1	The hypothetical model of the flavocytochrome b_2 interaction with cytochrome *c*, as predicted by Tegoni *et al*, 1993.	63
3.1.4.2	The interface between flavocytochrome b_2 and cytochrome *c* in the hypothetical model.	65
3.2.1	The second-order rate constants for the wild-type and mutant enzymes designed to test the Tegoni model.	70
3.3.1	The σ-tunnelling pathway proposed in the hypothetical model.	73
4.2.1	Bimolecular rate-constants for the reduction of cytochrome *c* with targeted point mutations designed to affect cytochrome *c* binding.	79
4.2.2	Redox potential determination for the double mutation E63K:D72K.	80
4.2.3	The effect of ionic strength on the interaction of cytochrome *c* with the double mutation, E63K:D72K.	81
4.2.1.1	The model produced, based on the kinetic data, of where cytochrome *c* binds to flavocytochrome b_2.	82
4.2.1.2	The interface between flavocytochrome b_2 and cytochrome *c*.	83
4.2.1.3	The proposed σ-tunnelling pathway from flavocytochrome b_2 to cytochrome *c*.	85
4.3.2.1	Brownian dynamics results for the interaction of flavocytochrome b_2 with cytochrome *c*.	88

TABLES

		PAGE
3.2.1	Steady-state kinetic parameters for the Wild-Type and mutant-enzymes designed to test the Tegoni model.	68
3.2.2	Pre-steady-state reduction of the flavin and haem prosthetic groups, and haem mid-point potential, for the mutant enzymes used to test the Tegoni model.	69
4.2.1	Pre-steady-state reduction of the flavin and haem prosthetic groups for the mutant enzymes that affect the second-order rate constant with cytochrome *c*.	77

1. GENERAL INTRODUCTION

1.1 ELECTRON TRANSFER

1.1.1 Introduction

To generate energy in eukaryotic cells, electrons are transferred via a system of redox co-factors that are arranged within membranes to assist electron flow from NADH to oxygen. The electron flow is directed down a potential gradient of greater than 1 volt, and in the confined area of the cell, specificity must be assured to ensure against 'short circuiting' (Mclendon & Hake, 1992). A fundamental problem in biology is understanding the mechanism by which molecules recognise and bind to one another. Indeed, the degree of specificity required for electron transfer may be more critical than the actual rate of the electron transfer itself (Mclendon, 1988). A great deal of attention has been directed in understanding not only how these proteins recognise one another, but by what means does the protein medium facilitate electron transfer (Moser *et al*, 1995; Curry *et al*, 1995; Baum, 1993).

Several systems have been studied with a view to elucidate the nature of this electron transfer. In the case of ruthenated proteins (Lloyd *et al*, 1994) and the photosynthetic reaction centre (Moser *et al*, 1992), this involves a fixed donor-acceptor distance, and a purely intra-molecular electron transfer step. Cytochrome *c* peroxidase and cytochrome b_5 have both been studied with respect to their interaction with cytochrome *c* (Millett *et al*, 1995; Mauk *et al*, 1995), this involves the formation of a complex of the reacting proteins prior to the inter-molecular electron transfer. In both systems there are a number of different parameters to entertain: The driving force of the reaction; the reorganisation energy; the distance and route of the electron transfer; and the kinetics of the association of the proteins.

1.1.2 Theory

Electron transfer in proteins can take place over long distances, typically 10-30Å from one redox centre to another. The redox centre itself can be thought of as a localised potential well, so when modelling the reactant and product redox centres, they can be thought of as two similar simple harmonic oscillator potentials (Fig. **1.1.2.1**). The potential minima of these wells are separated on the nuclear co-ordinate, which represents atomic displacement, and by the free energy of the

reaction, ΔG. The point of intersection of the two potentials represents the activation energy for the reaction which can be expressed algebraically, incorporating the free energy of the reaction and the reorganisation energy. The reorganisation energy is the energy needed to move along the product potential surface as the geometry is distorted from the average product geometry, to the average reactant geometry, before an electron can be transferred.

Fig. 1.1.2.1

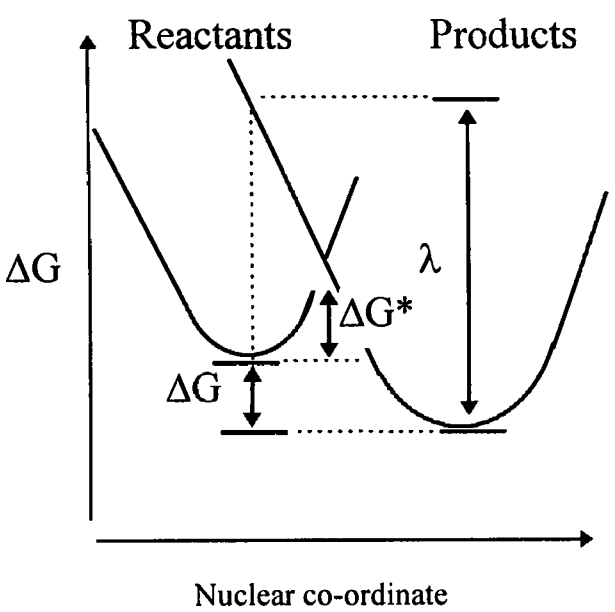

$$\Delta G^* = (\Delta G + \lambda)^2/4\lambda$$

ΔG^*= Activation energy

ΔG = Free energy of reaction

λ = Re-organisation energy

In intra-molecular electron transfer there is only one event, the electron transfer itself; in inter-molecular electron transfer a pre-cursor complex has to be formed with sufficient binding affinity, before the electron can be transferred. When the proteins are 'docked' in this complex there may be a conformational change, or there might be an increase or decrease in redox potential before electron transfer can take place. Such events are known as conformational gating. Once the electron transfer has taken place, the successor complex dissociates into the products.

$$A + D \underset{k_{off}}{\overset{k_{on}}{\rightleftharpoons}} [A:D] \overset{k_{et}}{\rightleftharpoons} [A^-:D^+] \underset{k_{on}^*}{\overset{k_{off}^*}{\rightleftharpoons}} A^- + D$$

pre-cursor complex successor complex products

The above scheme represents the mechanism for biological electron transfer. The usually asymmetrically positioned redox centre is thought to be situated near to the centre of the binding site, so as to reduce the distance between the redox centres when the pre-cursor complex is formed. If the complex is formed as is thought, to exclude water from the interface (Rodgers & Sligar, 1991; Salemme, 1976), then the electron transfer is purely through the protein medium itself. How does the protein matrix mediate electron transfer?

For any first-order reaction:

$$k_{et} = A\ e^{-\Delta G^*/kT}$$

k_{et} = electron transfer rate
A = electronic term
ΔG = activation energy
k = Boltzmann constant
T = Temperature

When this standard equation is applied to a biological system, 'A' cannot be a simple collision frequency as proteins have areas on them that are 'hot' or 'cold' with respect to electron transfer. This pre-exponential factor actually is an electronic term that measures the extent of orbital overlap between the donor and acceptor. The extent of this overlap decays exponentially with distance, and is proportional to an attenuation factor β. At van der Waals contact $A \approx 10^{13} s^{-1}$ (Moser *et al*, 1992).

$$A_R^{\,2} = A_o^{\,2} \exp\ [\ -\beta R\ ]$$

A_R = Electronic coupling
A_O = Maximum electronic coupling
R = Distance: centre of edge atom of donor to centre of edge atom of acceptor
β = Beta, attenuation factor: exponential coefficient of decay of electronic coupling with R

If we look at electron transfer through a covalently linked system, the attenuation or decay factor β, is 0.7 $Å^{-1}$. Through a vacuum it's 2.8 $Å^{-1}$. The β value for a frozen organic glass is 1.2 $Å^{-1}$ (Moser *et al*, 1992). If we look at the protein medium as a

homogeneous insulator, then the asymmetrically positioned redox centre is designed to transfer electrons through the least amount of polypeptide. This means that an area around the redox centre will be 'hot' for electron transfer, and the specificity is assured by the recognition between proteins. In this case the average value for β in proteins is 1.4 $Å^{-1}$.

We can also think of the protein medium as a conductor. In this case, the path of lowest resistance would be for the electron to travel through a system of covalent bonds (Wuttke *et al*, 1992; Regan *et al*, 1993; Moser *et al*, 1992), and the idea of a universal value of β becomes meaningless (Curry *et al*, 1995). This leads to the question of distance. If the electron was to travel through bonds, the path between the redox centres will be longer than the direct distance, but this is compensated for by the lower resistance afforded by the covalent bonds. The path of lowest resistance will provide the dominant electron transfer pathway from one redox centre to another. A computer program to calculate the optimal path has been developed by Onuchic *et al* (1991), and the electronic coupling between redox centres now becomes separated into three factors, and is not dependant on one universal decay factor:

$$\text{Electronic coupling} \propto (\text{Through bond distance})(\text{Through hydrogen bond distance})(\text{Through space distance})$$

If a number of optimal paths are found, as this is a quantum event, they may interfere constructively or destructively (Curry *et al*, 1995). Constructive interference will create a family of paths, or a pathway tube, and just as different model compounds give different values for β, different secondary structures will give different tubes (Beratan *et al*, 1991). However, if a large number of pathways are important, then no specific details of the protein structure will affect the rate (Onuchic *et al*, 1991).

The experimental method of testing the pathways theory is to attach pentaaminoaquaruthenium II to a histidine ligand on the surface of the protein. The direct distance to the redox centre from the ruthenium can be calculated from the

high resolution crystal structure, as well as the through-bond pathway. Once the electron transfer rate has been measured, the rate enhancement afforded by the through bond approach can be seen (Wuttke *et al*, 1992; Lloyd *et al*, 1994). These experiments are intra-molecular and avoid the rate limitation of complex formation.

A combination of the above equations leads us to Marcus' theory of electron transfer, which is independent of both the through bond approach, and the direct distance approach:

$$k_{et} \alpha \exp - [(\Delta G - \lambda)^2 / 4\lambda k_b T]$$

ΔG = free energy of reaction
λ = re-organisation energy
k_b = Boltzmann constant
T = Temperature

This equation shows the Gaussian dependence of electron transfer on free energy. The electron transfer is optimised when $\Delta G = \lambda$. When ΔG is greater than λ, the reaction is overdriven, and the electron transfer rate drops (Figs.**1.1.2.2 & 1.1.2.3**). This defines the Marcus inverted region (Miller *et al*, 1994; Marcus, 1956).

The photosynthetic reaction centre has proved to be an excellent model with which to study the dependence of free energy on the electron transfer rate (Moser *et al*, 1992,1995). The reaction centre provides an energy optimised system for the study of electron transfer, and therefore allows the examination of the dependence of electron transfer on purely the electronic coupling between donor and acceptor. The results suggest that electron transfer cannot be controlled by a fragile arrangement of polypeptide connecting the two redox centres, instead electron transfer can be more easily directed, or controlled, using more robust methods such as changing the polarity of the amino acids surrounding the cofactor, to modify the free energy and reorganisation energy (Moser *et al*, 1996). The relative proximity of the redox centres in the photosynthetic centre is apparently all that is needed to direct electron transfer.

The use of ruthenium modification on proteins of known structure provides a unique semi-synthetic system with which to study electron transfer where the driving force, distance, and intervening medium are known. Surface residues chosen are

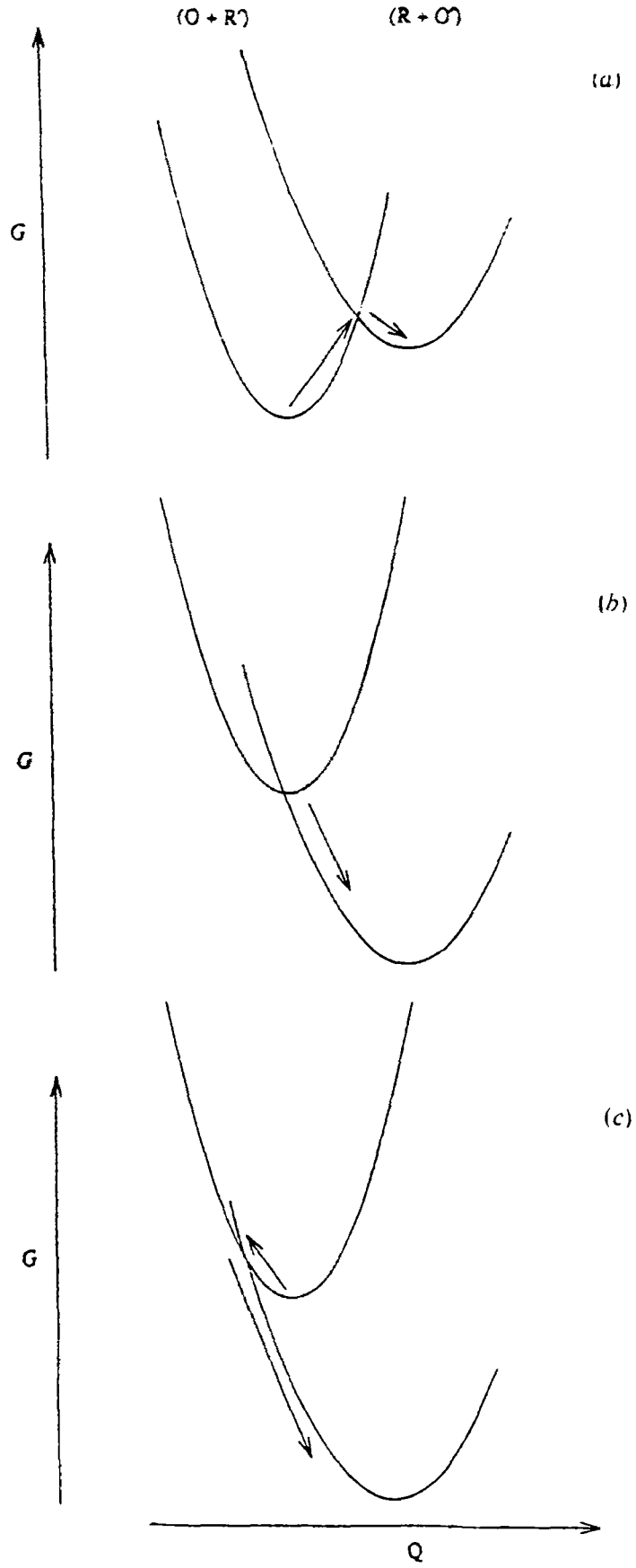

Fig. 1.1.2.2 Typical energy diagrams for the a) normal ($\Delta G + \lambda > 0$), b) activationless ($\Delta G + \lambda = 0$), and c) inverted ($\Delta G + \lambda < 0$) regions. The left hand bowl represents the reactants, and the right hand bowl the products. The arrow denotes the reaction pathway (Adapted from Chapman & Mount, 1995).

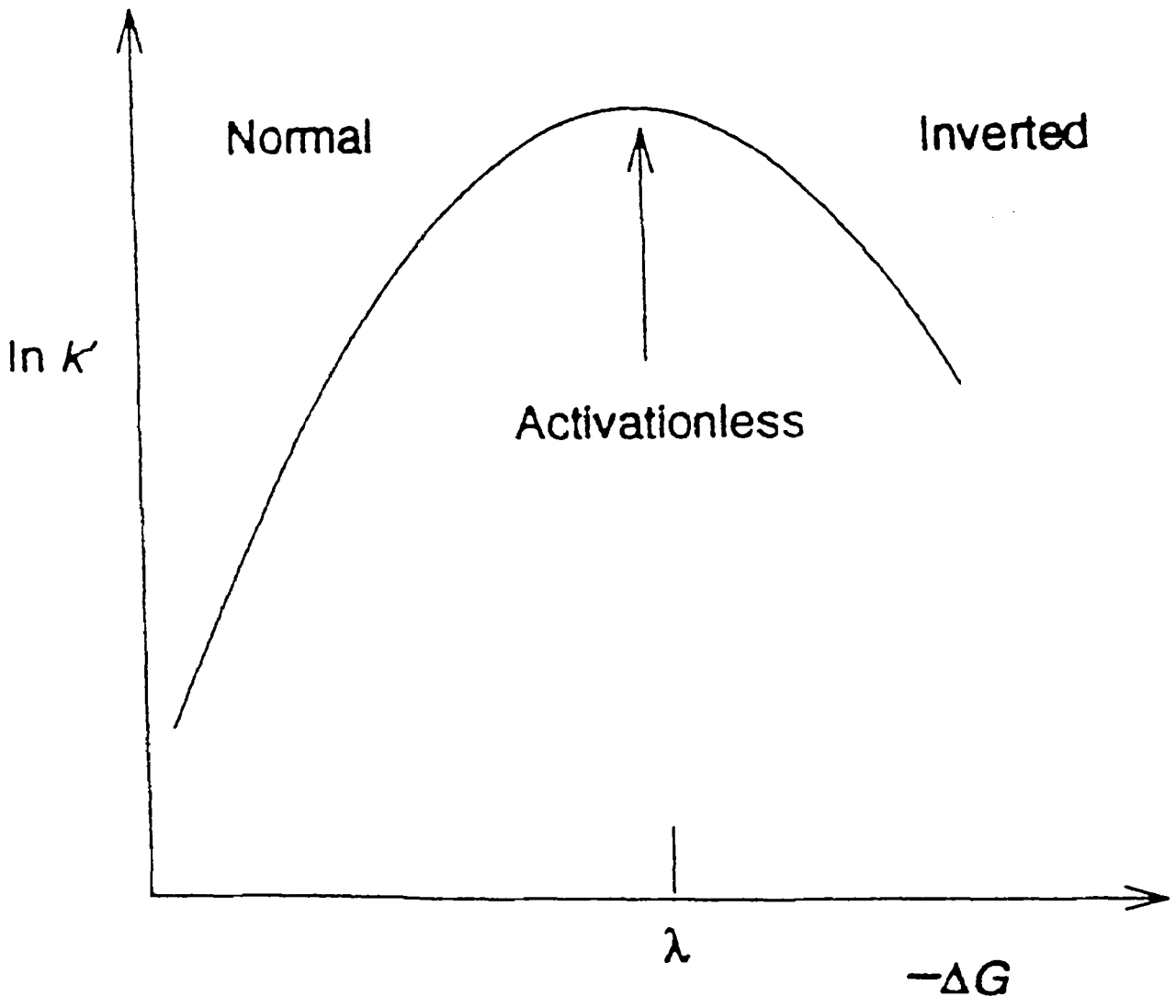

Fig. 1.1.2.3 The variation of the logarithm of the electron-transfer rate constant (k') with free energy between reactants and products (Adapted from Chapman & Mount, 1995).

mutated to a histidine prior to ruthenium modification. The direct distance between the donor and acceptor can be calculated using energy minimisation techniques, and then a program can be used to predict the best pathway connecting the two centres. The comparison can then be made to see if there is any rate enhancement afforded by the covalent pathways (Wuttke & Gray, 1993).

The fragility of the through bond theory can be seen in the mobility of the protein structure. The crystal structure provides us with a very complete, but time averaged structure that sometimes cannot account for the dynamic nature of the protein structure. The specific nature of the polypeptide acting as a conducting wire may be offset by the individual motion of amino acids, of water molecules, or by larger structural changes involving the secondary structure (Moser *et al*, 1995). When looking at inter-protein electron transfer, it's not just the dynamics of one protein that need to be addressed. This helps us in some ways when examining how the protein structure guards against energy wasteful reactions, as can be seen in amicyanin's reaction with cytochrome *c*551i (Davidson & Jones, 1995), and also in the photosynthetic reaction centre (Moser *et al*, 1992, 1995). In these cases a maximum electron transfer rate can be theoretically reached but cannot be obtained in practice, due to the lack of a binding site. In conclusion, the physiological dependence of electron transfer seems to be modulated by more 'robust' features than intermolecular wires.

1.2 PROTEIN-PROTEIN ASSOCIATIONS

1.2.1 Cytochrome b_5:Cytochrome *c*

In 1976 Salemme produced a hypothetical complex to illustrate how two proteins may interact. It had been observed that cytochrome *c* contained a highly conserved belt of positively charged residues surrounding the exposed haem edge (Fig. **1.2.1.1**). The partner it was to be matched with, cytochrome b_5, contained a conserved belt of negative residues surrounding its exposed haem edge. The two proteins are each composed of a single domain, and the crystal structures of both proteins were known. Although the interaction between cytochrome b_5 and

cytochrome *c* may not be a physiological reaction (Bernardi & Azzone, 1981), the rate *in vitro* is substantial enough to merit attention. The fact that the two proteins contain these highly conserved residues led to the theory that molecular recognition, and protein complex stability, were determined by complementary ionic interactions. The bimolecular rate constant was found to be dependent upon ionic strength and the two interacting surfaces were complementary, so that when the two proteins were aligned to produce the first hypothetical complex, the bulk of the solvent was found to be expelled from the interface between the proteins, by the tight fitting rigid conformation afforded by the close association of the hydrophobic and polar side chains. This tight association was thought to lower the dielectric constant, and therefore facilitate electron transfer. The haem groups were found to be parallel, and were separated by 8.4Å. Four ion pair interactions were postulated by Salemme to stabilise the complex, and were later confirmed by chemical modification studies (Daily & Strittmatter, 1979; Ng *et al*, 1977).

The cytochrome b_5:cytochrome *c* interaction has been the most extensively studied system to date (Mauk et al, 1995; Durham et al, 1995), and has proved to be a paradigm for other protein complexes. A hypothetical complex was also proposed for the physiological interaction between cytochrome b_5 and *met*hemoglobin (Poulos & Mauk, 1983). The conclusions were almost identical to the cytochrome b_5: cytochrome *c* complex, involving the same acidic residues on cytohrome b_5. Investigation into the position of the lysyl groups in *met*hemoglobin involved in binding cytochrome b_5 surprisingly revealed corresponding analogues in the cytochrome *c* structure. Four hydrogen bonds were proposed to lock the haems together in a parallel geometry thought to facilitate electron transfer by way of a conjugated π-system. Solvent was excluded from the interface between the two proteins by the hydrophobicity afforded from the complementary charge neutralisation of the interacting proteins.

1.2.2 Cytochrome *c* Peroxidase: Cytochrome *c*

In the same manner as Salemme, Poulos and Kraut (1980) tried to illustrate the Cytochrome *c* peroxidase:cytochrome *c* interaction with a hypothetical model.

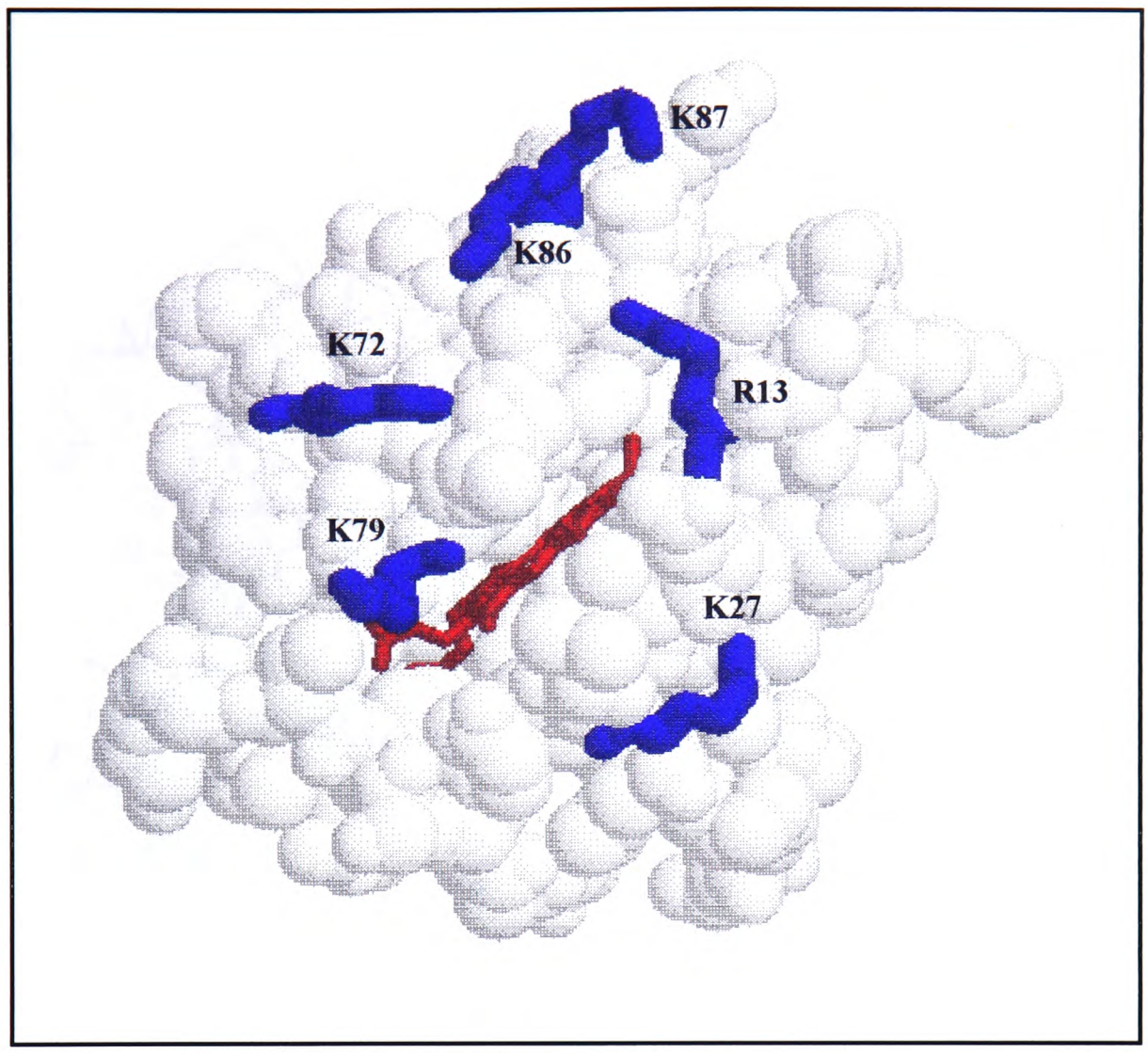

Fig. 1.2.1.1. The reacting face of cytochrome *c* showing the residues important for molecular recognition (Mclendon & Hake, 1992).

Fig. 1.2.1.2. Two orthogonal views of Salemme's original model of the interaction between cytochrome b_5 (bottom), and cytochrome c (top).

This is a physiological interaction, except for the purposes of this model, Tuna cytochrome *c* was used with yeast cytochrome *c* peroxidase. This was justified by the high degree of homology between the yeast and tuna cytochromes *c*. Again, a static docking model complete with specific interacting residues was produced. Seven main ionic interactions were named, and an inter-haem distance of 16.5Å was measured. The haems were seen to be parallel, in agreement with Salemme's model, and a very close fit between the two interacting surfaces was found. Unfortunately, there was a lack of data available to confirm the model.

12 years later Pelletier & Kraut (1992) produced co-crystals of the complex which did not confirm the hypothetical model (Fig.**1.2.2.1**). Two different sources of cytochrome *c* were used to form the co-crystals, as well as two differing conditions for crystallisation, yet two very similar structures were obtained. The theory is that the most stable complex in solution must be the complex that crystallised. However, does this necessarily have to be the optimal, or active complex for electron transfer? The crystals showed the two haem groups not to be parallel but made an angle of 60°, and the predominant forces holding the complex together were hydrophobic. Several possible ionic interactions could be made, but the authors had to concede that they just didn't form in the crystal. There were slight differences in the two crystal structures, however this was stated not to constitute 'multiple binding'. This crystal structure has been tested in two different ways: The point of closest contact between cytochrome *c* peroxidase and cytochrome *c* is residue 193 on cytochrome *c* peroxidase. This residue was converted to a cysteine which was then modified with a bulky reagent (Miller *et al*, 1994; Miller *et al*, 1996). The idea was that this steric crowding of the binding area between cytochrome *c* peroxidase and cytochrome *c* would inhibit the formation of the complex. The specificity of the interaction was indicated by the fact that the yeast cytochrome *c* was inhibited from binding to cytochrome *c* peroxidase much more strongly than the horse heart cytochrome *c*. This result indicates there are two closely linked binding modes for cytochrome *c* which the authors state should not be viewed as rigid structures, as recent work indicates that some surface diffusion is required to produce a productive complex. Experiments involving charge reversal on residues on and around the binding site

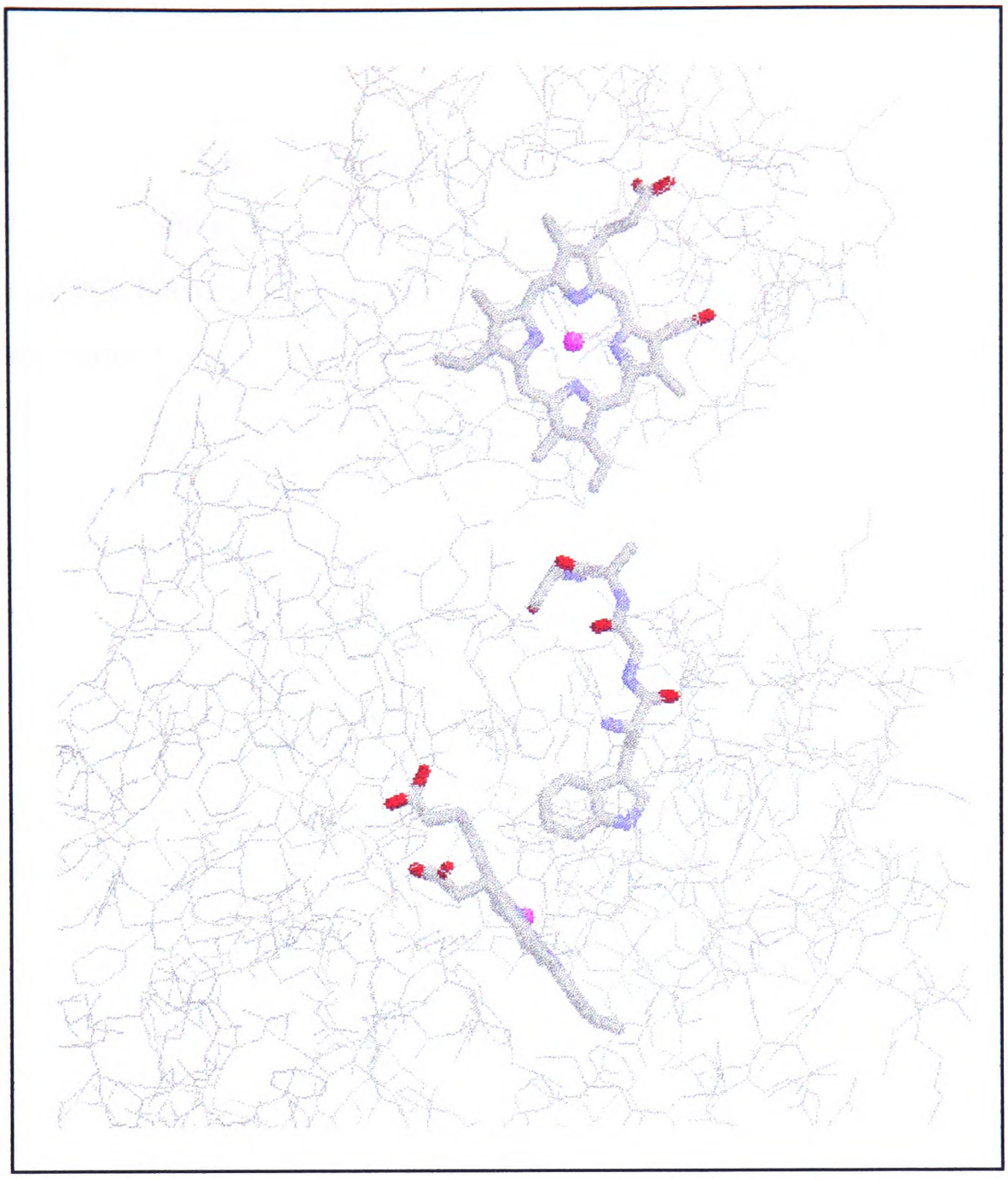

Fig. 1.2.2.1. The Cytochrome *c* Peroxidase (bottom):Cytochrome *c* (top) interaction as seen in the crystal structure of the complex. The proposed electron transfer pathway is shown to join the two haems, and involves residues Ala194, the backbone of residues Ala193 and Gly192, and the side chain of Trp191 (Pelletier & Kraut, 1992).

also confirmed that the solution interaction domain is similar to that seen in the crystal (Miller *et al*, 1994).

1.2.3 The Blue Copper Proteins: Plastocyanin and Amicyanin

Plastocyanin is a copper containing protein. Physiologically it acts as an electron shuttle between cytochrome *f* and the reaction centre chlorophyll (P700) in the photosystem I of plants and some algae (Gross, 1993). Like cytochrome b_5 and cytochrome *c* peroxidase, plastocyanin contains two localised acidic patches on its surface inclusive of residues 42-45, and 59-61 (Fig. **1.2.3.1.**). However, unlike cytochrome b_5 and cytochrome *c* peroxidase, this patch does not surround the redox centre, instead the copper resides in a hydrophobic pocket at the northern end of the molecule (Guss & Freeman, 1983). Also, these proteins do not seem to have a single site for electron transfer. In cytochrome b_5, cytochrome *c* peroxidase, and cytochrome *c*, the point of entry or exit of the electron occurs at the exposed haem edge. The copper proteins do have a site of maximum electronic coupling with a redox partner, as close to the copper as possible, but the protein seems to regulate the electron transfer by placing the binding sites a fixed distance away from the copper.

In the studies on the interaction between plastocyanin and cytochrome *c* (Roberts *et al*, 1991), the pre-orientation of cytochrome *c* was examined before a complex was formed. This produced several families of orientations with differing haem angles on various areas of the protein surface. These locations for electron transfer have also been examined in terms of the strength of the electronic coupling between the redox centres (Ullmann & Kostic, 1995). A pertinent conclusion from the two studies is that the alignment of electrostatic residues to produce an optimal docking complex may not necessarily be the optimal complex for the transfer of electrons. Cross-linking studies demonstrate that a rearrangement by surface translation or rotation is a requirement for the efficient transfer of an electron (Qin & Kostic, 1993; Peerey & Kostic, 1989).

Plastocyanin does have two physiological sites for electron transfer. It has been proposed that while the acidic patches on plastocyanin must provide the initial molecular recognition for its redox partners, the electron transfer sites are different.

In the interaction with cytochrome *f*, plastocyanin uses the acidic residues 42-45 and the electron is transferred via Tyr 83 (Lee *et al*, 1995). Photosystem I uses both acidic patches, 42-45 and 59-61, and the electron is transferred from plastocyanin through the imidazole ring of His 87 (Lee *et al*, 1995; Sigfridsson *et al*, 1996).

Methylamine dehydrogenase (MADH) provides an extremely interesting system for examining the importance of complex formation. The enzyme contains the unusual tryptophan tryptophylquinone cofactor, and oxidises methylamine to methanal and ammonia with the liberation of two electrons. These are passed singly to amicyanin, a blue copper protein, and then to cytochrome *c*551i. Studies seem to indicate that a ternary complex must form before electron transfer can take place from MADH to cytochrome *c*551. Cytochrome *c*551 does not accept electrons directly from MADH (Husain & Davidson, 1986), and the reaction with free amicyanin in the absence of MADH is thermodynamically unfavourable (Gray *et al*, 1986; Davidson & Jones, 1995). The formation of the binary complex between amicyanin and MADH induces a redox potential shift of 73mV for amicyanin from 294mV to 221mV. This greatly facilitates electron transfer to cytochrome *c*551 which has a redox potential of 190mV (Gray *et al*, 1988).

A crystal structure has been solved for the ternary complex (Chen *et al*, 1994). Cytochrome *c*551i does not make any contact with MADH, binding solely to amicyanin. The two interacting complex surfaces of amicyanin are also quite different. The interaction with MADH is mostly hydrophobic, the two cofactors are positioned as close together as possible. On the other side of amicyanin, the highly acidic cytochrome *c*551i forms a mainly polar complex with interacting charged residues (Chen et al, 1994).

From the crystal structure the copper-iron distance is quite large at ~25Å (Fig. **1.2.3.2**), and the redox potential difference is also unfavourable for the reduction of the cytochrome, however the rate of electron transfer does not reflect these parameters, and the two centres seem to be well electronically coupled considering the distance (Davidson & Jones, 1996). The unfavourable forward reaction of the electron exchange is further aided by the fact that the electron transfer from the copper to the iron is slower than the rate of dissociation of the cytochrome *c*551i

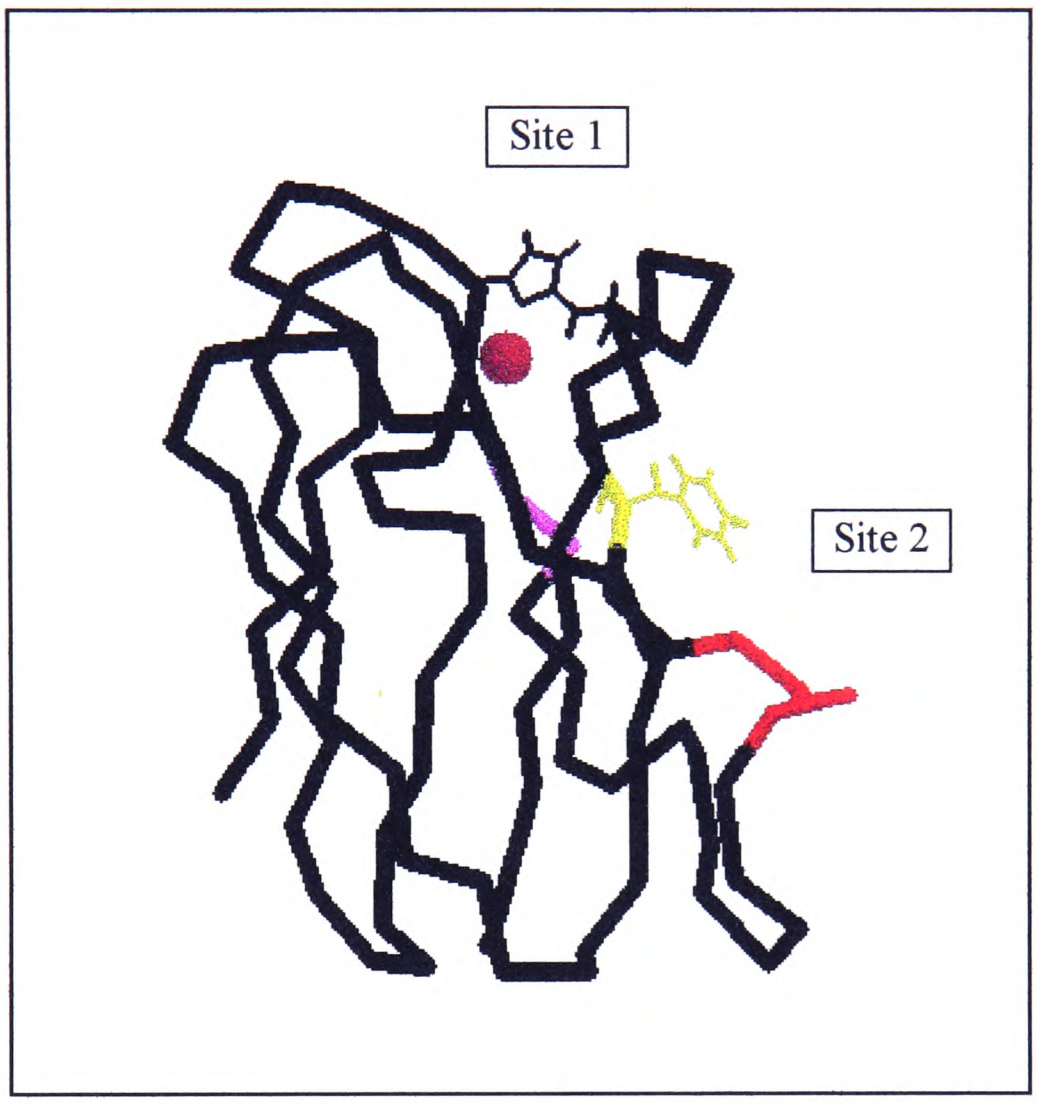

Fig. 1.2.3.1. The backbone of the blue copper protein plastocyanin showing the two sites of electron transfer. Site 1 is located at the hydrophobic end of the protein, and the electron is delivered from the copper to photosystem I via His 87. Site 2 is the location of Tyr 83, which is the point of electron entry from cytochrome *f*. The red section of backbone shows the area of acidic residues 42-45 implicated in forming the complex with cytochrome *f*, and the magenta indicates the residues 59-61 which are thought to help form the complex with photosystem I.

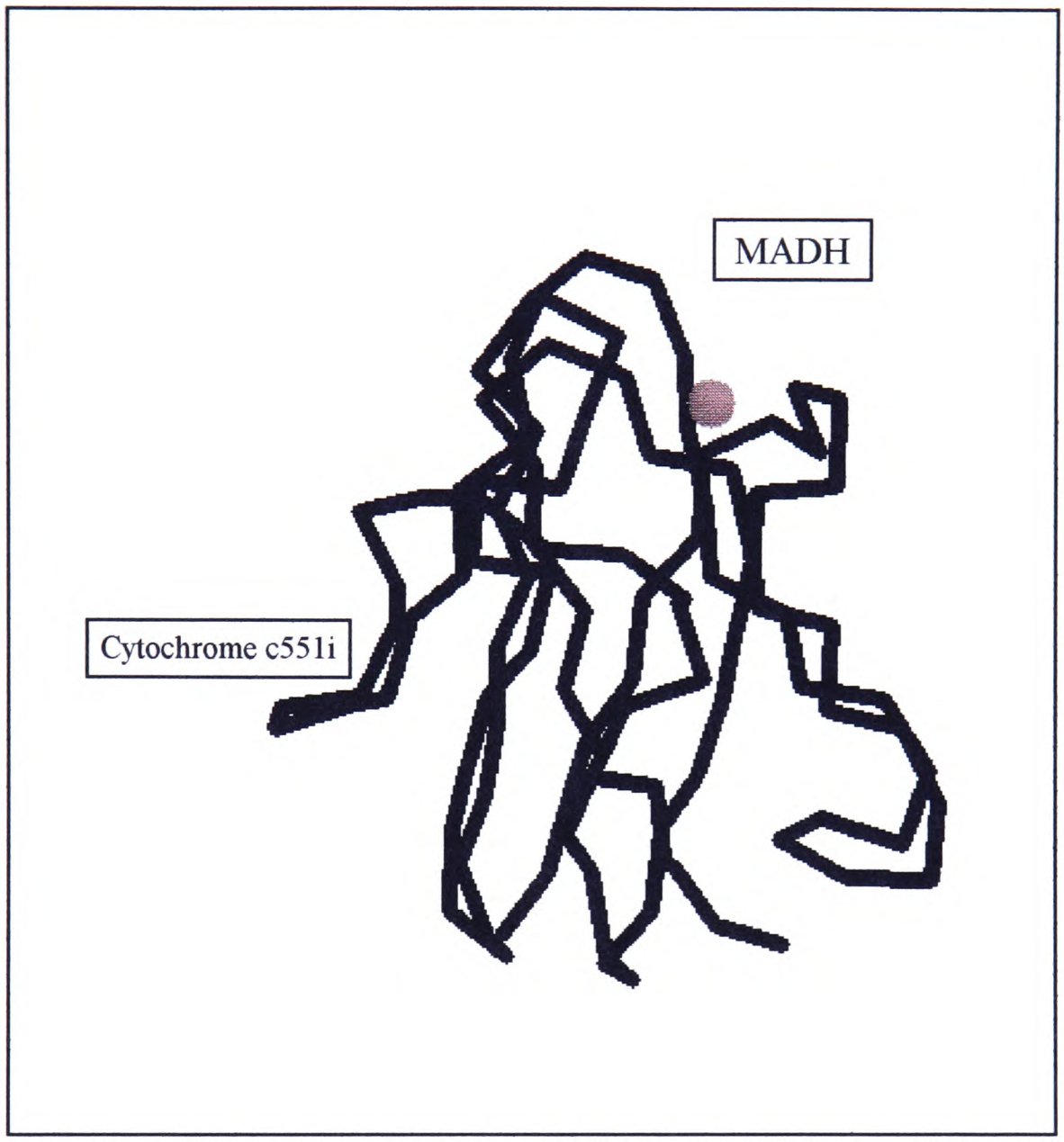

Fig. 1.2.3.2 The blue copper protein amicyanin showing the two binding sites proposed for electron transfer. The MADH co-factor binds 9.4Å from the copper at the hydrophobic end of the molecule. Cytochrome *c*551i is restricted to binding on the opposite side of amicyanin forming mainly polar interactions. This places the haem 24.8Å from the copper.

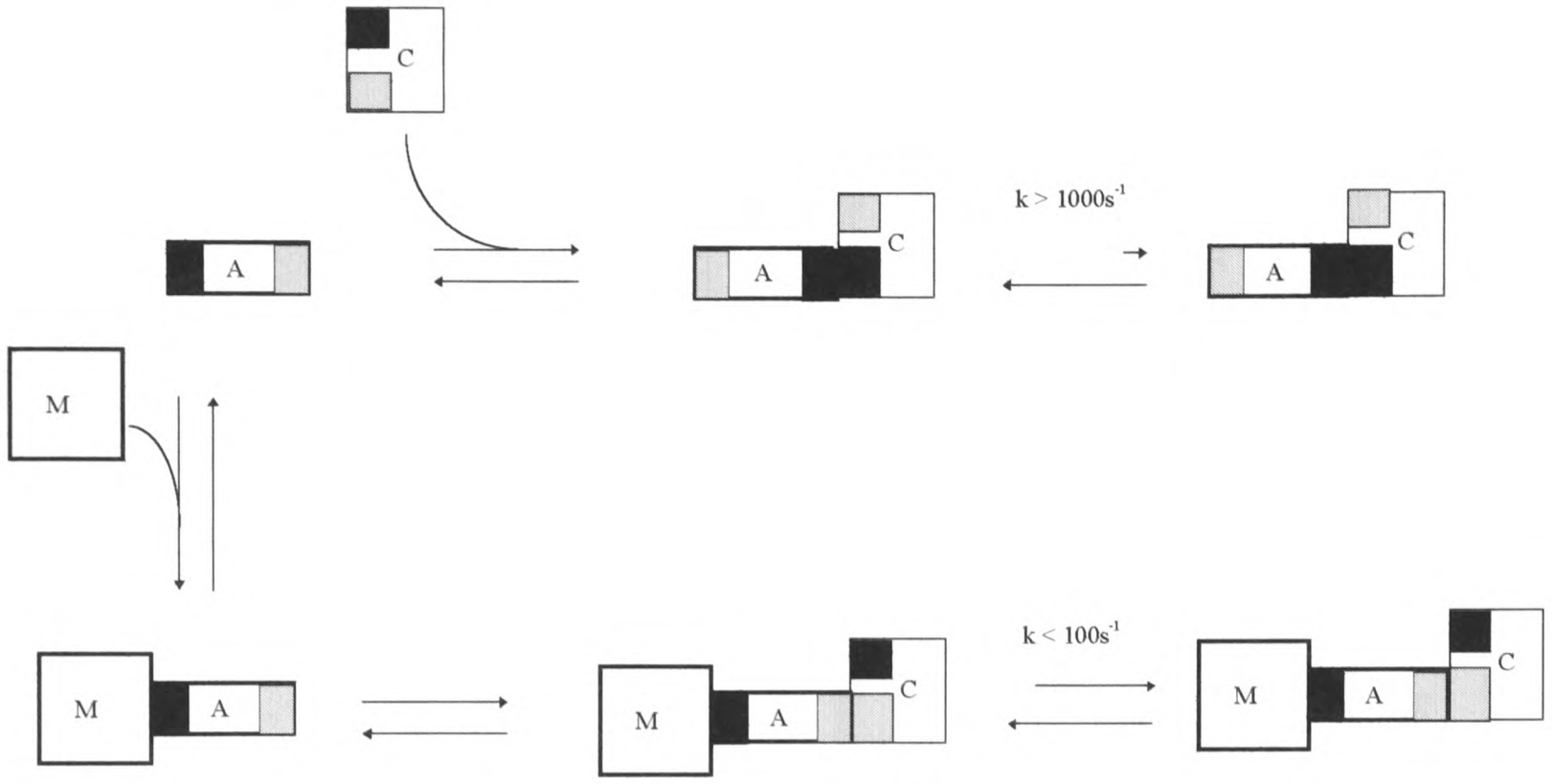

Fig. 1.2.3.3. Model for the electron transfer reactions between amicyanin and cytochrome *c*551i. The squares represent Methylamine dehydrogenase, (M), Amicyanin, (A), and cytochrome *c*551i, (C). The black patch indicates a hydrophobic region, and a striped black patch indicates a polar region. The most direct access to the copper and haem cofactors is via these hydrophobic patches (Adapted from Davidson & Jones, 1995).

from the ternary complex. This means that the thermodynamic equilibrium, as calculated from the redox potentials of the two centres does not reflect the kinetic reality (Fig.**1.2.3.3**).

Analysis of these two systems involving plastocyanin and amicyanin provides an important insight to the modulation of biological electron transfer. In the case of plastocyanin the specificity of the interaction is governed by electrostatics that allow interfacial motion. The initial docking geometry not being the optimal geometry for electron transfer. The electron transfer itself is seen to occur through two separate residues, differing in distance form the redox centre. Amicyanin forms a highly specific, yet a weakly bound hydrophobic complex with MADH (Gray *et al*, 1988; Chen *et al*, 1994). The redox centres are placed as close together as possible, and this binary complex only allows cytochrome *c*551i to bind on the polar side of amicyanin, and means that the copper-iron distance is approx. 25Å. The thermodynamics become more weighted for the electron transfer to the iron in terms of a redox potential shift (Gray *et al*, 1988), and a dissociation rate of the reduced cytochrome that is faster than the electron transfer (Davidson & Jones, 1995). This may be another example of how proteins modulate their electron transfer by distance. When free amicyanin reacts with cytochrome *c*551i, although the equilibrium is heavily weighted against the reaction, the electron transfer is in excess of $1000s^{-1}$ (Davidson & Jones, 1995). This electron transfer rate is purely a result of the close proximity of the redox centres, despite the large redox potential against the transfer (104mV, Gray *et al*, 1988). The reason for this not being the physiological electron transfer site, and the need for a binary complex, is the lack of molecular recognition provided by the hydrophobic protein surface. The same result can be seen when Roberts *et al* (1991) modelled the plastocyanin interaction with cytochrome *c*.

1.2.4 The nature of the association

Hypothetical models of protein complexes seem to present static, rigid docking models of how two proteins interact (Salemme, 1976; Poulos & Kraut, 1980). There is some evidence that this is the case, however, there is also a great deal of work indicating that these complexes are not static, or rigid, but dynamic and

flexible. If the interaction is flexible, we have to ask the question: How is specificity achieved? To examine this conflict we have to look closely at the formation of the complex itself. When Salemme modelled his complex between cytochrome b_5 and cytochrome *c*, it was a very tight association of hydrophobic and polar side-chains. The year before, Chothia and Janin (1975) had theorised that the major factor stabilising the protein-protein association was this hydrophobicity of the interacting surfaces. The complementary side-chains were there for recognition, deciding which proteins are to associate, and then to pre-orientate the molecules for complex formation. Recent research has indicated that hydrophobicity plays a key role in molecular recognition (Lijnzaad *et al*, 1996).

Molecular recognition is proposed to start with the non-specific ionic attraction, which leads to a "reduction in dimensionality" (Adam & Delbruck, 1968), or a "diffusive entrapment" effect (Northrup *et al*, 1992). This meant that the initial ionic attraction and recognition resulted in a non-specific complex, so that there was a greater chance of achieving the optimal configuration for electron transfer as the proteins had only two dimensions to deal with. Clearly in this case the complementary ionic charges are providing a pre-collisional orientation effect (Roberts *et al*, 1991; Koppenol & Margoliash, 1982; Chothia & Janin, 1975), and once the proteins have formed a complex these interactions cannot be too strong as to impede the formation of an optimal geometry, yet cannot be too weak so as to allow dissociation of the newly formed complex. This was the basis of the theory that proteins formed a flexible complex that could sample inter-haem geometries (Eley & Moore, 1983; Wendoloski *et al*, 1987; Northrup *et al*, 1988, 1992), and to achieve a correct geometry for electron transfer, proteins undergo many small collisions without actually dissociating. This flexibility was used to explain the compatability of the non-physiological interaction of cytochrome b_5 and cytochrome *c*, and is used to explain the small electron transfer rates of cross-linked complexes (Peerey & Kostic, 1989; Quin & Kostic, 1993).

Experiments on the rigidity of protein complexes seemed to illustrate that if the binding was too tight, then the complex was seen to be inefficient. Low temperature work indicated that the cytochrome *c* peroxidase:cytochrome *c* complex was not

necessarily restricted to a single docking geometry (Nocek *et al*, 1990), and at low ionic strength the electron transfer rate could be lowered, indicating that the complex formed was too tightly bound (Hazzard *et al*, 1988). This shows that the most stable complex may not be the most favourable for electron transfer (Pelletier & Kraut, 1992; Meyer *et al*, 1993), and that the ionic contribution to complex stability may be solely confined to molecular recognition.

To test the tightness of the protein-protein association, nmr experiments have been carried out involving deuterium exchange of amide protons on the backbone of the protein. The idea is that the area involved in forming the complex will show slowed exchange, and a 'footprint' of the binding site can be seen. The extent to which the exchange is slowed will reflect the tightness of the association. Two differing results illustrate the problem. Jeng *et al* (1994) found no significant slowing of exchange in the Cytochrome *c* Peroxidase:Cytochrome *c* complex, and therefore concluded that the protein complex interface must be highly mobile, and not a static model as previously thought. In direct contrast Yi *et al* (1994) reported that the same complex was highly specific. The difference in the experiments was the ionic strength. The small difference in ionic strength was probably enough to make a weak association of two proteins into a tightly bound complex. A more dynamic interaction was also found by Eley & Moore (1983) when they examined the formation of the cytochrome b_5:cytochrome *c* complex.

Pressure is another tool used to investigate the formation of protein complexes (Mozhaev *et al*, 1996; Rodgers & Sligar, 1991). In conjunction with site-directed mutagenesis the interaction area for the formation of a protein complex can be mapped, and the number of ionic interactions determined (Kornblatt *et al*, 1988, 1993). These experiments led to the conclusion that protein complex formation is entropy driven. The decrease in entropy from the actual formation of the complex is offset by the expulsion of water from the interface between the two proteins to the bulk solvent. Rodgers & Sligar (1991) proposed from their work involving pressure on the cytochrome b_5:cytochrome *c* complex that there is only one major orientation of the complex, and this is attained without the formation of electrostatically stable encounter complexes.

1.3 FLAVOCYTOCHROME b_2 (From *S.cerevisiae*).

Flavocytochrome b_2 provides an ideal system for the study of biological electron-transfer. It combines intra-molecular electron transfer with inter-molecular electron transfer to its physiological partner, cytochrome *c*. It is perfectly amenable to study as the crystal structure has been solved (Xia & Matthews, 1990), and the gene has been expressed in *E.coli* (Black *et al*, 1989a). This not only allows a detailed study of the molecular structure of the enzyme, but also avails itself to genetic manipulation, and kinetic analyses.

1.3.1 The Physiological Role of Flavocytochrome b_2

Flavocytochrome b_2 is an L-lactate:cytochrome *c* oxidoreductase that can be found in the intermembrane space of yeast (Daum *et al*, 1982). It allows yeast to respire on L-lactate when the main respiratory pathway is blocked, for example by antimycin (Pajot & Claisse, 1974). The two electrons resulting from the oxidation of L-lactate are transferred singly from the flavin domain via the cytochrome domain to cytochrome *c*, which acts as a one electron shuttle between flavocytochrome b_2 and cytochrome *c* oxidase (Fig. **1.3.1.1**).

1.3.2 The structure of Flavocytochrome b_2 (Xia *et al*, 1987; Xia & Matthews, 1990)

Flavocytochrome b_2 is a tetramer of M_r 230, 000 (Fig. **1.3.2.1**). Each subunit is composed of two separate domains that bind their prosthetic groups non-covalently. The two domains are joined by a polypeptide linker. The cytochrome domain comprises of residues 1-99, and folds in a similar fashion to cytochrome b_5. The ligands to the iron of the haem group are histidines 43 and 66. The flavin containing domain consists of residues 100-486, and forms a $\beta_8\alpha_8$ structure, similar to glycolate oxidase (Lindqvist & Branden, 1985; Linqvist *et al*, 1991) but with a significantly different orientation of the FMN that reflects the separate functions of the enzymes. The final 25 residues form a C-terminal tail that makes contact with each of the other subunits.

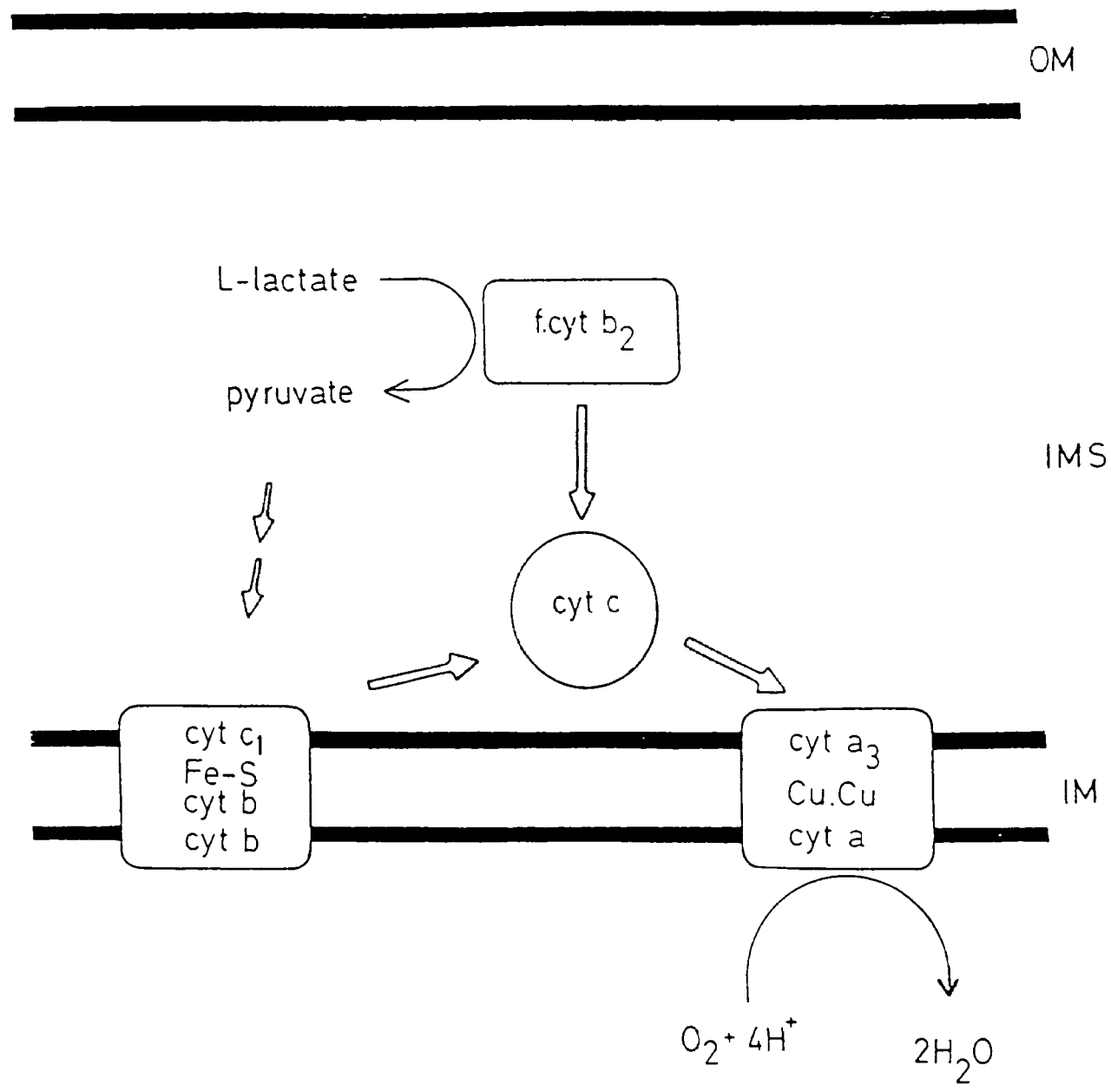

Fig. 1.3.1.1. The position of flavocytochrome b_2 in relation to the the intermembrane space of yeast mitochondria, and other electron-transport enzymes. OM = outer-membrane; IMS = intermembrane space; cyt, cytochrome; f.cyt.b_2, flavocytochrome b_2 (Chapman *et al*, 1991).

The subunits are related by a pseudo-four fold axis of symmetry. The flavin domain and the C-terminal tail form all the intersubunit contacts, and resemble an ellipsoid disc in the absence of the cytochrome domains. The cytochrome domains are positioned on the periphery of the disc (Fig. **1.3.2.1**). In the crystal structure two of the four cytochrome domains are disordered, and do not appear on the electron density map. In subunit one, the ordered cytochrome domains make more contacts with other tetramers in the crystal lattice, and also a pivotal hydrogen bond can be seen between the two domains from Tyr 143 to the haem propionate. No substrate is seen at the active site. In subunit two, where the cytochrome domain is found to be disordered, pyruvate is seen bound in the active site. The pyruvate carboxylate forms a hydrogen bond with Tyr 143. So it appears that Tyr 143 is important not only for communication between the two domains, but also for binding substrate in the active site (Miles *et al*, 1992).

The positional disorder of the cytochrome domain in subunit two means that the folded chains occupy a number of discrete orientations in the crystal. The first visible residue is Gly 100, and this provides the arbitrary start of the interdomain hinge. Experiments have shown that this hinge regulates interdomain electron transfer from the flavin to the haem (White *et al*, 1993; Sharp *et al*, 1994), and without it, communication between the two independently expressed domains is undetectable (Balme *et al*, 1995). Nmr experiments on the *H.anomala* flavocytochrome b_2 (Labeyrie *et al*, 1988) seemed to confirm that the disordered cytochrome domains were mobile, however this is currently being investigated by way of a disulphide lock, and with nmr experiments on the recombinant *S.cerevisiae* flavocytochrome b_2 (Bell *et al*, 1996). Mutations made to residues buried at the interface suggest that the degree of mobility of the haem domain is small, consistent with a close association rather than a loose tethering (Kay & Lippay, 1993).

1.3.3 Comparison of *S.cerevisiae* and *H.anomala* flavocytochromes b_2

Flavocytochrome b_2 has been isolated from two different sources of yeast: *Hansenula anomala*; and *Saccharromyces cerevisiae*. The *H.anomala*-b_2 enzyme has a higher molar activity than *S.cerevisiae*-b_2, and the rate-limiting steps are also found

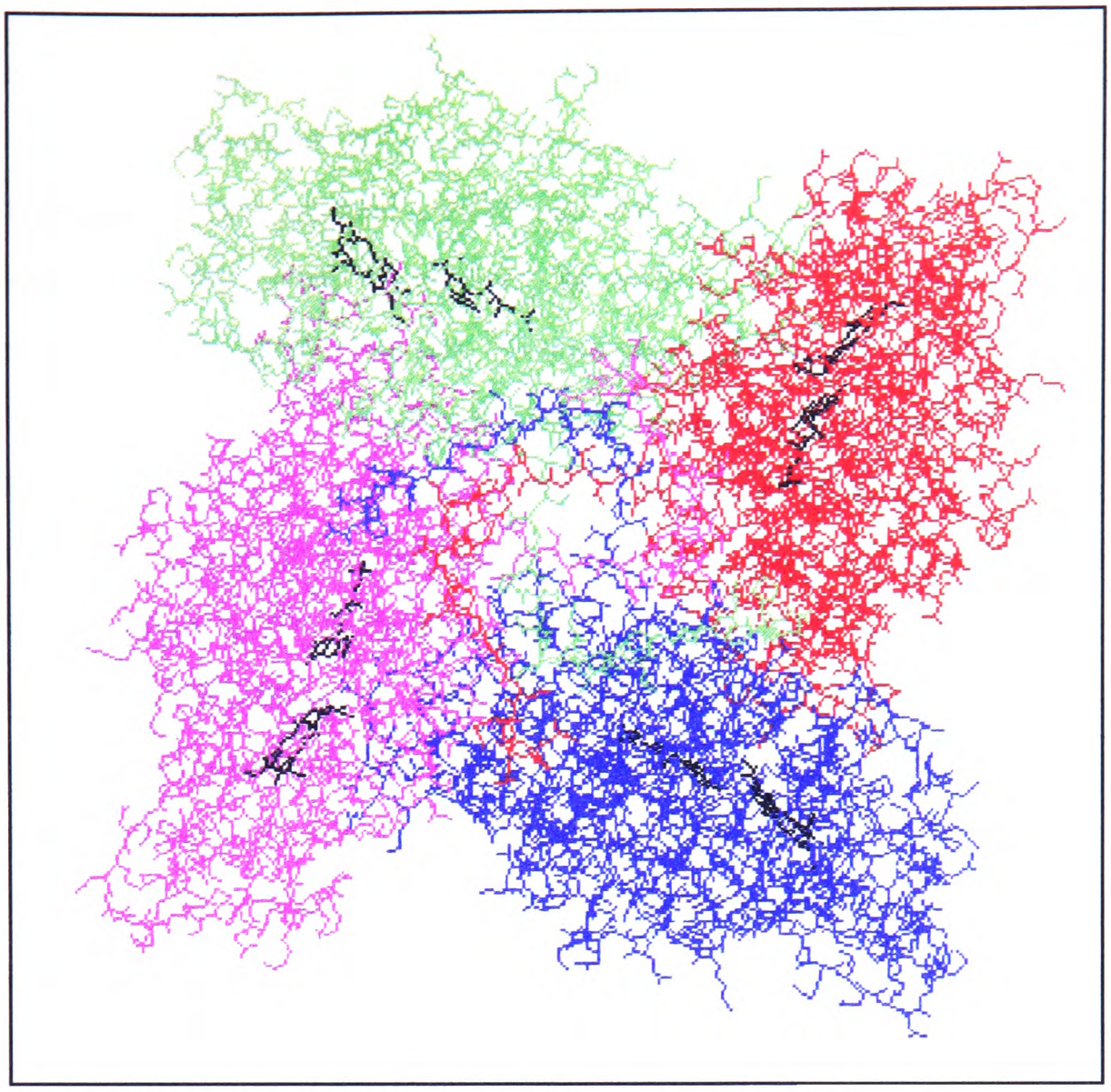

Fig. 1.3.2.1. Top. The Flavocytochrome b_2 tetramer viewed down the pseudo-four fold axis of symmetry. the individual domains are shown in red, blue, magenta and green. The flavin and haem prosthetic groups are shown in black.
Bottom. A single Flavocytochrome b_2 protomer. The flavin domain is shown in green, the cytochrome domain in red. The polypeptide linker is shown in blue, and the C-terminal tail in magenta. The flavin and haem prosthetic groups can be seen in black.

to differ (Capeillere-Blandin *et al*, 1986). The recent structure determination of the *S.cerevisiae-*b_2 and expression of the gene, has led to the production of a plethora of mutant-enzymes used to investigate the structure-function relationship of the enzyme. However, conclusions on function can also be drawn from analogues based on sequence homology. The gene from the *H.anomala* enzyme has been cloned and sequenced (Black *et al*, 1989b), and reveals a 60% homology with *S.cerevisiae-*b_2. All the active site residues thought to be important for catalysis are conserved, as are the residues involved in binding the prosthetic groups. This homology has led to a number of assumptions for the structure of the enzyme from *H.anomala*, for which no crystal structure has been derived. The haem domain is suspected to fold in a similar fashion to *S.cerevisiae-*b_2 (Haument *et al*, 1987), and it is expected that the $\alpha_8\beta_8$ barrel found in *S.cerevisiae-*b_2 will be present in the *H.anomala* structure.

Comparison of the primary sequences of both enzymes reveals that the *H.anomala* enzyme is much more acidic in two specific areas (Black *et al*, 1989): The interdomain hinge and the proteinase sensitive loop. The interdomain hinge in *H.anomala* is shorter and more acidic than the *S.cerevisiae* hinge. This observation has led to mutagenesis experiments on how this affects the kinetics of the enzyme (White *et al*, 1993; Sharp *et al*, 1994), especially on the interdomain electron transfer and on the interaction with cytochrome *c* . The basic proteinase sensitive loop in *S.cerevisiae-*b_2 has also affected the kinetics of the enzyme after mutagenesis (Reid *et al*, 1988). The corresponding area in *H.anomala-*b_2 in contrast is very acidic.

1.3.4 The active site

The flavin prosthetic group is almost completely buried within the flavin binding domain and is stabilised by a number of hydrogen bonds and ionic side-chain interactions, solvent access to it is small. An increased solvent access to the active site, by removal of the cytochrome domain, results in a decreased rate of L-lactate dehydrogenation (Balme *et al*, 1995). The C-terminal tail has also proven to be necessary to retain the structural integrity of the enzyme around the active site, despite the fact that the two are well separated in space (White *et al*, 1989).

In subunit two the reaction product, pyruvate, can be seen at the active site (Fig.**1.3.4.1**). The pyruvate carboxylate is proposed to be stabilised in the active site by Arg376 and Tyr143, and the carbonyl by His373 and Tyr254 (Xia & Matthews, 1990). Leu230 and Ala198 have been shown to restrict the size of the active site of flavocytochrome b_2 and thus confer specificity for the short chain (S)-2-hydroxy acid L-lactate (Daff *et al*, 1994).

The first step in the reaction mechanism is the α-hydrogen abstraction (Miles *et al*, 1992), as illustrated by the deuterium isotope effect of 8.1. There is some debate on how this hydrogen is abstracted: as a proton, or as a hydride (Lederer & Matthews, 1987; Lederer, 1991; Chapman *et al*, 1991). The arguments for the formation of a carbanion, indicating the abstraction of a proton, derive from experiments by Urban & Lederer (1985), and Lederer (1974), but are not entirely conclusive. One problem with the theory that the mechanism goes by way of a carbanion, is that the active site base that is proposed to abstract the α-hydrogen, His373, would have to have a pK_a of 15 which would necessitate a pK_a shift enforced by the protein structure of around 8 pH units. How this would be achieved is not quite clear (Lederer & Matthews, 1987). A hydride mechanism would not involve such a forcing of conditions. The His373 could quite easily remain with a 'normal' value for pK_a, and would abstract the more easily abstractable hydroxyl proton. This would then give rise to a concerted mechanism resulting in a hydride transfer to the flavin N5 position (Fig. **1.3.4.2**).

1.3.5 The Catalytic Cycle

The catalytic cycle has five steps (Fig. **1.3.5.1**). These have been thoroughly examined individually in *S.cerevisiae-*b_2 with experiments on the active site (Daff *et al*, 1994), flavin to haem electron transfer (Chapman *et al*, 1994, 1996; Daff *et al*, 1996b), and in the interaction with cytochrome *c* (Tegoni *et al*, 1993; Chapman *et al*, 1996; Daff *et al*, 1996a).

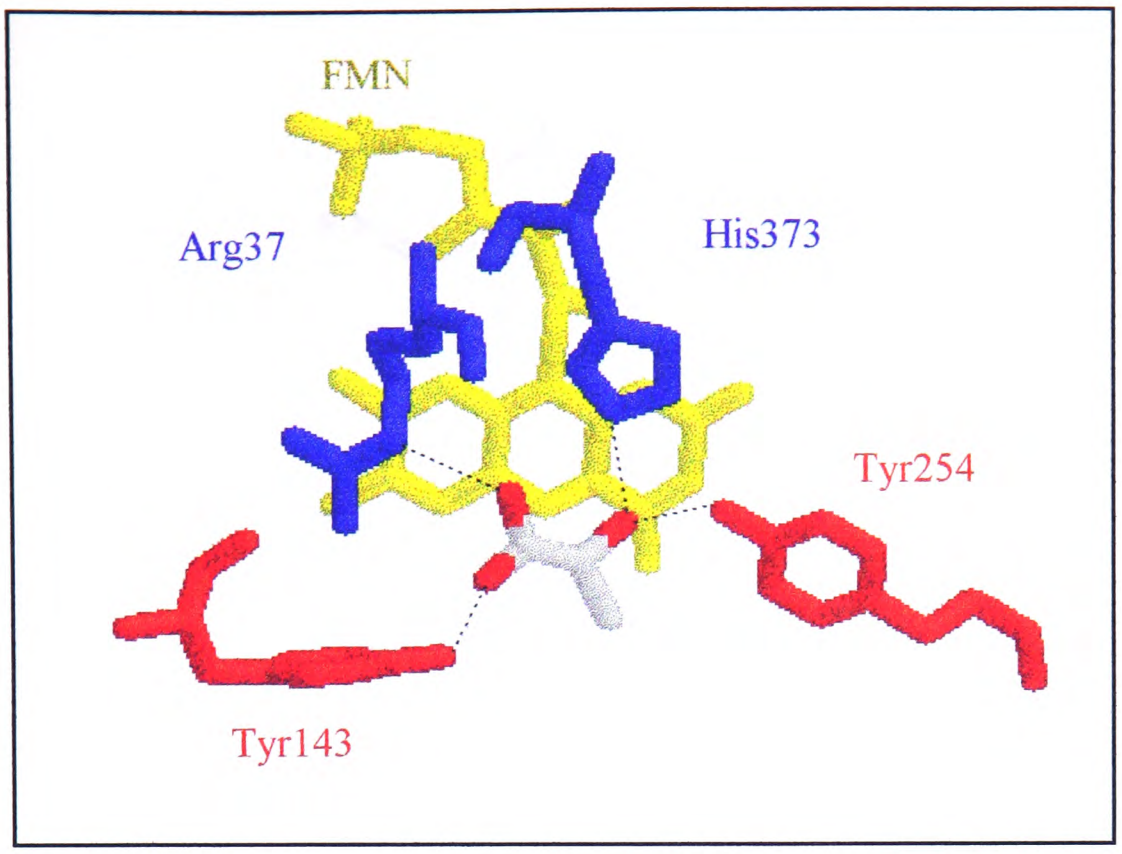

Fig. 1.3.4.1. The active site of flavocytochrome b_2 illustrating the residues that are seen to stabilise pyruvate, shown here in grey and red. For reasons of clarity, the residues that form hydrophobic interactions with the methyl group of pyruvate, Ala198 and Leu230, have been omitted.

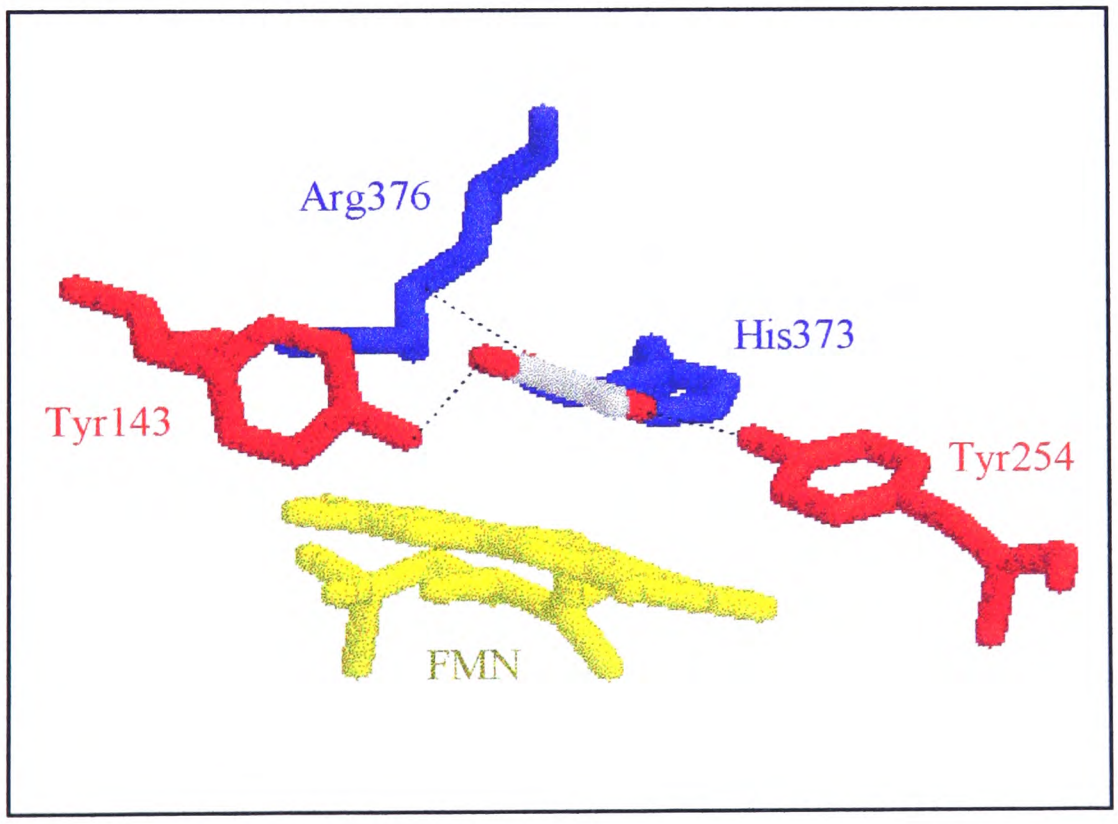

The active site of flavocytochrome b_2 differing from the above view by a 90° rotation. Pyruvate lies parallel to, and 3Å above the flavin.

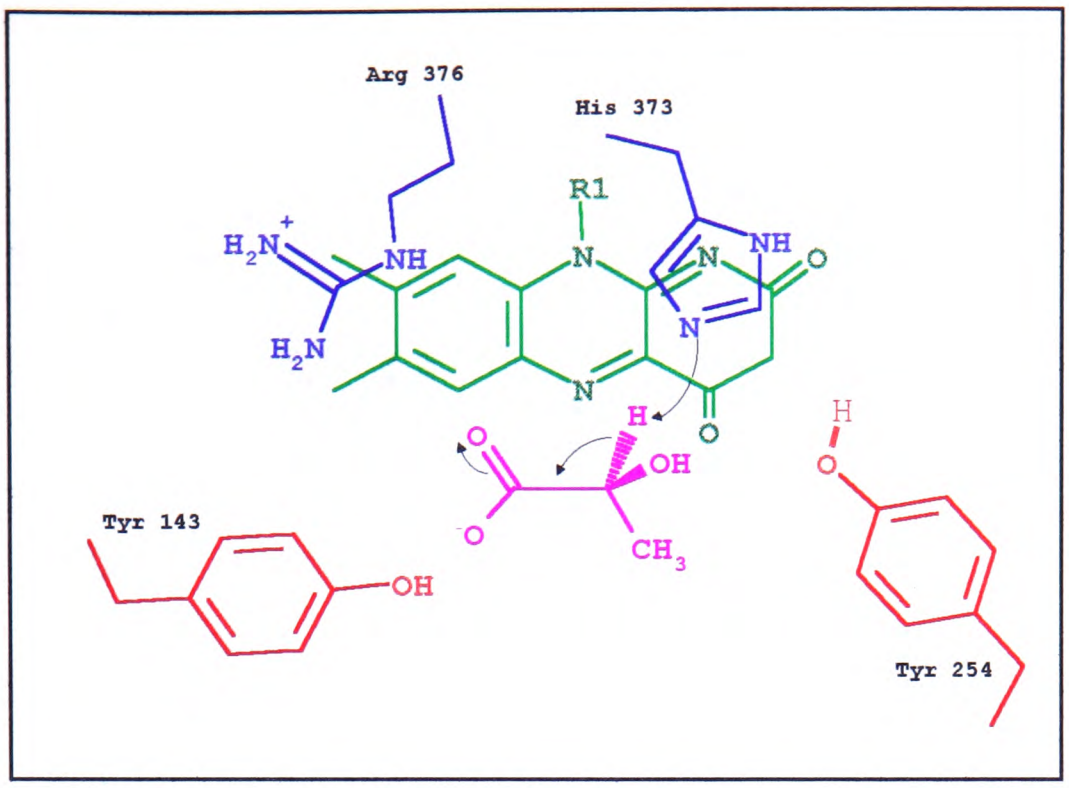

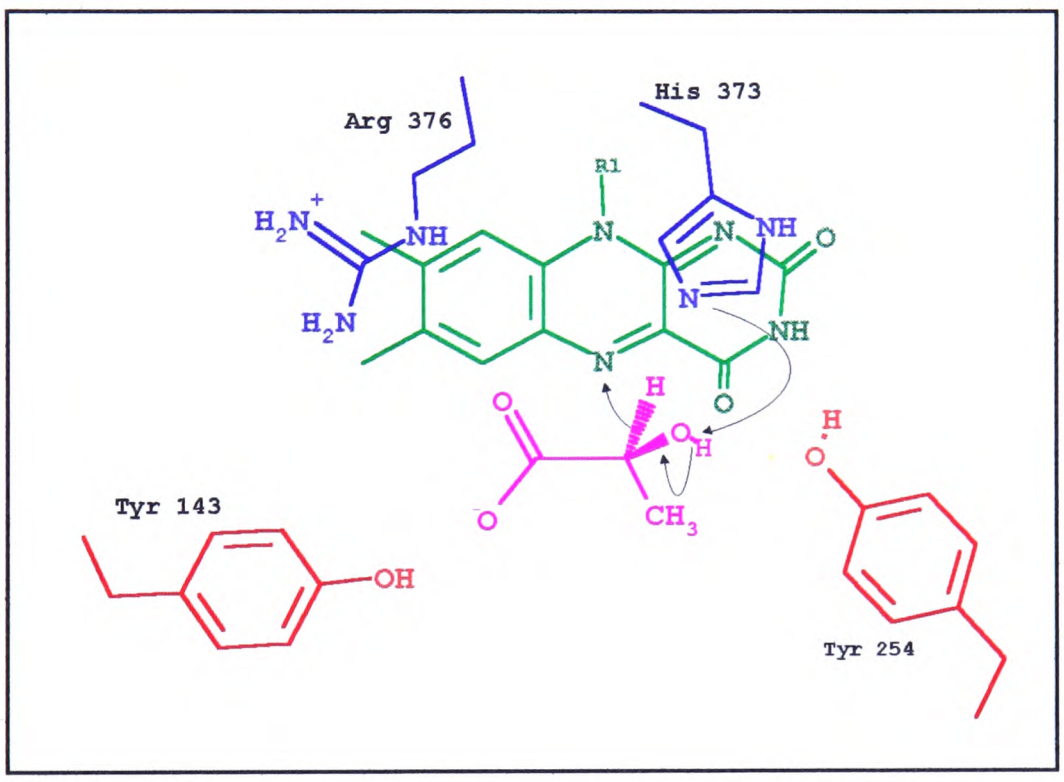

Fig. 1.3.4.2. The two possible mechanisms of L-lactate dehydrogenation, as catalysed by flavocytochrome b_2.
Top. The carbanion mechanism, which results in covalent addition to the flavin N5.
Bottom. The hydride mechanism, which involves a direct hydride transfer to the flavin.

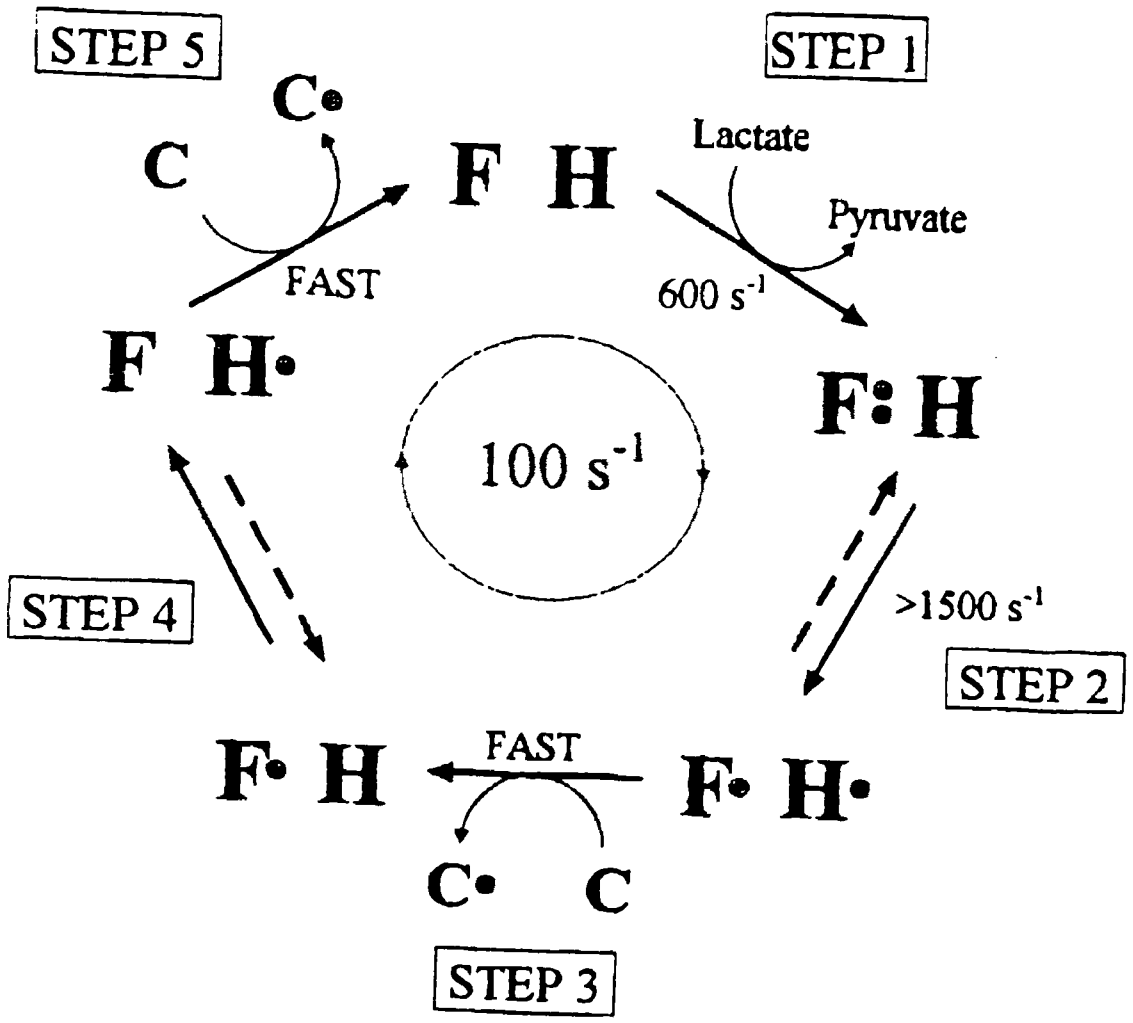

Fig. 1.3.5.1. Model proposed to explain the catalytic cycle of flavocytochrome b_2 based on the individual electron-transfer processes. The action of a single subunit of the enzyme is described as it turns over at its maximum rate of ~$100s^{-1}$ in the presence of saturating amounts L-lactate and ferricytichrome *c*. **F**, FMN; **H**, b_2-haem; **C**, ferricytochrome *c*;●, electron (Daff *et al*, 1996a).

Flavin to haem electron transfer

Flavin to haem electron transfer involves two intramolecular electron transfer steps (Capeillere-Blandin *et al*, 1975; Capeillere-Blandin, 1982): From fully reduced flavin hydroquinone to haem and from flavin semiquinone to haem. In the absence of an electron acceptor the enzyme can accommodate three electrons per protomer, a situation that does not arise during turnover of the enzyme (Capeillere-Blandin *et al*, 1975). Biphasic traces are used to follow the reduction of both flavin and haem domains, and give rates of reduction of $604 \pm 60\ s^{-1}$, and $445 \pm 50\ s^{-1}$ respectively (Miles *et al*, 1992). This value for the reduction of the haem domain is however an approximation, as the haem reduction shows a definite lag behind the flavin reduction, and three steps are shown to be involved (Chapman *et al*, 1994). By taking into account these two factors, a rate of reduction the haem domain by the fully reduced flavin domain can be evaluated to be $\sim 1500 s^{-1}$ (Chapman *et al*, 1994).

The flavin and haem prosthetic groups are separated by ~9.7Å, and lie in approximately in the same plane (Xia & Matthews, 1990). The two domains are joined by a polypeptide linker, without which electron transfer between the two domains does not occur (Balme *et al*, 1995). From the crystal structure two out of the four haem domains are disordered. In subunit one the haem domain is clearly visible and Tyr143 can be seen to be binding to the haem propionate. In subunit two however, the haem domain is not visible and Tyr143 is seen to be stabilising pyruvate, by hydrogen-bonding to the carboxylate. Mutation of this Tyr143 to a phenylalanine (Miles *et al*, 1992) results in a change in the rate determining step from the breakage of the Cα-hydrogen bond in the wild-type enzyme, to haem reduction in the mutant-enzyme. This decrease in the rate of haem reduction is most likely due to the removal of the interdomain hydrogen bond formed between the haem propionate and Tyr143. This theory is corroborated by the fact that flavin to haem electron transfer is decreased at low pH (Chapman *et al*, 1994), probably due to the protonation of the haem propionate that binds to Tyr143.

The interdomain hinge also plays an important part in the regulation of interdomain electron transfer (Balme *et al*, 1995; White *et al*, 1993; Sharp *et al*, 1994). From the crystal structure (Xia & Matthews, 1990) and nmr data (Labeyrie *et*

al, 1988), the haem domain was thought to be mobile with respect to the flavin domain. To test this theory various mutations have been made in the region of the hinge to shorten this polypeptide tether and perhaps restrict mobility. A 'hinge-swap' enzyme was created with the domains from *S.cerevisiae-*b_2, but with the shorter and more acidic hinge from *H.anomala-*b_2 (White *et al*, 1993). More subtle mutations were also produced which introduced 3, 6 and 9 amino acid deletions from the hinge (Sharp *et al*, 1994, 1996). The conclusions from this work showed that the hinge was of little importance for lactate dehydrogenation, but had a great effect on the rate of flavin to haem electron transfer.

Flavin oxidation has also been shown to be inhibited by pyruvate (Daff *et al*, 1996b; Lederer, 1978; Tegoni *et al*, 1984). In binding studies, the flavin semiquinone state is more stabile than the flavin hydroquinone, or the oxidised flavin in the presence of pyruvate (Tegoni *et al*, 1990). The presence of pyruvate not only stabilises the flavin semiquinone but increases the redox potential of the flavin semiquinone by about 100mV (Tegoni *et al*, 1983). This means that the flavin semiquinone rate-limits the catalytic cycle.

1.3.6 The interaction with cytochrome *c*

The formation of a complex between flavocytochrome b_2 and cytochrome *c* is dominated by electrostatic interactions (Capeillere-Blandin, 1982; Daff *et al*, 1996a). Work on the location and nature of the association has been limited mostly to the *H.anomala-*b_2 enzyme, however recent work has been successfully completed for the *S.cerevisiae-*b_2 enzyme. The location of the binding site for cytochrome *c* will be discussed later, however, a brief description of the kinetics will be given here. Studies have been carried out on both the *H.anomala-*b_2 and the *S.cerevisiae-*b_2 forms of the enzyme with respect to their interactions with cytochrome *c*. Due to the higher molar activity of the *H.anomala-*b_2, the reactions are carried out at 5°C, and so a direct kinetic comparison cannot be made.

The specific electron donor to cytochrome *c* is the flavocyochrome b_2 haem domain (Iwatsubo *et al*, 1977; Capeillere-Blandin *et al*, 1980; Balme *et al*, 1995), however, the flavin domain has been shown to contribute a great deal towards the

stabilisation of the complex (Capeillere-Blandin & Albani, 1987; Daff *et al*, 1996a). The fully reduced flavocytochrome b_2 acts as a three electron donor to cytochrome *c*, one electron is provided by the cytochrome domain, and a 'reservoir' of two electrons can be provided to the oxidised cytochrome domain from the flavin hydroquinone. Therefore, pseudo-first order kinetics are still be observed in this bimolecular reaction even when stoichiometric amounts of reactants are used (Capeillere-Blandin, 1982). The cytochrome domain of flavocytochrome b_2 in the course of these experiments has been shown not to exceed 30% oxidation, its 70% reduced state being maintained by the supply of electrons from the flavin domain.

The reaction between flavocytochrome b_2 and cytochrome *c* is proposed to follow a two step process: A reversible association resulting in the formation of a stable complex, which rate limits the electron transfer; and an irreversible electron transfer step. The traces recorded from the reduction of cytochrome *c* can be fitted to single exponentials, indicating that the reaction is controlled by a single rate determining step (Capeillere-Blandin, 1982; Daff *et al*, 1996a), the reversible formation of the complex. The irreversible electron transfer step arises due to the large redox potential difference between the two haems.

In the reaction between *H.anomala*-b_2 and cytochrome *c* the first order rate constant has been measured to be $380s^{-1}$ at 5°C (Capeillere-Blandin, 1982). The corresponding rate of electron transfer, at 25°C, for *S.cerevisiae*-b_2 has been estimated at $>1000s^{-1}$ in the preformed complex (Daff *et al*, 1996a), in approximate agreement with the *H.anomala*-b_2 value. The second-order rate constant for the *S.cerevisiae*-b_2 reduction of cytochrome *c* is $34.8 \pm 0.9\ \mu M^{-1}s^{-1}$ (Daff *et al*, 1996a), which, as has already been discussed, is purely a measure of the rate of association of the two proteins. Investigation into the effects of inhibition revealed a K_d of 8μM (Daff *et al*, 1996a). A residual rate was also observed indicating that the inhibition is only partial and that alternative lower affinity binding sites exist, a finding that is tentatively corroborated by brownian dynamics calculations on the flavocytochrome b_2 monomer (Dr. Sue Brown, Dept. of Biochemistry, University of British Colombia).

2. Materials and Methods

2.1 GROWTH AND MAINTENANCE OF STOCKS

Bacterial stocks.

E.coli TG1 Gibson & Hastings, 1962

E.coli BW313 Kunkel,1985

E.coli growth

All bacteria were grown in standard Luria Broth made from Difco Bacto yeast (5g/l), Difco Bacto tryptone (10 g/l), and sodium chloride (5 g/l), dissolved in dH_2O and autoclaved. Carbenicillin (final concentration, 50µg/ml) was dissolved in dH_2O, sterilised by filtration, and was added to the cool Luria Broth after it had been autoclaved.

'Starter flasks' of Luria Broth, 150ml of Luria Broth in a 250ml flask, were inoculated with a single colony of bacteria selected from an agar plate with a sterile loop. The bacteria were then grown overnight at 37°C on an orbital shaker at approximately 180rpm. Larger flasks, 500ml of Luria Broth in a 1l flask, were then inoculated with 1ml from the starter flask showing the best expression of flavocytochrome b_2.

Storage of bacterial cultures

For long term storage, approximately 1ml of bacterial culture was stored at -70°C with 20% glycerol in a labelled eppendorf. Cultures streaked onto agar plates (Luria Broth mixed with the same volume of 15g/ml Difco Bacto agar, with the appropriate amount of sterilised carbenicillin) were used for short term storage of up to 2 weeks.

2.2 SOLUTIONS.

2.2.1 DNA manipulation

TE buffer

tris/HCL	10mM
EDTA	1mM

10 x TBE

Tris base	108g/l
Boric acid	55g/l
0.5M EDTA pH 8.0	40ml

10 x loading buffer

0.25% Bromophenol blue

15% Ficoll 400

DNA sequencing gel (6% acrylamide)

	per 60ml
Urea	25.2g
Protogel (30% acrylamide; 0.8% bis-acrylamide)	12 ml
10 x TBE	6 ml
dH_2O	to 60 ml
10% Ammonium persulphate	140 µl
TEMED	140 µl

All reagents, except APS and TEMED were mixed thoroughly. APS and TEMED were added immediately prior to pouring the gel.

2.2.2 Protein buffers

0.1M purification buffer

0.2M K_2HPO_4 solution (~600ml) is titrated against 400ml of 0.2M KH_2PO_4 solution to pH 7.0, with 5mM L-lactate, and 1mM EDTA. The final volume is 2l.

10mM Tris/HCl buffer, pH 7.5 (I 0.10)

NaCl	5.265g/l
1M HCl	10ml
dH_2O	to 1l

adjusted to pH 7.5 with Tris base.

2.3 SUPPLIERS

Enzymes

T_4 DNA ligase, restriction endonucleases, T4 polynucleotide kinase and the Klenow fragment of DNA polymerase were obtained from Gibco-BRL, Paisley, UK. Lysozyme and pancreatic ribonuclease A were obtained from Sigma. The ribonuclease was boiled for 10 minutes to remove any DNAse activity before use. Sequenase™ was obtained from the United States Biochemical Corporation, Cleveland, Ohio.

General laboratory chemicals

Sigma chemical company, Poole, Dorset. Or BDH, Poole, Dorset.

2.4 DNA MANIPULATION

2.4.1 Plasmids

	Description and use	Reference
pGR401	phagemid/yeast shuttle vector	Reid *et al* (1988)
pDS6	transcriptional vector	Black *et al* (1989a)

2.4.2 Oligonucleotide primers

Primers used to sequence the flavocytochrome b_2 gene

Sequence 5'-3'	Name	Priming position relative to the start of flavocytochrome b_2 presequence coding region.
CTGCACAATATTTCAAGC	102A	primes in ADH promoter
TAGACAACAAGCCGAA	EIK	233to 248
CTACCAAATATGCCAGGTGGG	H43M	358 to 378
TCCTCCTTTTGCTCCTTG	Y97F	522 to538
AATGCGTATCATAGG	$b_2$730	715 to 729
CCAACTATTTGTTAACTC	Y254F	993 to 1009
GGTCCAAAATCGATGAAG	Cla 1155	1147 to 1164
GTTATCAGAGGTGTTCAA	K349R	1279 to 1296
CTTGAAAGCTTTATGTCT	Hind 1500	1494 to 1511

Oligonucleotides used for mutagenesis reactions

ATGCCTCCT(A,C)AACTTGTCTG	E91K/Q	501 to 520
GTTATCAAGGCTAATGCCGG	F52A	386 to 405
TGCTATTTTTAAACCATTACATG	E63K	417 to 439
CCTAATGTCATCAAGAAGTATAT AGCTCC	D72K	442 to 470
CATGTTCCCCCRAGGAAATTATTR AAGCAGCACCC	E236K/E240K	935 to 969
TAACAAGCCCRAKRAKTGTTGGGTTG	D23K/D24K	297 to 322
TACGTATACAAGTTAACGCGA	D35K	334 to 354

An underlined base indicates the position of a base-pair mismatch with the flavocytochrome b_2 gene. R denotes a purine base and K denotes a G or a T.

The close proximity of the nucleotide bases coding for D23 and D24, as well as for E236 and E240 enabled a mix of oligonucleotides to be used, capable of a double mutation as well as either individual single mutation. The mutant-enzymes that were eventually constructed and expressed were D35K, E63K, D72K, E236K and E240K.

2.4.3 Transformation and selection procedures

Preparation of competent cells

5ml of Luria Broth, inoculated with culture strain BW313 or TG1, was grown overnight to stationary phase. 2ml of this was then added to 100ml of fresh media, and shaken until its optical density at 600nm was 0.3 exactly. This took approximately 1.5 to 2 hours. The cells were then spun down at 10 000 rpm for 5 minutes in sterile tubes at between 0 and 5°C. The supernatant was poured off, and the pellets were collected and resuspended in a total volume of 50ml cold, sterile 100mM calcium chloride. The solution was then spun again, in the cold, the pellets were collected and resuspended in a total volume of 10ml of 100mM calcium chloride. The cells were then stored in this state with 20% glycerol at -70°C.

Transformation of E.coli

One eppendorf of competent cells was taken from the frozen stocks and allowed to defrost slowly on ice (Once thawed, any left over cells should not be re-frozen for a second use). Between 2 and 5µl of DNA from the mutagenesis reaction was then added to 200µl of competent cells, which were then mixed thoroughly and left on ice for 30minutes. The cells were heat shocked for 1.5 to 2 minutes at 42°C, and left on ice for 5 minutes. 1ml of Luria Broth was added, and the mixture was left incubated with shaking for 1 hour at 37°C. The cells were then spun down and all but approximately 150µl of the supernatant was removed. This was used to resuspend the

cells so they could be spread onto an agar plate with the appropriate antibiotic. The plates were then left incubated overnight at 37°C.

2.4.4 Preparation and isolation of DNA

Isolation of plasmid DNA from E.coli

5ml of cells grown overnight at 37°C were spun down and the pellet resuspended in 0.1ml TEG, and transferred to a 1.5ml centrifuge tube. 0.2ml of 0.2M NaOH with 1%SDS was added to the mixture which was then vortexed and left on ice for 5 minutes. 0.15ml of 3M sodium acetate, pH 5, was added to the solution which was mixed by inversion, and left on ice for 5 minutes before being spun for 10 minutes in the cold. The supernatant was then removed carefully and extracted with 0.5ml of a 1:1 phenol:chloroform solution. The aqueous phase was then extracted with 0.5ml of Chloroform. To precipitate the DNA, 0.9ml of ethanol was added to the aqueous phase, which was placed at -20°C for 30 minutes. The DNA was precipitated after spinning for 10 minutes at 4°C, the pellets were dried and finally resuspended in 50µl of TE.

Preparation of single stranded DNA

The *E.coli* host containing the respective plasmid-borne flavocytochrome b_2 gene was grown up overnight to stationary phase. 200µl of this culture was used to inoculate to 5ml of fresh medium with ampicillin (100µg/ml) and grown to mid-log phase (an optical density at 600nm of between 0.5 and 0.8). 2ml of this culture was then removed and incubated for 1 hour with 1µl of helper phage M13K07, multiplicity of infection ≥10:1 (Vieira & Messing, 1987). After 1 hour, 400µl of the infected cells were inoculated with 10ml of Luria Broth, containing ampicillin (100µg/ml) and kanamycin (70µg/ml), and were shaken with good aeration overnight at 37°C.

The *E.coli* host BW313 was used for the production of uracil incorporated DNA template for use in mutagenesis.

Isolation of single stranded DNA from E.coli

For a standard preparation of single stranded DNA for use as a template for mutagenesis, six 1.5ml centrifuge tubes were filled with culture, prepared as above, and spun for 5 minutes. The resulting supernatant was then added to 0.3ml of 2.5M NaCl with 20% PEG 6000 in a fresh, sterile eppendorf mixed well by inversion, and was left for 15 minutes at room temperature. The tubes were then spun for five minutes and all traces of residual supernatant removed. Then the pellets were suspended in 0.1ml of TE buffer and extracted against 50µl of phenol. The upper aqueous layer was removed to fresh tubes, extracted with 0.5ml of chloroform, spun again, and the upper aqueous phase retained. 10µl of Na acetate (pH 5.5), and 250µl of ethanol were then added to precipitate the single stranded DNA after being left at -20°C for 1 hour. The DNA pellets were then dried, and finally dissolved in a total volume of 50µl TE, and stored between 0 and 5°C.

2.4.5 Gel electrophoresis of DNA

Agarose gel electrophoresis of DNA

To monitor the amount of DNA after each step of the mutagenesis, it was analysed on a 0.8-1% BRL electrophoresis grade agarose gel containing 0.5µgml^{-1} ethidium bromide. The buffer used throughout was 1 x TBE. The DNA samples were mixed with 1 x loading buffer, and loaded into the horizontal wells created in the gel. Bacteriophage λcI857 DNA, restricted with HindIII, was used for size markers.

Recovery of DNA from agarose gels

An ideal way to separate DNA fragments after a digest with restriction enzymes is to run an agarose gel with ethidium bromide. The degree of separation of the fragments can be seen under a UV lamp, and the desired fragment can be cut out. To extract the DNA from the gel Geneclean™ was used. The required fragment of DNA was cut from the gel and weighed, and the appropriate amounts of TBE modifier and 6M NaI were added. The agarose was dissolved in this solution by heating to 55°C for 5 minutes with occasional mixing. The solution was then cooled on ice and treated with 5µl of 'glass milk' (a silica matrix suspended in water). The mixture was

thoroughly mixed and kept on ice to get as much DNA to bind to the silica as possible. The silica was then pelletted by centrifugation, the supernatant was poured off but was not discarded and the pellet was washed three times with 500µl of 'New wash' (NaCl/ethanol/water mix). After the final wash, the silica was dried thoroughly and the DNA was eluted with 10-20µl of TE buffer at 55°C. The recovery checked qualitatively by running 1-2µl on an agarose gel.

2.4.6 Digestion and ligation

Cleavage of DNA with restriction enzymes

All restriction enzyme digests were performed using BRL enzymes and buffers. DNA (0.1 to 20µg) was cut using the appropriate restriction enzymes dissolved in 10-200µl of the specified 1x 'react' buffer for 2-8 hours at the appropriate temperature, usually 37°C.

Ligation of DNA ends

50-100ng of vector was incubated with an excess of insert fragment in 1x ligation buffer (10mM Tris/HCL pH 7.2; 1mM EDTA; 10mM $MgCl_2$; 10mM DTT; 1mM ATP) with 10 units of T_4 DNA ligase. The reaction was made up to a final volume of 10µl and was incubated overnight at 16°C.

2.4.7 Site-directed mutagenesis

This was performed by the method of non-phenotypic selection, adapted from Kunkel (1986). The oligonucleotides used are listed in section **2.4.2,** along with the appropriate priming positions on the flavocytochrome b_2 gene sequence. The mutants that I was unable to construct within the allotted time were D23K, D24K and the double mutants D23K/D24K, and E236K/E240K.

Phosphorylation of the Oligonucleotide:

Reaction mix:

200 pmol oligonucleotidein a volume of 23µl	
1M Tris/HCl pH 8.0	3µl
0.3M $MgCl_2$	1µl
0.1M DTT	1.5µl
20mM ATP	1.5µl
5 units Polynucleotide kinase	0.5µl

The reaction mix was incubated at 37°C for 45 minutes and then heated to 68°C for 10 minutes to inactivate the enzyme and stop the reaction. The phosphorylated enzyme was used immediately.

Mutagenesis

Annealing:

Single stranded (Uracil incorporated) DNA template	
from a standard miniprep (ca.0.5-1pmol).	5µl (in TE)
Phosphorylated oligonucleotide (from above: ca.4pmol)	0.6µl
0.2M Tris/HCl, pH7.5	3.5µl
dH_2O	7.9µl

The annealing mix was incubated at 70°C for 3 minutes and then allowed to cool to 4°C over 30 minutes, and was finally placed on ice.

Extension/Ligation

To the annealing mix add:

100mM $MgCl_2$	5µl
0.9mM of each dNTP(for a final concentration of 40µM)	4 x 2µl
50mM ATP	1µl
0.1M DTT	2µl
dH_2O	15µl
Total volume	48µl

3 units of Klenow fragment of DNA polymerase	0.5µl
3 units of T_4 DNA ligase	1µl

The mixture was then incubated at 16°C for 20 hours.

In order to test the efficiency of the extension/ligation reactions, a 5µl volume of the SDM reaction mix was electrophoresed in a 1.5% agarose gel alongside single and double stranded pGR401 as controls. If the reaction product DNA co-migrated with the double stranded DNA and not the single stranded DNA, the reaction was considered a success, and 10µl was transformed into *E.coli* TG1 competent cells as described in section **2.4.3**. Potential mutants were screened directly by DNA sequencing of single stranded DNA extracted from a 5ml overnight growth of the colonies resulting from the transformation.

2.4.8 Sequencing of single stranded DNA

Sequencing of DNA was carried out using the Sequenase™ Version 2.0 kit (United States Biochemicals), which uses the dideoxy chain termination method. The flavocytochrome b_2 gene was sequenced using a combination oligonucleotide primers listed in section **2.4.2**.

The appropriate sequencing primer (1µl of 3 ng/µl^{-1}) was annealed to 7µl of template DNA (approximately 1µg DNA) with 2µl of 5 x reaction buffer (200mM Tris/HCl, pH 7.5; 100mM $MgCl_2$; 250mM NaCl) by heating to 65°C for 2 minutes, then being cooled slowly to below 37°C over 30 minutes. Extension from the annealed primer was carried out by adding 1µl 0.1M DTT, 2µl dGTP label mix (a 1 in 4 dilution of 7.5µM dGTP, dCTP, dATP, dTTP), 0.5µl α-[^{35}S]-dCTP (400 Ci/mmol) and 2µl of diluted sequenase™ (a 1 in 8 dilution of sequenase at 13units µl^{-1} in 10mM Tris/HCl, pH 7.5; 5mM DTT; 0.5mgml^{-1} BSA). The extension mixture was left at room temperature for 2-5 minutes. Further extension and termination was performed by dispensing 3.5µl of extension mix into 4 tubes preheated to 37°C containing 2.5µl of one of the four termination mixes:

ddGTP mix 80µM dNTPs; 8µM ddGTP; 50mM NaCl

ddATP mix 80µM dNTPs; 8µM ddATP; 50mM NaCl

ddCTP mix 80µM dNTPs; 8µM ddCTP; 50mM NaCl

ddTTP mix 80μM dNTPs; 8μM ddTTP; 50mM NaCl

The termination reaction was allowed to proceed at 37°C for 5 minutes and the reaction was stopped by the addition of 4μl of stop solution (95% formamide; 20mM EDTA; 0.05% bromophenol blue).

Sequencing reactions were denatured at 75°C for 3 minutes, loaded onto a 6% polyacrylamide gel, and electrophoresed in a 1 x TBE buffer at 65 watts for 1hour 45 minutes as standard. The gel was fixed in a 10% acetic acid, 45% methanol (v/v) aqueous solution, and dried under vacuum at 80°C for 1hour. The gel was then autoradiographed overnight at room temperature.

2.5 PURIFICATION OF FLAVOCYTOCHROME b_2

Growth and harvesting of E.coli cells over-expressing flavocytochrome b_2

Single bacterial colonies were taken from an agar plate, and were initially grown separately in 150ml of Luria Broth inoculated with 50μgml^{-1} of carbenecillin and shaken at 180-200rpm overnight at 37°C. 1.5ml from each flask was then spun down in a micro centrifuge, and the tube containing the most pink cells, ie. the flask showing the greatest over-expression of flavocytochrome b_2, was selected for large scale growth. Typically 6 x 1l flasks, each containing 500ml of Luria Broth at 50μgml^{-1} carbenecillin, were each inoculated with 1ml of bacteria from the initial growth and grown overnight as before.

Bacteria were harvested by centrifugation using a GSA rotor in a Sorvall RC-5B centrifuge at 10 000rpm for 5 minutes at room temperature. The resulting wet pellets of cells were collected together and stored in sterilin tubes at -20°C until use.

Cell lysis

To extract the crude protein from the cell, one tube of frozen cells were first dissolved in 250-300ml of 0.1M Phosphate buffer containing L-lactate, EDTA and a spatula amount (approx. 50μg/ml) of lysozyme. The EDTA was used to chelate ions released upon cell lysis, and the lactate was to keep the protein in its more stable reduced form. The mixture was left stirring for at least two hours to ensure efficient lysis. To check the extent of the lysis, 1ml of the mixture was extracted and micro

centrifuged. If the pellet was still slightly red, more lysozyme was added and the mixture left for another hour. If the use of lysozyme had no effect, a second option was to use sonication.

After cell lysis, the solution was centrifuged using an ss34 rotor at 18 000rpm for 10 minutes at between 5 and 10°C. The resulting supernatant should be red in colour and quite viscous.

Ammonium sulphate fractionation

By increasing the salt concentration of a solution one can selectively precipitate proteins, above a certain concentration, using centrifugation. By taking the supernatant to 40% ammonium sulphate saturation a varying amount of protein impurity was removed from solution. When the supernatant was adjusted to 70% ammonium sulphate saturation, flavocytochrome b_2 precipitated. When collected together, the pellets were dissolved in the minimum amount of 0.1M phosphate buffer ready for dialysis.

Dialysis

Seamless dialysis tubing with a molecular weight exclusion limit of 12kDa was used for dialysis. Before use it was washed thoroughly with 0.1M phosphate buffer. The 70% ammonium sulphate cut of flavocytochrome b_2 was then poured into the dialysis tubing, with a sufficient gap at one end to allow for expansion. The protein was dialysed against 2l of 1/2 strength phosphate buffer overnight, and was kept between 0 and 5°C whilst being continually bubbled with nitrogen. This process is a gentle way of reducing the ionic strength by removing the ammonium sulphate so that an efficient purification will follow. After dialysis the protein was spun at 18 000rpm for 10 minutes in the cold to precipitate any insoluble impurities.

Column chromatography

DE-52

After the overnight dialysis, the protein was loaded onto an ion exchange Whatman DE-52 column. This column consists of diethyl-aminoethyl groups

covalently cross-linked to a cellulose matrix. The column was prepared by first equilibrating the chromatographic material with an excess of 0.1M phosphate buffer. The pH was then adjusted to 7.0 with the addition of 1M HCl. The material was then allowed to settle, and the supernatant was poured off and replaced with fresh buffer. The pH was checked again, and the column was poured. A typical column length was about 2.5cm x 10-15cm. Flavocytochrome b_2 does not bind to this column, and so runs straight through. The column itself acts as a filter. What was left at the top half of the column was a loose broad green/yellow band of impurities. The flavocytochrome b_2 eluant was collected and loaded onto a hydroxyapatite column.

Hydroxyapatite

Hydroxyapatite (BIO-RAD) is the crystalline form of $[Ca_5(PO_4)3OH]_2$. Bound proteins are eluted by increasing the salt concentration of the eluant by the addition of ammonium sulphate.

The column was equilibrated by repeated washing in a large volume of phosphate buffer. Two or three washes were usually sufficient. A column was then poured, of typical dimensions 3cm x 6cm. The eluant from the DEAE-52 was loaded straight away. Flavocytochrome b_2 bound in a tight red band at the top of the column. The column was then washed with buffer and spectra of the eluant were taken from 700nm to 250nm. The washing was repeated until the peak at 269nm disappeared. Once this had happened, an ammonium sulphate gradient was started. Flavocytochrome b_2 started to elute at around 8% and fractions were collected. The purest fractions, the ones with the smallest 269/423 peak height ratio were pooled together and precipitated at 70% ammonium sulphate. A 100% pure sample of flavocytochrome b_2 will have a 269/423 peak height ratio of 0.5.

For short term storage the pure flavocytochrome b_2 was refrigerated as a 70% ammonium sulphate pellet under nitrogen. For long term storage however, the 70% pellet was redissolved in a minimum amount of 0.1M Tris/HCl, pH 7.5, and was passed down a gel column to be oxidised and stored in liquid nitrogen.

G25

Gel filtration is used to separate species of different molecular weights. The resolution of this separation depends on the pore size of the column material. A G25 column will retard elution of material between 1 and 5kDa, as molecules of this size will have to travel through the pores of the column particles. Molecules larger than this will not be retarded, and are able to pass around the exterior of the column particles.

The G25 was equilibrated by washing with 0.1M Tris/HCl, pH 7.5, *I* 0.1. A large volume of buffer was needed to allow for the expansion of the gel material. When flavocytochrome b_2 was passed through the column, the lactate and ammonium sulphate were retarded by the gel pores. The protein then changed colour from a reduced red to an oxidised orange colour. On elution the concentration was measured along with the purity, and the protein was stored in 0.5ml or 1ml aliquots under liquid nitrogen indefinitely.

Regeneration

Hydroxyapatite was regenerated by washing with one column volume of 1M NaCl, and then with phosphate buffer to re-equilibrate. DEAE-52 had to be washed first with one column volume of 1M HCl, then with 1M NaOH, then with two column volumes of water. It was then returned to its original pH by repeated washing with 0.1M phosphate buffer. These two columns were used a maximum of three times, and different columns were used for each mutant enzyme. The gel can easily be regenerated by washing with a few column volumes of the buffer of choice.

Modification of the procedure for the preparation of the mutant enzymes

The mutant enzymes that did not purify in the same way as the wild-type enzyme were E63K, D72K, and the double-mutant E63K:D72K. E63K did not lyse as easily as the wild-type enzyme, and a small amount precipitated after the overnight dialysis. As a consequence the cells were lysed for up to 4 hours, and the preparation was continued as for the wild-type.

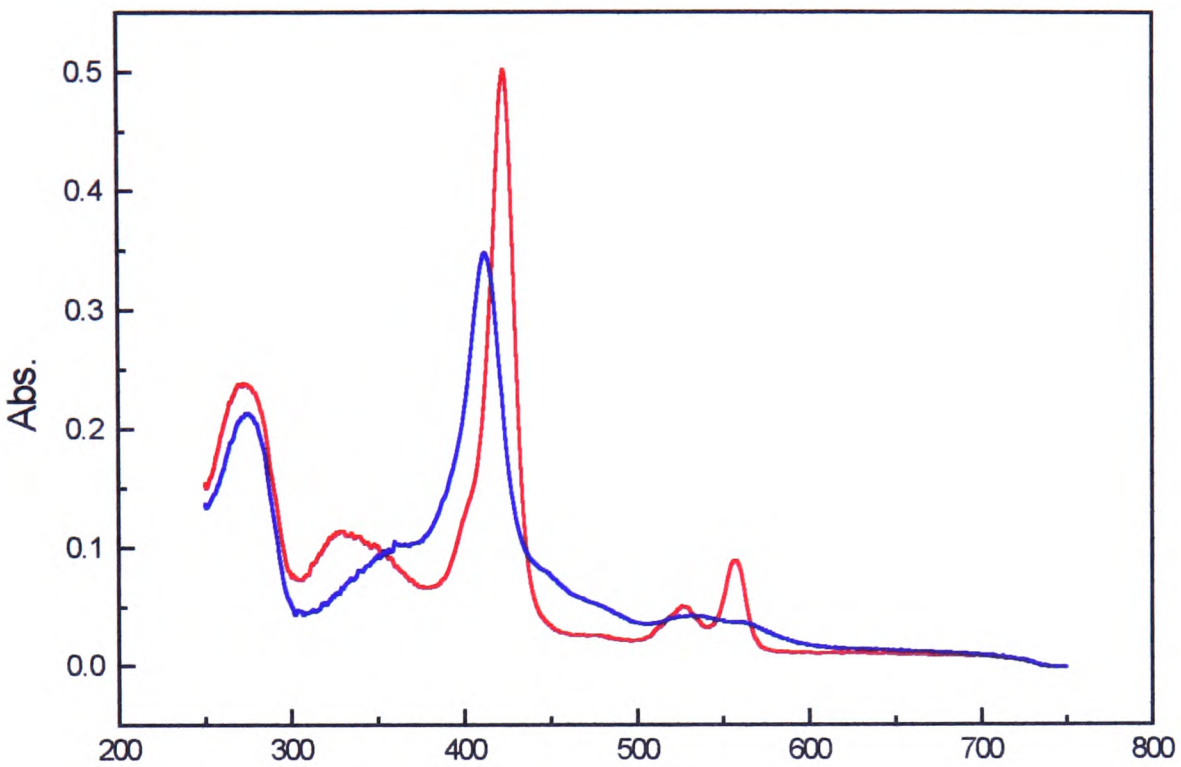

Fig.2.5.1. Oxidised (blue) and reduced (red) spectra of flavocytochrome b_2.

D72K did not lyse with lysozyme, instead the cells had to be sonicated. A 30% ammonium sulphate cut was not taken, but the protein was precipitated directly with 70% ammonium sulphate. After the overnight dialysis the protein was diluted about three fold, and was loaded onto a hydroxyapatite column, and the purification continued as with the wild-type. The protein was not spun after dialysis to avoid the partial precipitation.

Purification of the double mutant enzyme also deviated from the standard preparation. Again the cells were sonicated to extract the protein. When the cells were broken open there was a great deal of cell debris released. The cells are spun at 18, 000 rpm for 10 minutes, and the precipitate was discarded. The solution was then added to a small amount of hydroxyapatite that had been already equilibrated in phosphate buffer. This was left stirring for 10-15 minutes in the cold, then the hydroxy-apatite was allowed to settle. The murky supernatant was poured off, and the remaining red hydroxyapatite was washed with buffer. It was then poured onto an existing hydroxy-apatite column to be purified with washing and an ammonium sulphate gradient.

2.6 STEADY-STATE KINETIC ANALYSIS

All experiments were performed at 25 ± 0.1°C in 3ml quartz cuvettes with a 1cm path length, using either a Beckman DU62, or a Shamadzu 2102PC spectrophotometer. Tris/HCl buffer was used for all experiments (See section **2.2.2**).

ferricyanide

Assays were carried at 1mM ferricyanide, and a varying concentration of L-lactate to determine k_{cat} and K_m parameters. The activity was monitored by recording the rate of decrease in absorbance at 420nm as the ferricyanide was reduced. A ferricyanide extinction coefficient of $\Delta\varepsilon_{ox\text{-}red} = 1010 M^{-1}cm^{-1}$ was used.

Cytochrome c

Horse heart cytochrome *c* (type VI Sigma) was used at a saturating concentration of around 50μM for all the mutant enzymes. The cytochrome *c* used was always freshly dissolved in Tris/HCl buffer, and its concentration determined by measuring the reduced spectrum between 650nm and 500nm. The extinction coefficient at 550nm for reduced cytochrome *c* is $30{,}900M^{-1}cm^{-1}$. The assays were monitored at 550nm, and the rate for cytochrome *c* reduction was calculated using the extinction coefficient of $\Delta\varepsilon_{ox\text{-}red} = 22, 640M^{-1}cm^{-1}$.

Flavocytochrome b_2

All flavocytochrome b_2 concentrations were determined using the reduced spectrum taken from 700nm to 250nm. The Soret peak at 423nm has an extinction coefficient of ε_{red}=$183, 000M^{-1}cm^{-1}$.

2.7 STOPPED-FLOW KINETIC ANALYSIS

All pre-steady-state kinetic experiments were performed on an applied photophysics SF.17 Micro Volume stopped flow fluorimeter. Data were collected and analysed using non-linear regression analysis on the SF.17MV software package.

'Super-steady-state' reduction of cytochrome c

The steady-state reduction of cytochrome *c*, as described in the previous section, involves monitoring many assays at differing concentrations of cytochrome *c* typically up to a saturation concentration of 50μM, or a constant concentration of cytochrome *c* is used with a varying amount of lactate. This is not only time consuming, but uses a great deal of cytochrome *c*. A different way to measure the same constants, k_{cat} and K_m, has been investigated.

A 2-3ml solution of oxidised cytochrome *c* was made up to a concentration of 30μM. Flavocytochrome b_2 wild-type enzyme was made up to exactly about 0.1μM in 10mM L-lactate. All solutions were dissolved in Tris/HCl, pH 7.5, *I* 0.1, and at a temperature of 25°C. This gave reaction concentrations of ~15μM cytochrome *c*,

which when reduced will reach the practical limit for total absorbance using the stopped-flow apparatus, and ca. 0.05μM flavocytochrome b_2. The wavelength to monitor the reaction is 550nm, the usual wavelength for a cytochrome *c* steady-state experiment. The reactants were rapidly mixed together in the stopped-flow, and 1000 points were recorded over a time base of 5 seconds (as opposed to 10-20 individual points being recorded for a few minutes each). A few traces were collected and averaged. The data were then analysed on Microcal 'Origin'. A corresponding 'conventional' assay was carried out with ferricyanide to check the enzyme had full activity.

This first trace recorded represents the reduction of cytochrome *c* from fully oxidised to an approximately fully reduced state. A baseline is taken from the maximum absorbance, ie. where there is the greatest amount of **reduced** cytochrome *c*. This is when the gradient tends to zero, and the rate is slowest. This will give an approximation of when the concentration of **oxidised** cytochrome *c* is zero. The end-point is tricky to define, and as a consequence, the Michaelis-Menten curve will not go exactly through the origin. When this first trace is differentiated, a plot of rate (Absorbance per second) *vs.* time (seconds) is derived.

The differential plot represents the rate of reduction of cytochrome *c*, measured in absorbance change per second, at a concentration of oxidised cytochrome *c* defined by the time after the beginning of the reaction. Therefore, the absorbance needs to be quantified with respect to the amount of oxidised cytochrome *c*, and by the amount of flavocytochrome b_2 used to reduce it. This is done by dividing the baselined absorbances before differentiation, by the oxidised-reduced extinction coefficient for cytochrome *c* ($\Delta\varepsilon_{ox\text{-}red}$ = 22, 640$M^{-1}s^{-1}$) to give the oxidised cytochrome *c* concentrations. The differential values are also divided by the cytochrome *c* oxidised-reduced extinction coefficient, and then the exact flavoctochrome b_2 concentration, to give a rate of cytochrome *c* reduction per second per flavocytochrome b_2. The rate is then plotted against the concentration.

The result gives, to a good approximation, the rate of turnover of the enzyme and the dissociation constant, with the use of very little enzyme. The only problems arising from this experiment are that there will be slight inhibition when the reaction

is nearing completion ie. when the concentration of the reduced protein is large. This is also the end-point of the reaction, and therefore defines the beginning of the Michaelis-Menten plot. The plot therefore does not go exactly through the origin (fig. **2.7.2**).

Oxidation of L-lactate

All experiments were carried out in Tris/HCl, pH 7.5, I 0.1 buffer at 25 ± 0.1°C. Flavin reduction was monitored at 438.3nm, a haem isosbestic point. Haem reduction was monitored at the flavin isosbestic point of 557nm. Oxidised flavocytochrome b_2 was used directly after thawing from the liquid nitrogen.

Pre-steady-state reduction of cytochrome c

The pre-steady-state reduction of cytochrome *c* was carried out under pseudo-first order conditions in Tris/HCl, pH 7.5, I 0.1M buffer at 25 ± 0.1°C. The flavocytochrome b_2 isosbestic point 416.5nm was used to monitor cytochrome *c* reduction. 544.8nm was used for higher concentrations of protein.

Flavocytochrome b_2 was taken from storage in liquid nitrogen and allowed to defrost slowly. The concentration was measured, and the oxidised flavocytochrome b_2 stock solution could be diluted into 2ml reaction solutions ranging from 4μM to 20μM, all at 20mM L-lactate. The oxidised cytochrome *c* solution was made to 2μM. This meant that the reaction concentrations always involved an excess of flavocytochrome b_2 (2-10μM) reacting with 1μM cytochrome *c*. The reaction studied does not therefore involve turnover of the enzyme. Above 10μM flavocytochrome b_2, the protein concentration begins to affect the ionic strength and the traces become less accurate.

The effect of ionic strength on the second order rate constant with cytochrome *c* is carried out at 1mM lactate, in Tris/HCl buffer, 25°C. The ionic strength of the 10mM Tris/HCl can be varied by the addition of a calculated amount of sodium chloride. A number of second-order rate constants were measured at differing ionic strengths, and these were then plotted as a straight line according to the Debye-

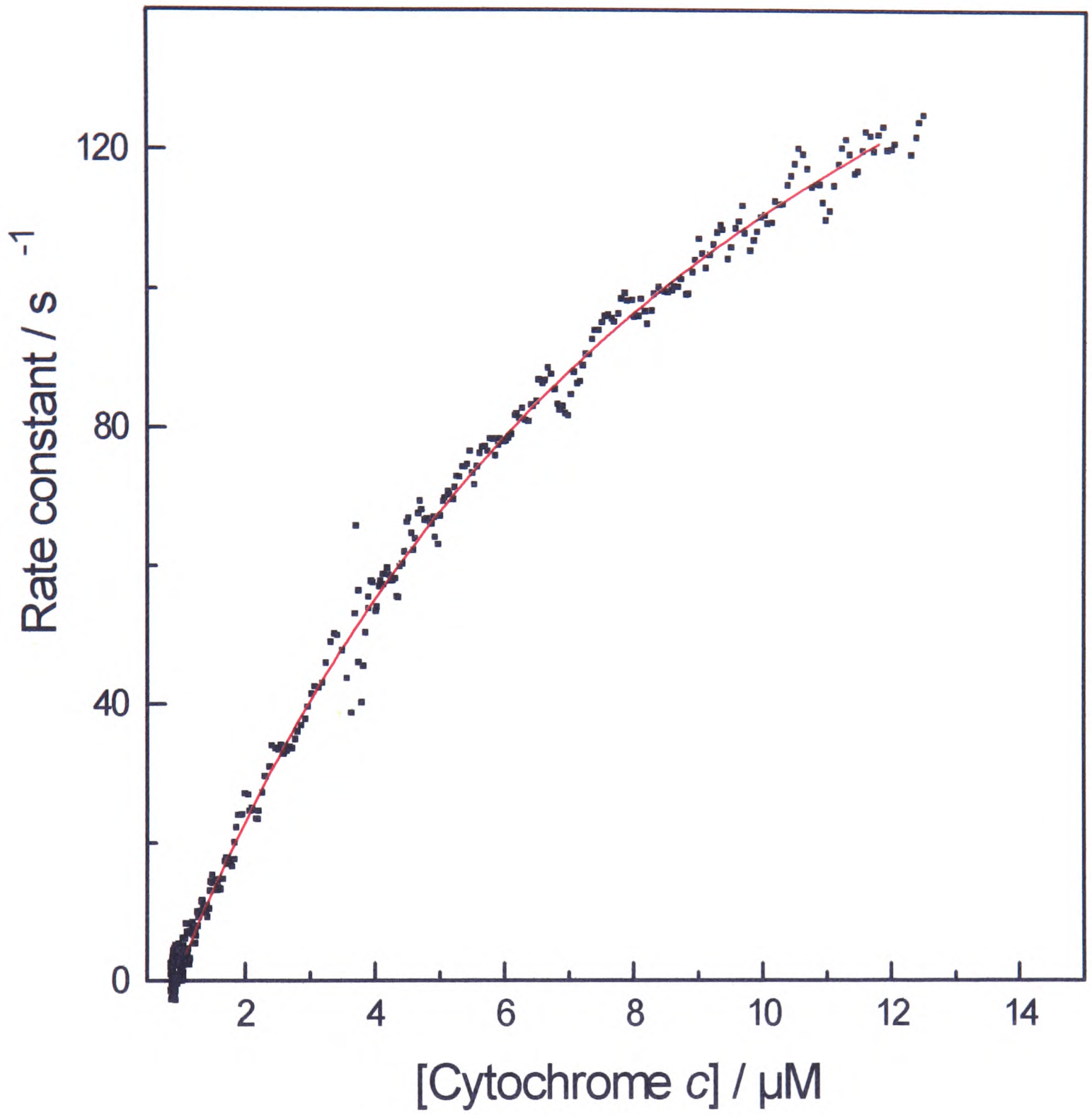

Fig.2.7.1.'Super-steady-state' reduction of cytochrome *c* , by Wild-type flavocytochrome b_2 in Tris/HCl,
pH 7.5, *I* 0.1M, 25 ± 0.1 °C, 10mM lactate.
k_{cat} = 228 ± 4 s-1
K_m = 10.6 ± 0.3 µM

Hückel equation, log.(rate constant) *vs.* square root ionic strength (See below). The gradient of the line indicates the strength and nature of the interaction.

The Simplified Debye-Hückel equation

$$\log k_2 = \log k_2^\circ + 2AZ_+Z_- \sqrt{I}$$

This is a simplified version of the Debye-Huckel expression that treats the proteins as point charges, and is only valid really for ionic strengths of 0.1 and below. However, it has been observed that saturation occurs at I ≈ 0.07 for the flavocytochrome b_2 cytochrome *c* interaction (for *H.anomala*-b_2, Capeillere-Blandin & Albani, 1987; for *S.cerevisiae*, Daff *et al*, 1996a). This point is more fully discussed in chapter **4**.

2.8 REDOX POTENTIOMETRY

Preparation of redox standard solutions

Iron III solution (Iron III Sulphate in 10mM EDTA, 0.1M acetate buffer, pH 5).

0.931g of EDTA was dissolved in 250ml of 0.1M acetate buffer, pH 5. 25mg of iron III sulphate was added, and the acetate buffer was titrated against sodium hydroxide to return to pH 5.

Iron II Sulphate

0.695g of Iron II Sulphate was made up to 25ml in a standard flask, and degassed with nitrogen.

Calibrating the electrode

The electrode used was a Platinum/Calomel electrode saturated with Potassium Chloride solution. All experiments were done at 25 ± 0.1°C, under a nitrogen atmosphere in a 10ml quartz cell. A small magnetic 'flea' was used to help keep the solutions homogeneous.

6 x 10µl aliquots of Iron II Sulphate solution were titrated into the Iron III Sulphate solution. The potential was recorded after each addition, and the temperature was maintained at 25°C. A plot of potential (plus 244.4mV to correct to the standard hydrogen electrode) against $\log_{10}([ox]/[red])$, should give a straight line of slope 59mV, and an intercept of 108mV.

Redox solutions

mediators		E_m/mV
2-Hydroxy-1,4-napthaquinone	(HNQ)	-140
Phenanzine methosulphate	(PMS)	+60
Phenanzine ethosulphate	(PES)	+80
2,3,5,6-tetramethyl-p-phenylenediamine	(DAD)	+220

Each mediator was made up to a concentration of 5mM in 0.1M Tris/HCl.

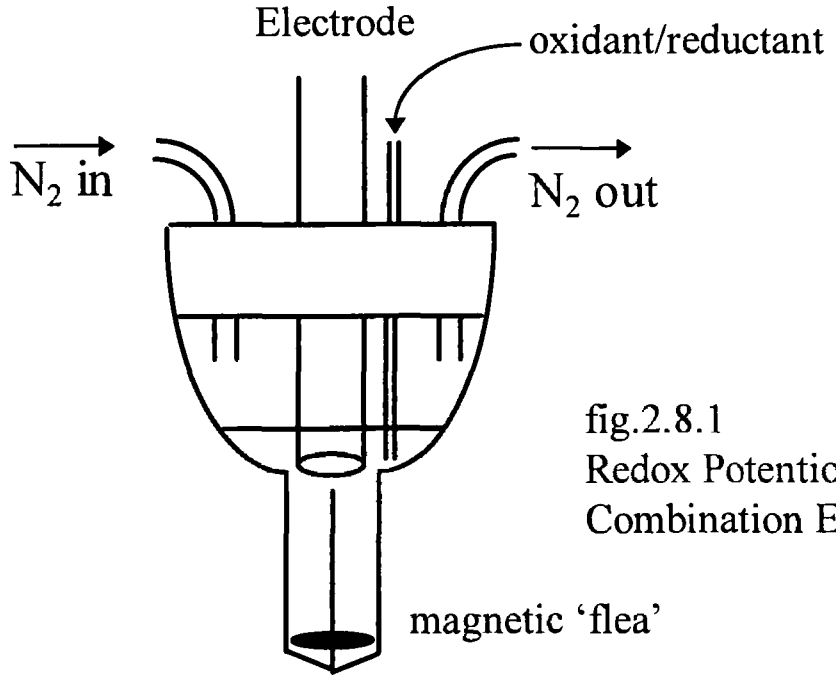

fig.2.8.1
Redox Potentiometry
Combination Electrode.

L-Lactate and ferricyanide

5mM solutions of both L-lactate and ferricyanide were made up in Tris/HCl buffer, and were used to reduce and oxidise the enzyme respectively. Both solutions were thoroughly degassed with nitrogen before used.

Measurement of the haem redox mid-point potential

Oxidised flavocytochrome b_2 was defrosted slowly from liquid nitrogen storage, and a sufficient amount was removed so that after dilution to 10ml a concentration of 15-20μM would be attained. 25μl of each mediator was then added to the protein, and the solution was made up to 10ml with Tris/HCl buffer. The solution was degassed gently under vacuum, then flooded with nitrogen. Once the solution was transferred to the quartz cell it was left stirring with a magnetic 'flea' under a nitrogen atmosphere to ensure it was fully degassed. The whole apparatus was kept in the dark as the mediators are light sensitive.

When the solution was thoroughly degassed, a spectrum was taken from 650nm to 500nm. L-lactate was added in 5μl amounts until the potential started to change. On each successive change in potential a spectrum was recorded, and the peak height at 557nm was measured (A flavin isosbestic). Upon full reduction, the enzyme was re-oxidised by addition of ferricyanide so as to ensure there was no hysteresis.

From the data, a Nernst plot of reduction potential vs. $\log_{10}([ox]/[red])$ should yield a straight line with a gradient of 59mV. The mid-point potential is the ordinate intercept.

Nernst equation

$$E = E_h + RT/nF \ln [ox]/red]$$

E is the measured potential, E_h is the mid-point potential, R is the molar gas constant ($Jmol^{-1}K^{-1}$), T is the absolute temperature (K), F is the Faraday constant ($Cmol^{-1}$), n is the number of electrons, [ox] is the concentration of the oxidised species, [red], is the concentration of the reduced species.

3. THE CYTOCHROME *c* INTERACTION WITH FLAVOCYTOCHROME b_2

3.1 INTRODUCTION

Flavocytochrome b_2 catalyses the reduction of cytochrome *c* by L-lactate in yeast mitochondria (Appleby & Morton, 1954). The enzyme can be extracted from two types of yeast; *Saccharomyces cerevisiae* and *Hansenula anomala*. The two proteins share a 60% sequence identity and all the active site residues are conserved (Black *et al*, 1989b). Only the crystal structure of the *S.cerevisiae* enzyme has been solved (Xia & Matthews, 1990), however, the flavin domain from *H.anomala*-b_2 is expected to share the same $\alpha_8\beta_8$ structural motif as in the *S.cerevisiae* enzyme. There are three major differences in the sequences: i) In the C-terminal tail, which forms a number of inter-subunit contacts which may explain why the *H.anomala* enzyme dissociates into monomers at low ionic strength (Baudras, 1971). ii) In the surface loops, and iii) in the 'hinge' region. The loop and the hinge regions in the *H.anomala* enzyme are shorter and more acidic than in the *S.cerevisiae* enzyme. These differences in sequence are likely to have an effect on the structure, and both the inter- and intra-molecular electron transfer kinetics of the enzymes (Capeillere-Blandin *et al*, 1986; White *et al*, 1993; Sharp *et al*, 1994). In particular, the greater amount of acidity in the *H.anomala* enzyme should affect the association with the positively charged cytochrome *c*.

3.1.1. The Stoichiometry of the interaction between *S. cerevisiae* flavocytochrome b_2 and cytochrome *c*

Flavocytochrome b_2 from *S. cerevisiae* forms a complex of high stability with cytochrome *c* that is dependent on ionic strength and pH (Baudras *et al* 1971, 1972; Prats 1977a). The complex has been shown to form under both crystalline and solution conditions. The haem ratio however, was somewhat surprisingly found to be one cytochrome *c* per tetramer. A value of two cytochromes *c* per tetramer was also recorded by Yoshimura *et al* (1977). One conclusion was that there was strong anti-co-operative binding between flavocytochrome b_2 and cytochrome *c*. This conclusion was based on the assumption that a tetrameric enzyme could maximise its efficiency by binding four cytochromes *c* at any one time. A stoichiometry of one cytochrome *c*

per tetramer would indicate either that there was only one binding site, or that the binding of one cytochrome *c* made the other three binding sites unstable (Yoshimura *et al*, 1977; Baudras *et al*, 1971). A stoichiometry of one cytochrome *c* per protomer was reported in the crystal lattice by Tegoni *et al* in 1983. Cytochrome *c* was found to diffuse into the crystal channels of flavocytochrome b_2 at low ionic strength, and could be removed at a higher ionic strength. The complex was found to be catalytically competent, although clearly the cytochrome *c* reductase activity of the enzyme in the crystal could not be compared to the activity in solution, as the limiting factor is the diffusion of cytochrome *c* through the channels of the crystal.

3.1.2 The Stoichiometry of the interaction between *H. anomala* flavocytochrome b_2 and cytochrome *c*

A great deal of work on the interaction between flavocytochrome b_2 and cytochrome *c* has come from the studies on the enzyme from the yeast *Hansenula anomala*. Baudras (Biochimie, 1971) found this enzyme to be more amenable for study as the purification was reportedly more simple and effective than that for the *S.cerevisiae* enzyme. The kinetics of the bimolecular reaction of the enzyme with cytochrome *c* were found to be first order, with the haem ratio reported to be clearly four cytochromes *c* per tetramer (Baudras 1971, Thomas *et al* 1983, Capeillere-Blandin, 1982; Capeillere-Blandin & Albani, 1987).

3.1.3 The Effect of Electrostatics

Before inter-molecular electron transfer can occur, a protein complex has to be formed. What determines the stability of this complex is debatable, however, the importance of electrostatics within the flavocytochrome b_2:cytochrome *c* assembly has already been established (Capeillere-Blandin & Albani, 1987; Daff *et al*, 1996a). What was found to be unusual about this association was that the flavin domain showed a stronger affinity for cytochrome *c* than the haem domain (Thomas *et al* 1983, Capeillere-Blandin & Albani, 1987, Capeillere-Blandin, 1982). This result is unusual, as the specific electron donor to cytochrome *c* is the haem domain (Celerier *et al*, 1989; Balme *et al*, 1995; Iwatsubo *et al*, 1977). Also the association

did not depend on the quaternary structure of flavocytochrome b_2 (Gervais *et al*, 1982), but efficient binding to cytochrome *c* did depend on both domains being present (Prats, 1977b). This is illustrated when b_2-core (the flavocytochrome b_2 haem domain expressed independently of the flavin domain), is reacted with cytochrome *c* (Daff *et al*, 1996a; Capeillere-Blandin & Albani, 1987). The second-order rate constant is found to be two-fold lower than that for the reduction of cytochrome *c* by intact flavocytochrome b_2. The reason for this decrease must be due to the low stability of the complex, as the redox potential is approximately the same for both flavocytochrome b_2 haem domain, and for b_2-core (Brunt *et al*, 1992).

3.1.4 The Hypothetical Complex between Flavocytochrome b_2 and Cytochrome *c* (Fig. 3.1.4.1)

Tegoni *et al* (1993) produced a hypothetical complex for the flavocytochrome b_2:cytochrome *c* assembly based on the method used by Roberts *et al* (1991), and his modelling of the plastocyanin:cytochrome *c* interaction. By employing the use of molecular modelling and energy minimisation techniques on the known three dimensional structures of flavocytochrome b_2 and cytochrome *c*, a hypothetical model for the interaction of these two redox partners in the crystal lattice was generated (Tegoni *et al*, 1993). The most probable binding area for cytochrome *c* was deduced to be located around the interdomain border. Out of an initial selection of possible binding sites situated close to this area, only one was selected on the basis that it gave better surface complementarity and a closer haem-b_2 to haem-*c* distance than the others. On this site two possible orientations of cytochrome *c* were produced, differing by a 180° rotation. One model, which had the two haem groups in a perpendicular orientation, was discarded as only two out of four binding sites were available in the crystal lattice, and would therefore give a stoichiometry of 2 cytochromes *c* per tetramer, which the authors incorrectly state is unreported in the literature.

The best model actually predicts a parallel orientation of the haem groups, as has been predicted for other complexes (Poulos & Kraut, 1980; Salemme, 1976), despite

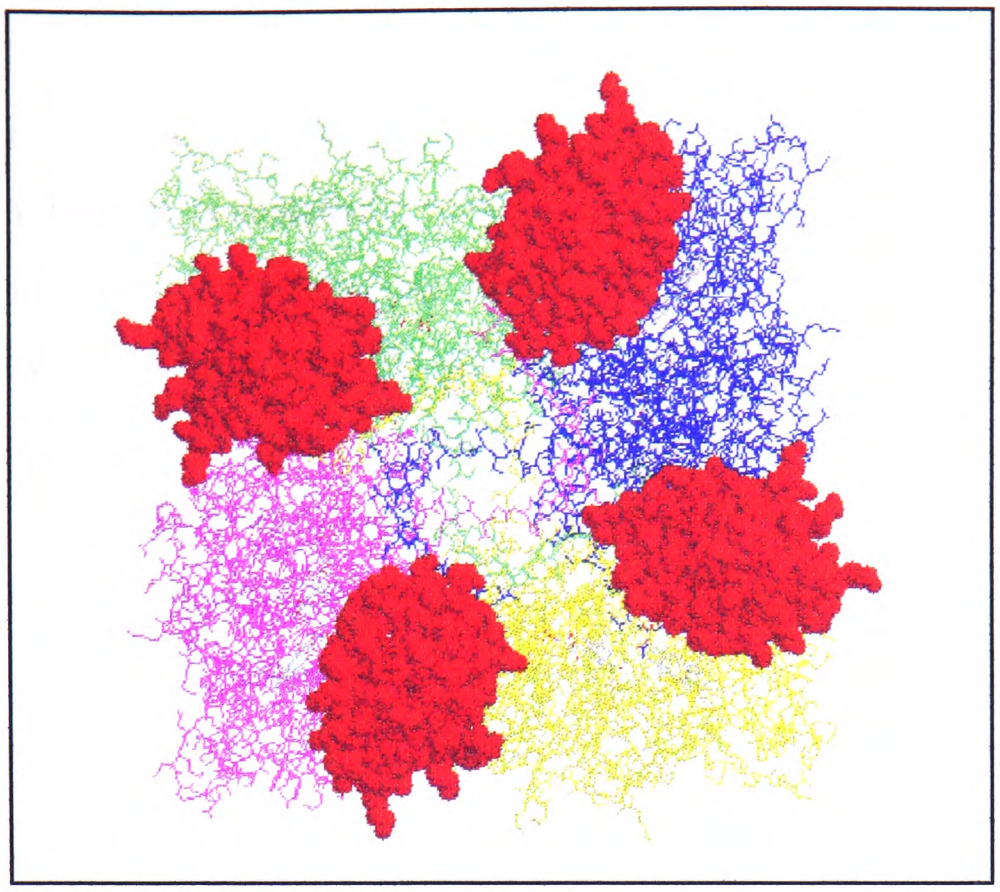

Fig. 3.1.4.1 Four cytochromes *c* (red space filled representation) are shown to bind to the flavocytochrome b_2 tetramer at sites predicted by Tegoni *et al* (1993). The four protomers are coloured individually: yellow, magenta, green and blue,

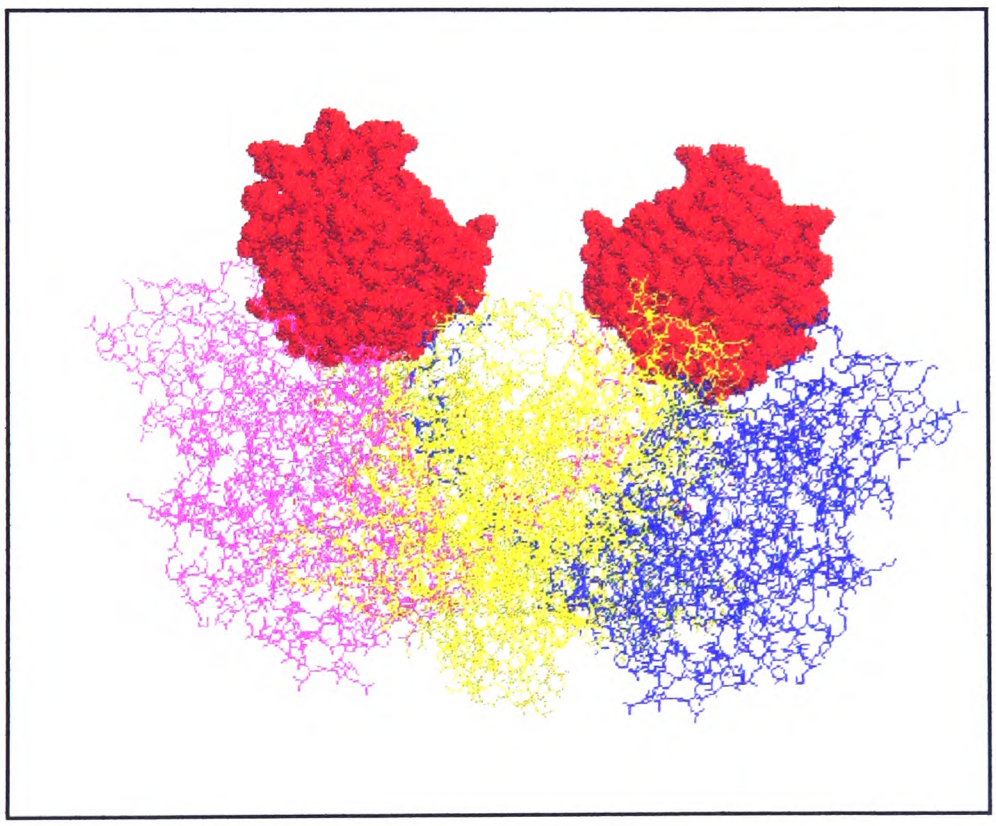

Fig. 3.1.4.1. A side view of the Tegoni hypothetical complex. Two cytochromes *c* (red space filled representation) are eclipsed behind the front two cytochromes. Flavocytochrome b_2 is shown in a wireframe representation (magenta, yellow, blue).

the fact that haem co-planarity was not used as a criterion. The haem propionates point in the same direction as in the cytochrome b_5:cytochrome *c* interaction. The haem to haem distance is acceptable within the parameters of other electron transfer complexes, however, the interacting surfaces of the proteins are not perfectly complementary, a fact noted by the authors (Fig.**3.1.4.2**). Cytochrome *c* interacts with three subunits in the tetramer: The greatest interaction is supplied by the flavin domain from one subunit, as indicated by previous equilibrium studies (Thomas *et al*, 1983; Capeillere-Blandin & Albani, 1987; Silvestrini *et al*, 1986); cytochrome *c* is further stabilised by the contacts with the C-terminal tail of one subunit, and the haem domain of another. The cytochromes *c* form identical contacts with the flavocytochrome b_2 tetramer, but individual cytochromes *c* also form contacts with other flavocytochromes b_2 in the crystal packing.

The principle interactions come from the alignment of the basic residues on cytochrome *c* with the acidic residues on flavocytochrome b_2. Arg13, Arg38, Lys 54 & Lys79 on cytochrome *c* are proposed to interact with Glu91, Glu110, Asp510, and Asp105 on flavocytochrome b_2 respectively. This means that the basic residues surrounding the exposed haem edge of cytochrome *c* are the ones involved in binding to flavocytochrome b_2 (Matsushma *et al*, 1986). A key residue in this alignment of residues is Glu91 on flavocytochrome b_2. It has been proposed to form three contacts with cytochrome *c*, the most important of which is the ion pair formed with Arg13 (Mclendon & Hake, 1992). An electron-transfer pathway has also been proposed, in accordance with other models such as cytochrome *c* peroxidase, for this static model which links the two haems. This σ-tunnelling pathway involves the side chain of Ile50, which is in van der Waals contact with the haem of flavocytochrome b_2, and joins to the backbone of Lys51. The final residue in the pathway is Phe52, which reportedly touches the haem of cytochrome *c* (Fig. **3.3.1**).

The model attempted to accommodate some of the parameters dictated by previous studies on the enzyme. The dependence of electron transfer on the stability of the protein complex has been clearly demonstrated (Capeillere-Blandin, 1982; Tegoni *et al*, 1983) in solution and in the crystal, and this dependence on electrostatics has been used as a tool to locate the cytochrome *c* binding site in the

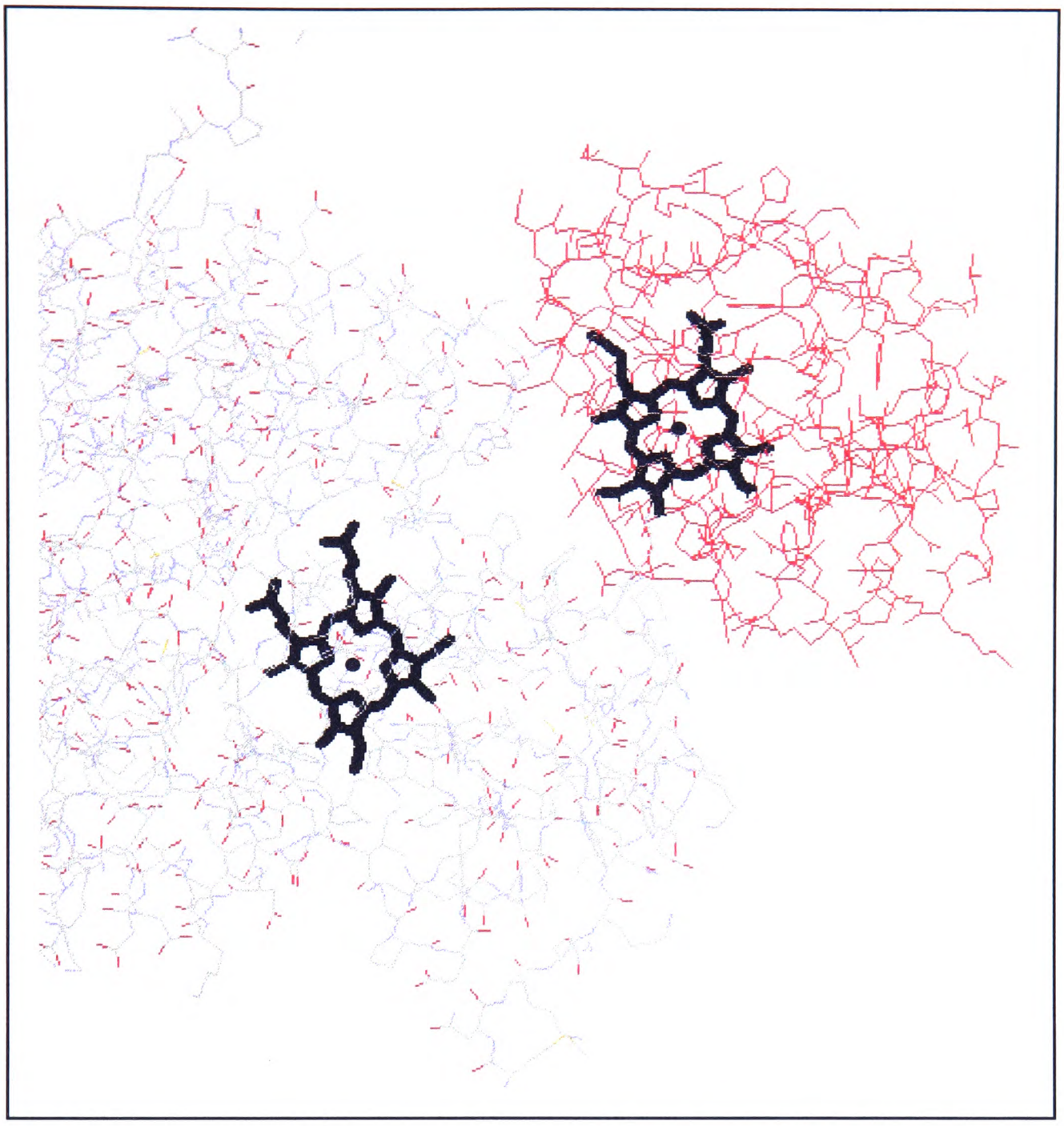

Fig. 3.1.4.2. The interface of the hypothetical model of the flavocytochrome b_2 cytochrome *c* interaction. Cytochrome *c* is shown in red, the two haem prosthetic groups are shown in black. The two surfaces can be seen not to be perfectly complementary (Tegoni *et al*, 1993).

crystal lattice. There are two ways to experimentally test this hypothetical complex: One is to test the dependence on electrostatics; and the other is to disrupt the pathway that is suggested to mediate the transfer of electrons between the two haem groups.

The importance of the basic groups in the reactivity of cytochrome *c* with flavocytochrome b_2, and its other redox partners has already been demonstrated (Matsushima *et al* 1986; Koppenol & Margoliash, 1982; Mclendon & Hake, 1992). Ionic strength experiments on interaction of flavocytochrome b_2 with cytochrome *c* (Daff *et al*, 1996a,b) indicate that the rate of the association is governed by this coulombic attraction. To test the hypothetical model, the negative residues on flavocytochrome b_2 predicted to be important for complex formation can be changed to positive residues using site-directed mutagenesis. If the model is correct, the charge reversal will disrupt, to a certain extent, the binding of cytochrome *c*. To test the electron-transfer pathway we need to increase the barrier for electron transfer. One approach is to shorten the covalent pathway, and perhaps to increase the through-space jump, thus increasing the σ-tunneling pathway length.

3.2 RESULTS

The two residues on flavocytochrome b_2 proposed from the model to be important for molecular recognition and electron transfer were Glu91 and Phe52 respectively. As mentioned in the description of the model, Glu91 is proposed to interact with Arg 13 on cytochrome *c*, and Phe52 is the final residue in the electron transfer pathway from flavocytochrome b_2 to cytochrome *c*. These two residues were independently mutated to produce three mutant-enzymes. The predicted ion-pair interaction was to be disrupted with a subtle mutation from a negative glutamate to an isoelectronic neutral glutamine, and in a second mutant-enzyme to a positive lysine. The electron transfer pathway was shortened to remove the predicted van der Waals contact between the Phe52 aromatic ring and the cytochrome *c* haem with the construction of a Phe52 to Ala mutation.

Using the relatively simple scheme of reversible association followed by irreversible electron transfer (Capellere-Blandin, 1982; Daff *et al*, 1996a), and

carrying out the bimolecular reaction between flavocytochrome b_2 and cytochrome *c* under pseudo-first order conditions, a second-order rate constant can be obtained.

● ~ denotes an electron, F = FMN, H = Haem-b_2, C = Haem-*c*.

In this scheme the rate limiting step is the formation of the complex (Daff *et al*, 1996a). The second step, k_2, is irreversible on account of the large redox potential difference between the flavocytochrome b_2 haem domain and cytochrome *c* (~270mV). In this case the experimentally measured second-order rate constant for the reduction of cytochrome *c* by flavocytochrome b_2 is purely a measure of the association of the two proteins and not a direct measure of the electron-transfer rate itself. Therefore, a decrease in the second-order rate constant will be seen if the rate of formation of the complex is lowered. If however the electron transfer itself is affected, then the rate of complex formation may reach a saturation limit, and be itself limited by the electron transfer.

All three mutant-enzymes were investigated to ensure that the mutations had little or no effect on the ability of the enzyme to act as a L-lactate dehydrogenase, so that any effect on the bimolecular rate constant with cytochrome *c* could be attributed solely to that step in the catalytic cycle. The results in of the steady-state and stopped-flow experiments with the mutant-enzymes are shown in tables **3.2.1** and **3.2.2**, and show that the mutations had essentially had no effect on the L-lactate dehydrogenase ability of the enzyme.

The second-order rate constants for the mutant-enzymes' reaction with cytochrome *c* are shown in figure **3.2.1**, along with the value for the wild-type enzyme for comparison. The results clearly illustrate that the mutant-enzymes show identical kinetics to the wild-type enzyme, and therefore cannot be involved in the molecular recognition and binding of cytochrome *c* (Chapman *et al* ,1996; Daff *et al*, 1996a).

Table 3.2.1. Steady-State Kinetic Parameters for the Wild-Type and Mutant-Enzymes designed to Test the Tegoni Model.

All experiments were performed at 25°C in 10mM Tris/HCl buffer, pH 7.5, *I* 0.10M.

Electron acceptor	Ferricyanide			Cytochrome c		
Mutant enzyme	k_{cat}/ s^{-1}	$^{1}K_m$/ mM (lactate)	$^{2}K_m$/ mM (ferricyanide)	k_{cat}/ s^{-1}	$^{3}K_m$/ mM (lactate)	$^{2}K_m$/ μM (Cytochrome *c*)
WT[a]	400 ± 10	0.49 ± 0.05	<< 0.07	207 ± 10	0.24 ± 0.04	10 ± 1
E91K	414 ± 10	0.46 ± 0.05	<< 0.07	200 ± 20	0.23 ± 0.03	14 ± 2
E91Q	320 ± 20	0.46 ± 0.05	<< 0.07	150 ± 20	0.33 ± 0.03	10 ± 2
F52A	400 ± 20	0.48 ± 0.07	<< 0.07	166 ± 20	0.37 ± 0.04	13 ± 2

1 : all assays were carried out at 1mM ferricyanide

2 : all assays carried out at 10mM lactate

3: all assays were carried out at ca. 50 μM cytochrome *c*.

[a] Miles *et al*, 1992.

Table 3.2.2. Pre-Steady-State Reduction of the Flavin and Haem Prosthetic Groups, and Haem Mid-point Redox Potential, for the Mutant-Enzymes Used to Test the Tegoni Model

	Flavin reduction		Haem reduction		Redox potential
Mutant-enzyme	k_{cat} / s^{-1}	Km / mM	k_{cat} / s^{-1}	Km / mM	mV
WT[a]	604 ± 60	O.84 ± 0.2	445 ± 50	0.53 ± 0.05	-17 ± 5
E91K[b]	681 ± 50	0.9 ± 0.3	470 ± 30	0.38 ± 0.15	-13 ± 5
E91Q	600 ± 50	1.2 ± 0.2	450 ± 50	0.66 ± 0.09	-
F52A[b]	580 ± 50	0.32 ± 0.1	570 ± 60	0.34 ± 0.06	-

a : Miles *et al*, 1992.

b : Chapman *et al*, 1996.

Fig. 3.2.1. Second-Order rate constants for the wild-type flavocytochrome b_2 and the mutant-enzymes designed to test the Tegoni model.

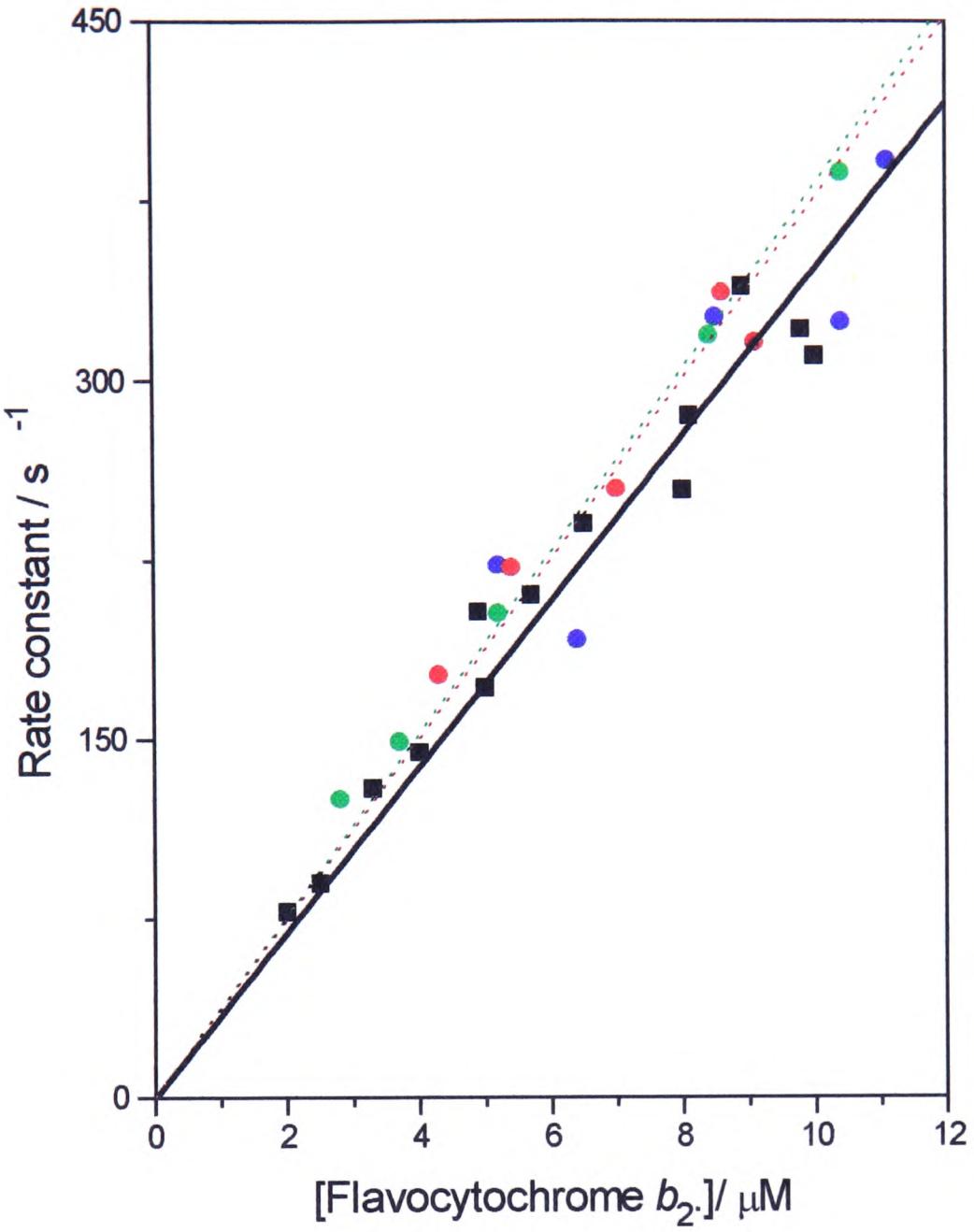

Mutant-Enzyme	Second-Order Rate Constant/ $\mu M^{-1}s^{-1}$
■ WT	34.8 ± 0.9
● E91K	37.7 ± 1.2
● E91Q	38.2 ± 0.8
● F52A	34.8 ± 1.9

*Daff *et al*, 1996

All experiments were carried out at 10mM L-lactate, in 10mM Tris/HCl, pH 7.5,

3.3 DISCUSSION

When a mutant-enzyme's properties are being studied, it is important to check that the mutation is having the desired effect in the targetted area. In this case, the mutations were designed to affect cytochrome *c* binding to flavocytochrome b_2. The residues that were targetted for mutation were predicted, in a hypothetical model, to be essential for binding cytochrome *c*. The two residues selected are on the surface of the protein, and therefore would be expected to have little effect on the overall function, or the structural integrity of the enzyme. The steady-state data confirms that the mutations have not affected the turnover of the mutant-enzyme with respect to the wild-type enzyme (Fig. **3.2.1**). The pre-steady-state data (Fig **3.2.2**) also shows that the catalytic steps prior to the reduction of cytochrome *c* have not, within experimental error, been affected. However, the pre-steady-state reduction of cytochrome *c* by flavocytochrome b_2 does not depend on these initial steps in the catalytic cycle, as the protein itself is kept fully reduced for the duration of the experiment.

The pre-steady-state reduction of cytochrome *c* by the mutant-enzymes of flavocytochrome b_2 designed to test the Tegoni model are, within error, the same as the wild-type enzyme (Fig.**3.2.3**). Glutamate 91 on flavocytochrome b_2 was the key residue for complex formation predicted by the hypothetical model. Therefore, the lowering of the second-order rate constant afforded by the alteration of this residue to a glutamine, would be less than the full charge reversal to a lysine, if the model was correct. As the results show, the two mutant-enzymes give the same second-order rate constants for the reduction of cytochrome *c*.

With hindsight, criticisms of the method with which the model was produced can be made. The calculations to predict the electrostatic potentials of the tetramer were simplified. They were not performed on the crystal packed complex, and they only incorporated two of the four haem domains in the calculations. The reactivity of crystalline flavocytochrome b_2 with cytochrome *c* (Tegoni *et al*, 1983) was used to further restrict the number of potential binding sites since the accessible surface area to cytochrome *c* is greatly reduced by the extent of the crystal contacts between the tetramers. As a result of these simplifications, a number of possible binding sites

were excluded. The model that was eventually produced did not have the almost perfect complementary fit of surfaces that was found in previous protein complex studies (Salemme, 1976; Poulos & Kraut, 1980; Pelletier & Kraut, 1992). An added complication in the construction of the model is that flavocytochrome b_2 is a tetramer, with each protomer being divided into two domains. This contrasts with the single domain proteins of cytochrome b_5 and cytochrome *c* peroxidase, where the locus of the binding site is centred around the exposed haem edge.

A conclusion made by the authors is that a functional role for the quaternary structure of flavocytochrome b_2 may have been provided by the fact that cytochrome *c* is shown to bind to three out of the four subunits. This is not in agreement with previous work (Gervais *et al* , 1982; Prats, 1977). Also, on examination of the co-ordinates of the hypothetical structure, it was noticed that there was a significant gap in the proposed σ-tunnelling pathway. It was this pathway that the authors stated was in contact with the haem of flavocytochrome b_2, and also touched the cytochrome *c* haem atom CBC. As is shown in figure **3.3.1.**, this is clearly not the case.

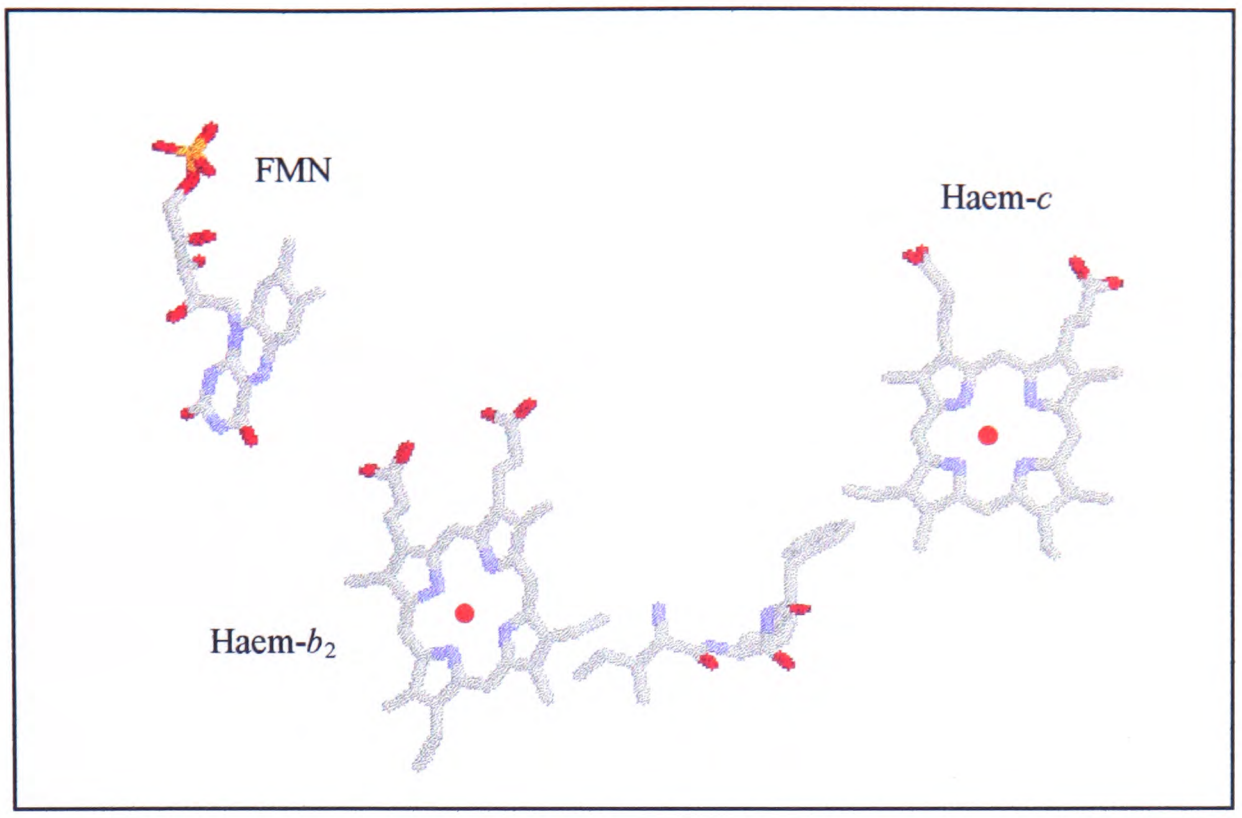

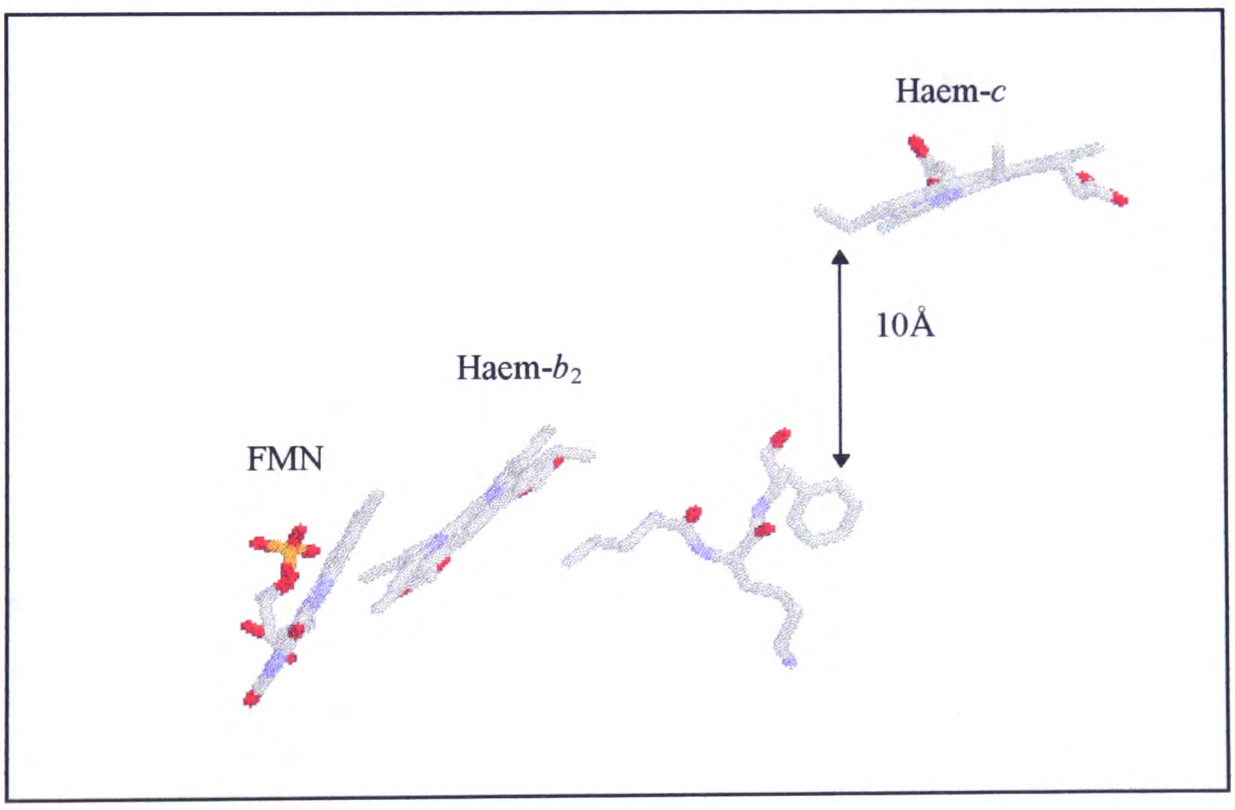

Fig. 3.3.1. Above. Illustration of the perspective of the published σ-tunneling pathway from flavocytochrome b_2 haem to the cytochrome *c* haem (Tegoni *et al*, 1993). **Below.** The same σ-tunneling pathway viewed from a different angle revealing a 10Å gap.

4. LOCATION OF A CYTOCHROME *c* BINDING SITE ON THE FLAVOCYTOCHROME b_2 STRUCTURE

4.1 INTRODUCTION

The interaction between wild-type flavocytochrome b_2 and cytochrome *c* has already been discussed in chapter **3** with respect to stoichiometry, the effects of ionic strength, and the areas on flavocytochrome b_2 which displayed the greatest affinity for cytochrome *c*. These data are important in this chapter. Other protein complexes, in particular the cytochrome b_5:cytochrome *c* complex, have been discussed in chapter **1**, and will be referred to in this chapter.

Unlike cytochrome b_5 and cytochrome *c* peroxidase, flavocytochrome b_2 is a tetrameric protein, with each protomer being divided into two separate domains. The examination of the crystal structure of flavocytochrome b_2 (Xia & Matthews, 1990) reveals a fairly uniform distribution of charge, however several areas of acidity can be found. These areas were looked at in terms of a location for a binding site for the positively charged cytochrome *c*. The prime concern in locating a possible binding site was that the haem-*c* was to get as close as possible to the haem-b_2. The residues that were thought to be involved in forming a binding site were then checked to see if they were conserved in the 'b_5-superfamily' (Lederer, 1994). The cytochrome domain, or b_2-core (Brunt *et al*, 1992), shares a great deal of homology with cytochrome b_5 (Lederer, 1994), and as has already been outlined in the first chapter, the cytochrome b_5:cytochrome *c* complex has attained pedagogical status (Mauk *et al*, 1995). This type of approach, looking at sequence homology to find a binding site, has already proved successful with cytochrome *c* oxidase (Witt, Zickermann & Ludwig, 1995).

Using a crude 'thought-experiment'; if the flavocytochrome b_2 haem domain was superimposed over cytochrome b_5 in the models derived for the cytochrome b_5:cytochrome *c* complex (Mauk *et al*, 1995), it would actually place the cytochrome *c* binding site on flavocytochrome b_2 at the interface between the flavin and haem domains. This is in agreement with Tegoni's conclusions on the general location of the binding site, and is also in accord with conclusions from work done by Moser *et al* (1995). He predicted the interdomain binding site on the basis of the relative efficiency of electron transfer from the redox centre to points on the surface of the

protein. This picture of an interdomain binding site must therefore involve the flavin domain in stabilising the complex. Kinetic evidence for this comes from the second order rate constant for the cytochrome domain, independently expressed from the flavin domain, with cytochrome *c* (Daff *et al*, 1996a). The decrease in the second order rate constant is more than two-fold. The tertiary structure has also been found to be important in other studies involving cytochrome *c* binding to flavocytochrome b_2 (Prats, 1977; Gervais *et al*, 1982).

Several residues were selected for investigation on the basis that they would provide a cluster of negative residues that cytochrome *c* would be attracted to, and that would place cytochrome *c* close to the flavocytochrome b_2 haem (see section **2.4.2**). These residues are also conserved in the 'b_5-superfamily'. In order to test the importance of these residues in binding cytochrome *c*, the aim was to introduce a charge reversal, and so aspartates and glutamates were replaced with lysines. The difference in steric bulk between a lysine and an aspartate or glutamate is small, allowing the major effect, if there is any, to be electrostatic.

4.2 RESULTS

Two point-mutations were found to affect the second order rate constant, Aspartate 72 to Lysine (D72K), and Glutamate 63 to Lysine (E63K). These mutant-enzymes were found to be kinetically identical to the wild-type enzyme in terms of the microscopic rate constants for flavin and haem reduction (Table **4.2.1**). The fact that they affected the second-order rate constant indicates that they must be involved in the molecular recognition and formation of a complex with cytochrome *c*. D72K and E63K lowered the second-order rate constant from $34.8\mu M^{-1}s^{-1}$ in the wild-type enzyme, to $24.3\mu M^{-1}s^{-1}$, and $13\mu M^{-1}s^{-1}$ respectively. A double mutation was also engineered (E63K:D72K). This caused the greatest decrease in second order rate to $6\mu M^{-1}s^{-1}$ (Figure **4.2.1**).

The reduction potentials were measured for each of the mutant enzymes to check that this fundamental electron-transfer parameter had not been inadvertantly altered by the introduction of the mutation. The reduction potentials were found, for all the mutant-enzymes, to be within error of each other, but approximately 20mV greater

Table 4.2.1. Pre-Steady-State Reduction of Flavin and Haem Prosthetic Groups of Mutant-Enzymes that affect the Second-Order Rate Constant with Cytochrome *c*.

	Flavin reduction		Haem reduction	
Mutant-Enzyme	k_{cat} / s^{-1}	K_m / mM	k_{cat} / s^{-1}	K_m / mM
WT[a]	604 ± 60	0.84 ± 0.2	445 ± 50	0.53 ± 0.05
E63K	677 ± 50	1.1 ± 0.3	363 ± 40	0.63 ± 0.1
D72K	595 ± 60	1.3 ± 0.4	504 ± 50	0.9 ± 0.1
E63K:D72K	600 ± 60	1.2 ± 0.2	415 ± 50	0.79 ± 0.2

a: Miles *et al*, 1992

All experiments were carried out in Tris/HCl buffer, pH 7.5, I 0.1M, and at 25°C.

than that for the wild-type enzyme (Figures **4.2.1** and **4.2.2**). This however should not affect the electron transfer step to cytochrome *c* as the driving force is still around 250mV, and the overall reaction is still rate limited by the complex formation (See section **3.2**).

The ionic strength dependence of the second-order rate constant has been carried out for the wild-type enzyme from *S. cerevisiae*, and is discussed in Daff *et al*, 1996a. A gradient was obtained by fitting the points to the simplified Debye-Hückel expression, and has a value of -5.9. This gives us a qualitative estimate of the strength, and nature of the interaction, in this case a positive-negative attraction. The same experiment was carried out for the double mutant enzyme E63K:D72K (Figure **4.2.3**). Again a straight line was obtained that indicated electrostatic attraction between the two proteins, however, the values for the rate constants at the different ionic strengths were lower than that for the wild-type enzyme. The gradient of the line was also smaller, with a value of -4.3. This decrease shows that there is not only a decreased rate of complex formation, but also that there is a decreased dependence on electrostatics.

4.2.1 Construction and description of the model

The model of the complex was developed by Dr. P. Taylor and Prof. M. D. Walkinshaw based on the kinetic data already gained from the charge reversal point mutations. The two proteins were first fitted together manually using molecular graphics, and the best complementary geometries were then energy minimised using X-PLOR version 3.1 (Brünger, A.T., Yale University Press, Newhaven). Two almost indistinguishable complexes were produced using this method. Both complexes were checked for unfavourable contacts, and then refined (Figures **4.2.1.1** and **4.2.1.2**).

The model centres around the residues that are known to have an effect on cytochrome *c* binding, Glu63 and Asp72, and can be therefore said to be kinetically relevant. Several important features can be highlighted. Unlike the Tegoni model, each cytochrome *c* only binds to one subunit of flavocytochrome b_2. Four cytochromes *c* can be accommodated on the tetramer and these cytochromes *c* are

Figure **4.2.1.** Bimolecular Rate Constant for the Reduction of Cytochrome *c* with Targeted Point Mutations Designed to Affect Cytochrome *c* Binding.

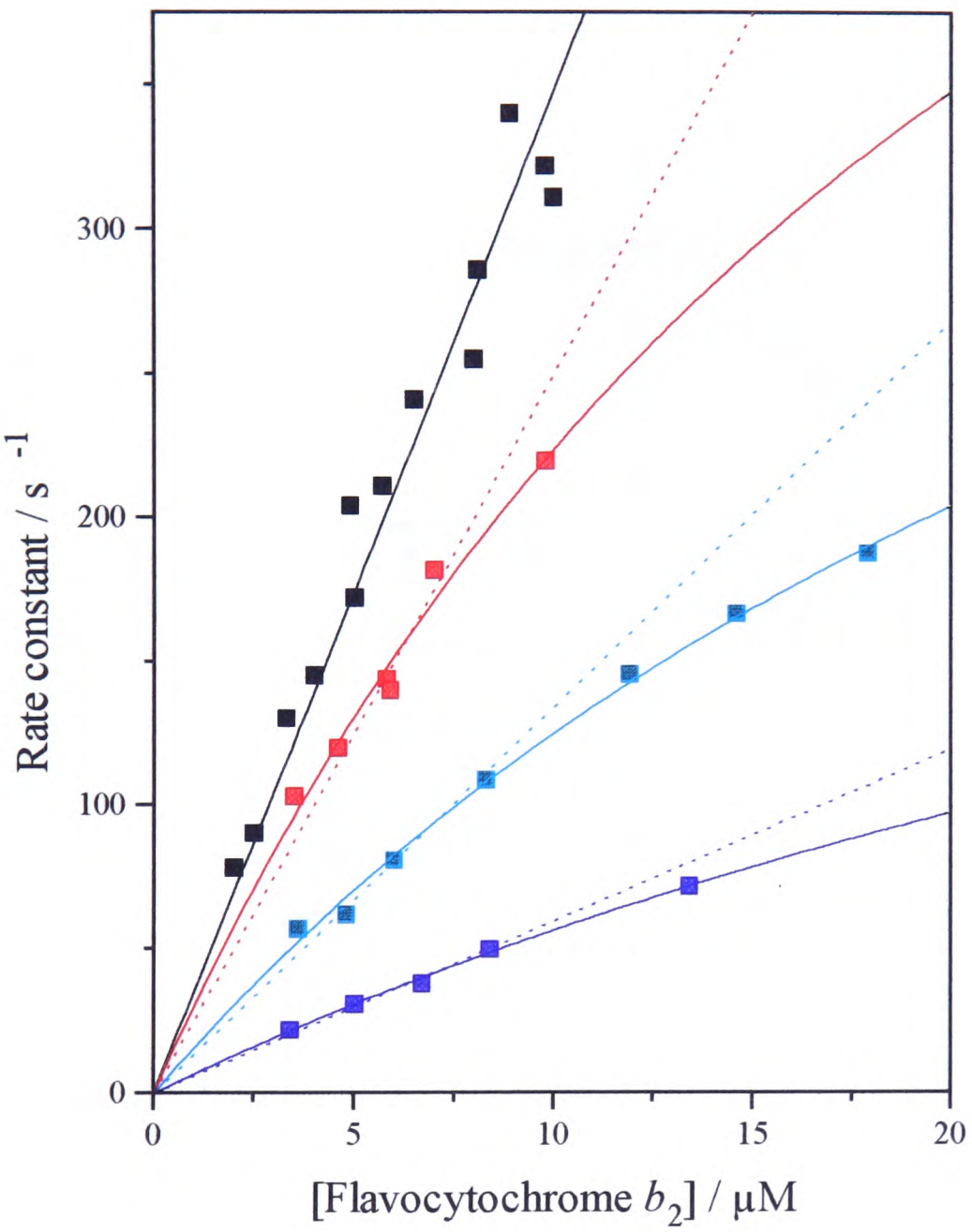

	Mutant-Enzyme	Second-Order Rate Constant /$\mu M^{-1}s^{-1}$	Redox Potential /mV
■	WT[a]	34.8 ± 0.9	-17.0 ± 3[a]
■	E63K	13.0 ± 0.7	-0.3 ± 5
■	D72K	24.3 ± 0.8	-1.8 ± 5
■	E63K:D72K	6.0 ± 0.05	+6.4 ± 5

a: Miles *et al*, 1992.

Fig. 4.2.2. Redox potential determination for the double mutation E63K:D72K, carried out as described in section **2.8**.

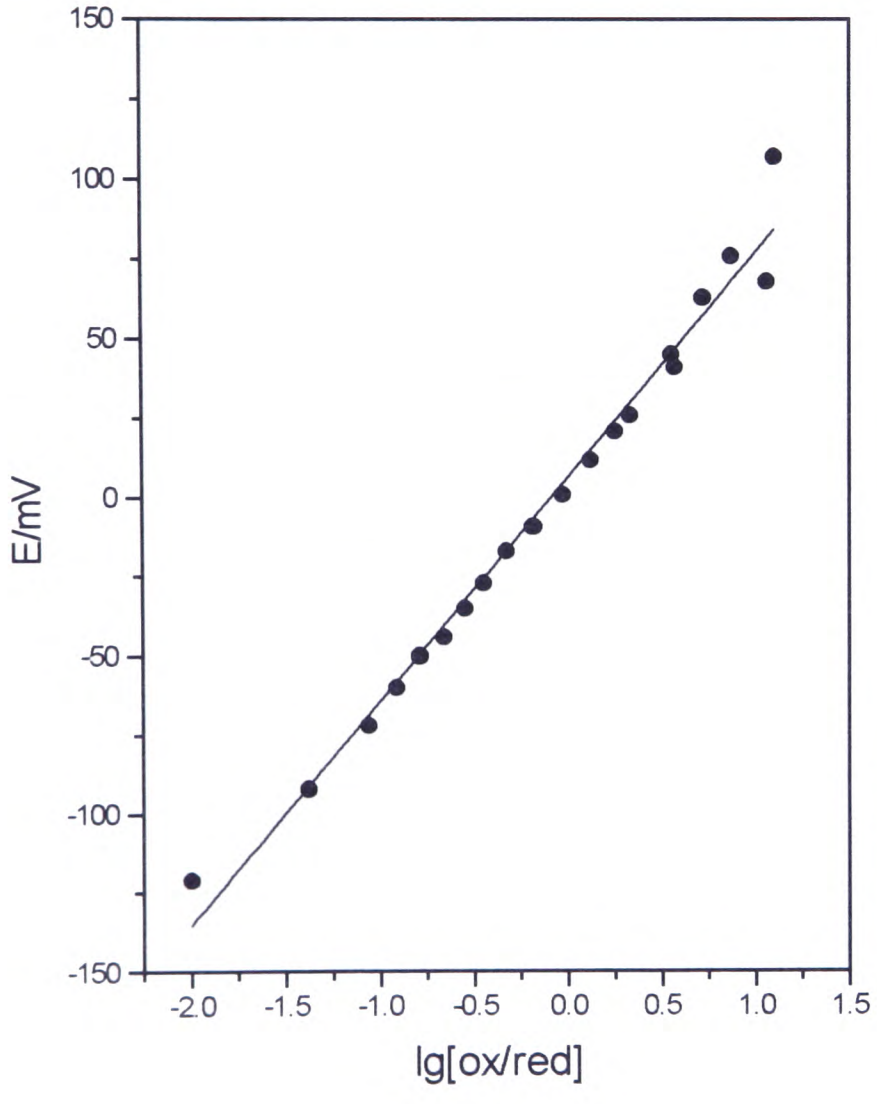

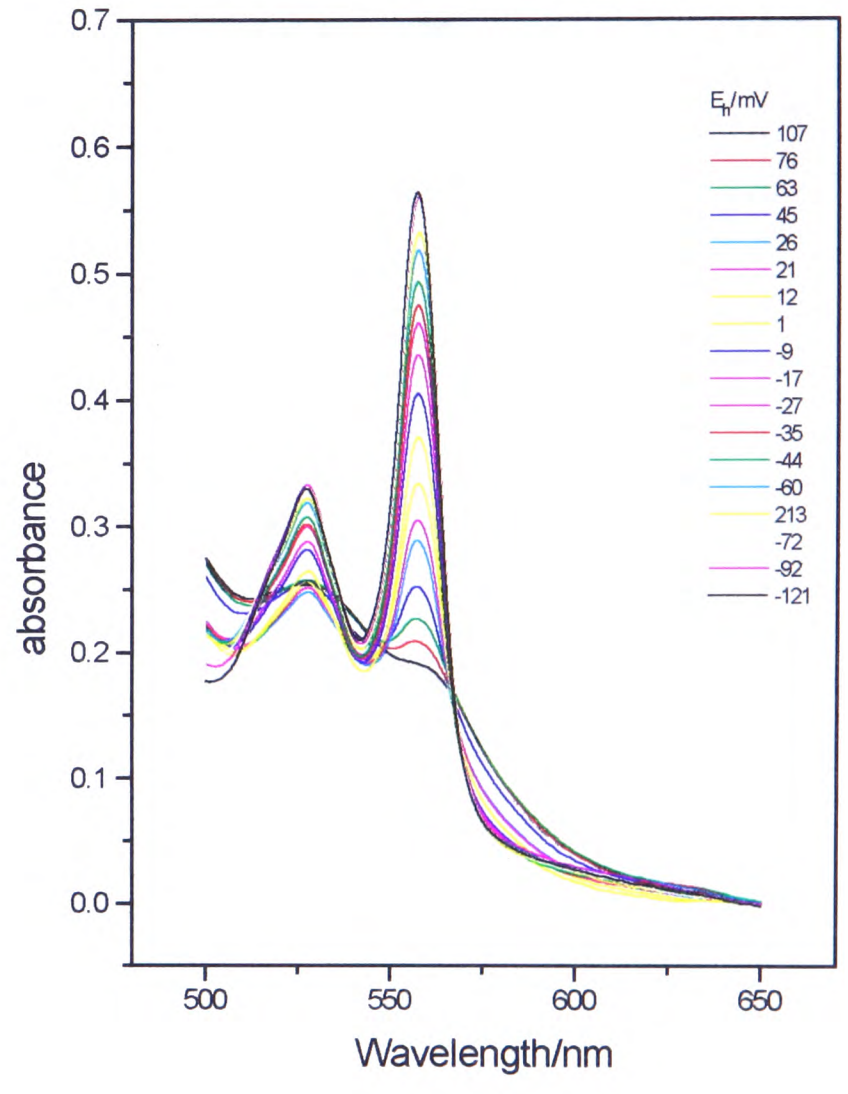

Figure **4.3.2.** Debye-Hückel plot showing the effect of ionic strength on the second-order rate constant for the reduction of cytochrome *c* by the double mutant enzyme E63K:D72K.
The gradient of the line $2AZ_+Z_-$ = -4.3 ± 0.44.

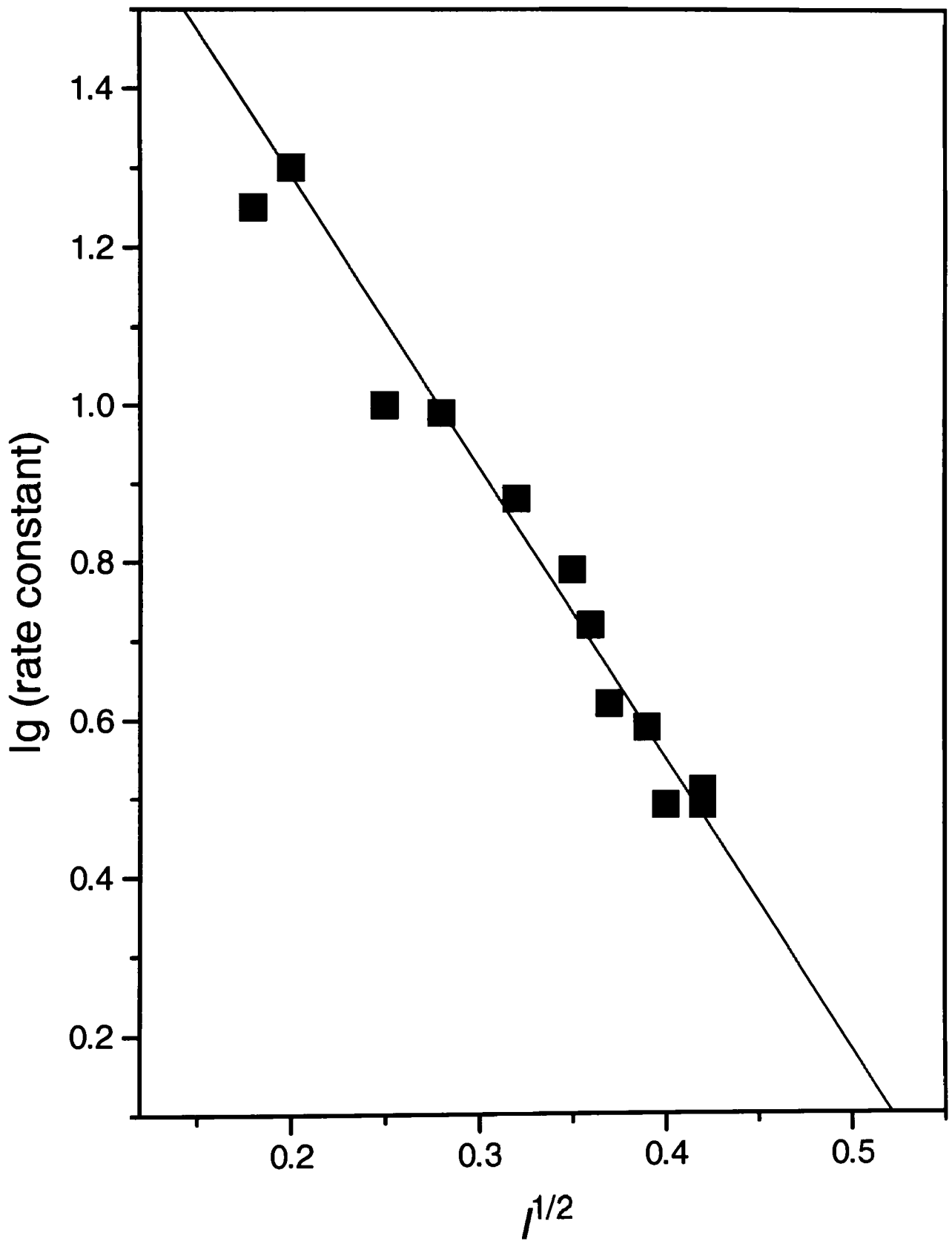

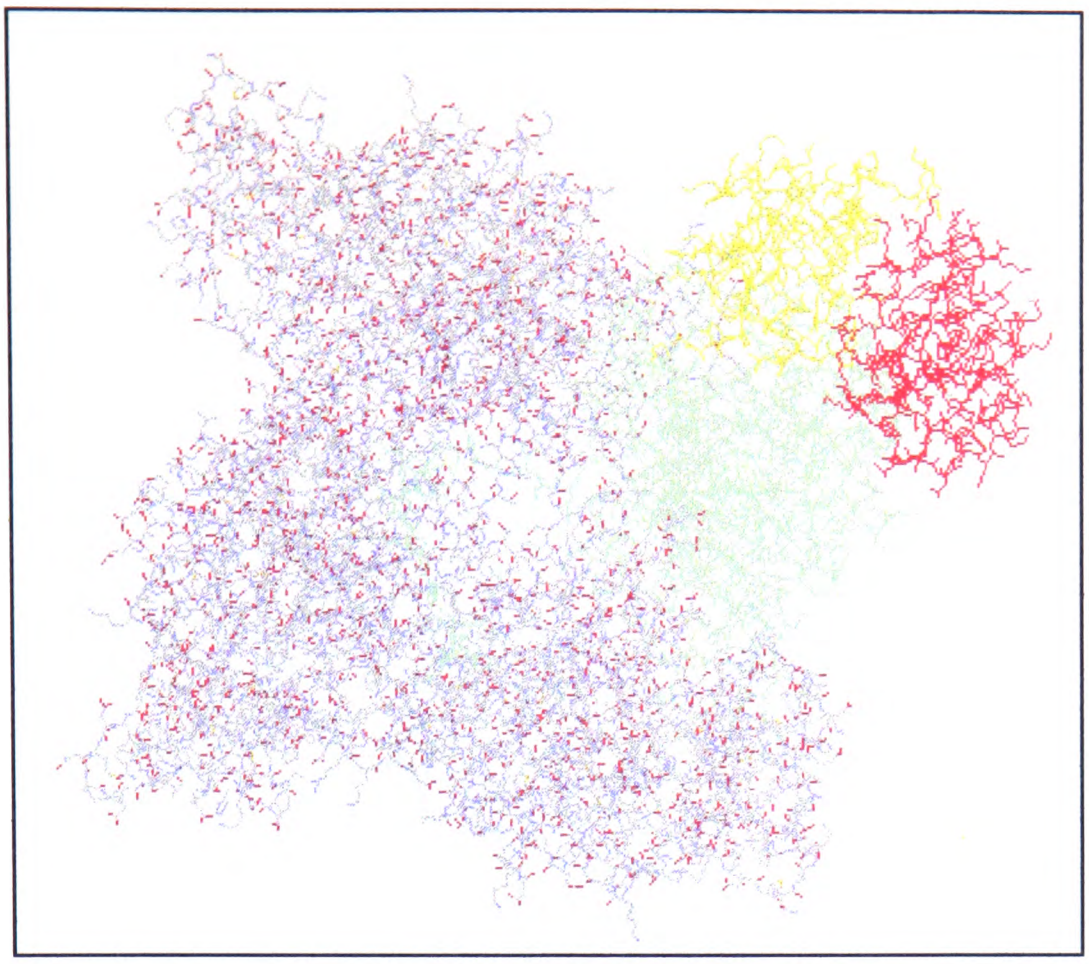

Fig. 4.2.1.1. One cytochrome *c* being shown to bind to the flavocytochrome b_2 tetramer, between the flavocytochrome b_2 flavin domain (green) and the haem domain (yellow). The stoichiometry is one cytochrome *c* per protomer. Rotation 90° around the pseudo-four-fold axis of symmetry reveals three other relevant catalytic sites.

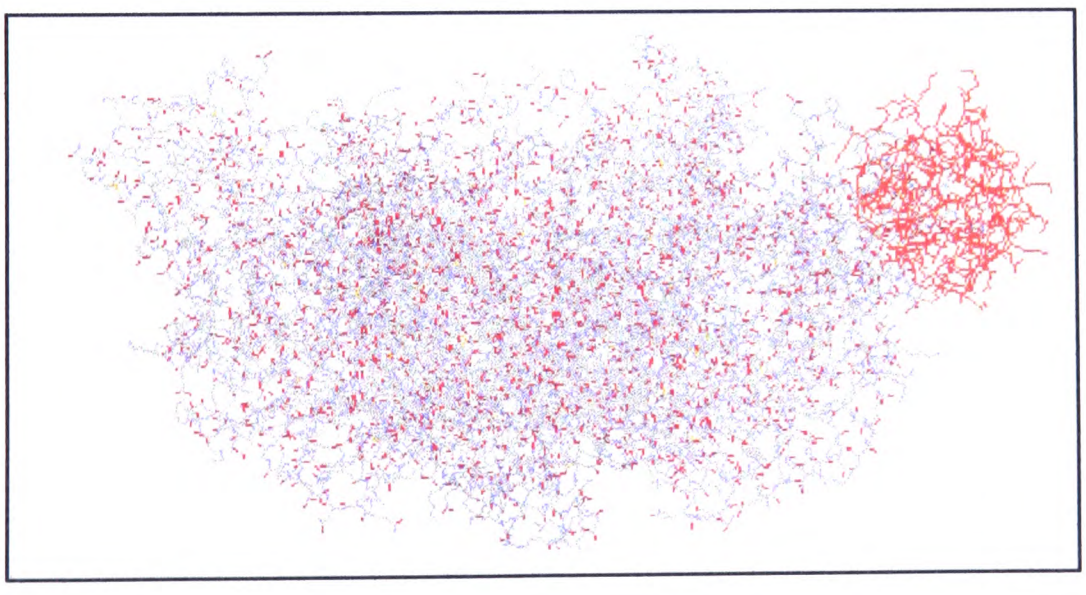

Fig. 4.2.1.1. A side view of one cytochrome *c* binding to the flavocytochrome b_2 tetramer. Rotation 90° around the pseudo-four-fold axis of symmetry reveals the other three binding sites.

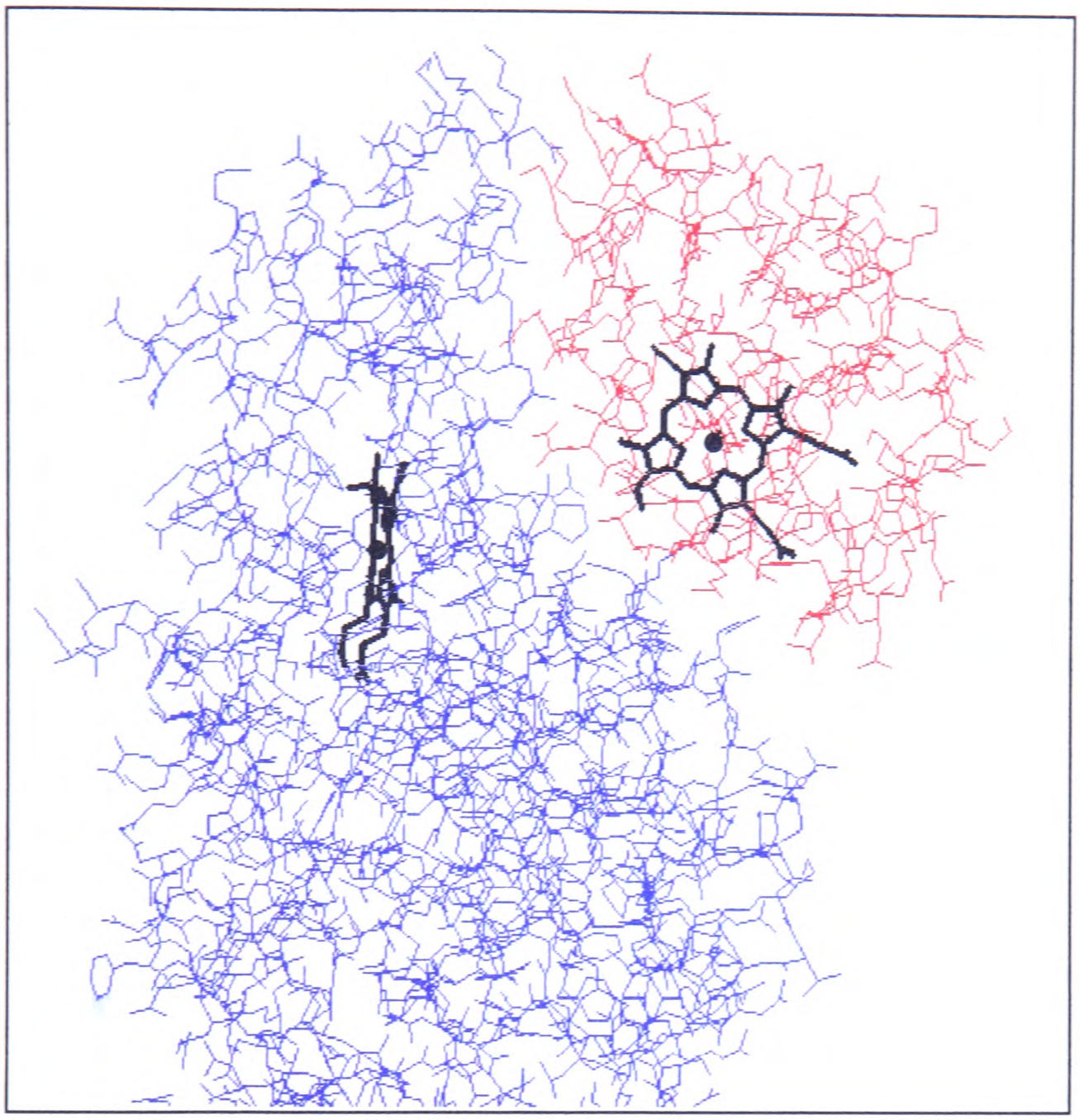

Fig. 4.2.1.2. The flavocytochrome b_2: cytochrome c interface showing the complementarity of the surfaces. Flavocytochrome b_2 is shown in blue, and cytochrome c is shown in red. The two haems are shown in black.

positioned on the interdomain border. Residues from both the flavin and haem domains are involved in the stabilisation of the complex. From the model, the residue that is implicated in stabilising the complex from the flavin domain is glutamate 237. The three residues form a triangular recognition site for cytochrome *c*. Asp72, Glu63 and Glu237 interact with Lys13, 27 and 79 respectively. Through the middle of this triangle runs a σ-tunnelling pathway (Figure **4.2.1.3**). This σ-tunnelling pathway spans residues 66 to 68, and starts with the flavocytochrome b_2 His66 axial ligand to the haem. This joins up with the backbone of Ala67 and ends with Pro68. The 'through space' jump is then 3Å to the cytochrome *c* haem. In total, the direct distance between His66 and the haem C3C pyrrole ring of cytochrome *c* is 13.1Å. This system provides cytochrome *c* with at least two similar alternative binding sites (as occurred in Salemme's original model of cytochrome b_5 and cytochrome *c*) to 'sample' without involving a separate electron transfer pathway. The rest of the interaction area, in agreement with other protein complexes, is made up of hydrophobic residues.

4.3 DISCUSSION

4.3.1 The kinetics of the association

The true rate of electron transfer from flavocytochrome b_2 to cytochrome *c* is estimated to be in excess of $1000s^{-1}$ (Daff *et al.*, 1996a), and so cannot be experimentally observed using stopped-flow kinetics. This means that the second-order rate constant is purely a measure of the rate of association of the two proteins *i.e.* the "on-rate". From Fig.**4.2.1** it can be clearly seen that data determined for the mutant-enzymes show a degree of curvature. This curvature may be real *i.e.* the electron-transfer rate is affected in the mutant enzymes and a saturation limit is being reached. In this case the points can be fitted to a Michaelis-Menton type equation which would reveal parameters equivalent to 'k_{cat}' and 'K_m' (listed in Table **4.3.1**). Alternatively, the curvature of the lines may arise from an artefact of the experiment. For example, the larger concentrations of protein used in these experiments may perturb the ionic stength which might well effect the rate of association of the proteins.

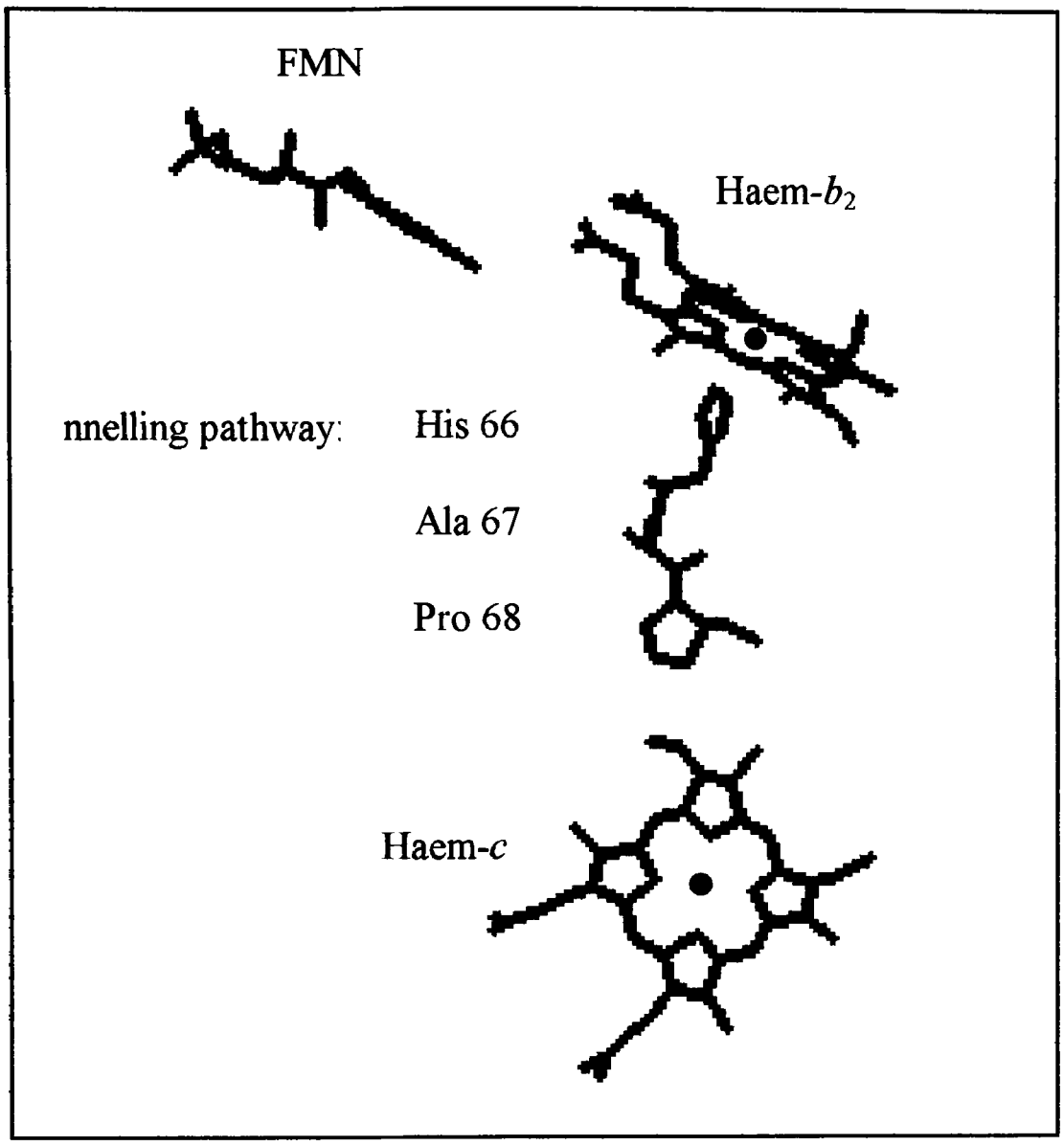

Fig. 4.2.1.3. The proposed σ-tunneling pathway from the flavocytochrome b_2 haem to the cytochrome *c* follows the covalently linked route through the side chain of His66, the backbone of residue 67, and the side chain of Pro68. There is then a through-space jump of 3Å to the cytochrome c haem.

If we assume that the curvature is indeed a real effect, then a possible explanation is that cytochrome *c* is unable to bind at its optimal location on the mutant flavocytochromes b_2. Cytochrome *c* may be forced to bind at an alternative adjacent site, this would increase the distance between the redox centres and thus lower the rate of electron transfer sufficiently to produce the saturation effect.

The results shown in Table **4.3.1** indicate that the introductions of charge reversals at positions 63, or 72, on flavocytochrome b_2 decrease the "on-rate" for the complex formed with cytochrome *c*. In addition the results would be consistent with the mutations resulting in a decrease in the rate-constant for electron transfer and an increase in the apparent dissociation constant. In each case, these results are strongly supportive of the idea that residues 63 and 72 on flavocytochrome b_2 are involved in the formation of a redox active complex between the two proteins.

4.3.2 The model of the complex

As with other models proposed to represent a protein-protein interaction (Salemme, 1976; Poulos & Kraut, 1980), this model can be thought of as a static representation of a dynamic interaction (Eley & Moore, 1983; Wendoloski *et al*, 1987; Northrup *et al*, 1988, 1993). Brownian dynamics experiments on the flavocytochrome b_2:cytochrome *c* interaction implicate not only residues 63, 72 and 237, but also the surrounding residues in the immediate vicinity (Dr. S. Brown, preliminary brownian dynamics work on the flavocytochrome b_2:cytochrome *c* complex, Figure **4.3.2.1**), which is in agreement with the model building work. Low affinity interactions are also shown *e.g.* the contact frequency with glu91, implicated in the Tegoni model, is extraordinarily high!

The brownian dynamics work, although very preliminary, does indicate that the complex forms many different geometries in agreement with other protein complexes such as cytochrome b_5:cytochrome *c*, and cytochrome b_5:hemoglobin. However, with cytochromes such as cytochromes b_5 and *c*, the clustering of binding sites predicted by brownian dynamics has a specific location around the exposed haem edge. In cytochrome b_5 the exposed haem edge may even participate in the formation of the complex (Salemme, 1976). In flavocytochrome b_2 the haem edge protruding from the

Table 4.3.1. k and K_d parameters are calculated assuming that the curvature is a 'real' effect, the points are fitted to a Michaelis-Menton type equation. The curvature reflects the decrease in the electron-transfer rate, and an increase in the K_d.

Mutant-enzyme	k (s^{-1})	K_d (μM)	k_{cat}/K_m^2 ($\mu M^{-1}s^{-1}$)	Straight line extrapolation ($\mu M^{-1}s^{-1}$)
Wild-type	~1000	~29	-	34.8
D72K	781 ±260	25 ± 11	31.2	24.3
E63K	555 ± 66	34 ± 6	16.3	13.0
E63K:D72K	349 ± 70	52 ± 12	6.7	6.0

Fig. 4.3.2.1. Brownian Dynamics results for the interaction of Flavocytochrome b_2 with cytochrome *c*.
(Dr. S. Brown, University of British Colombia, Vancouver).
Residues thought to be important for complex formation, as predicted by the Tegoni model are shown in blue.

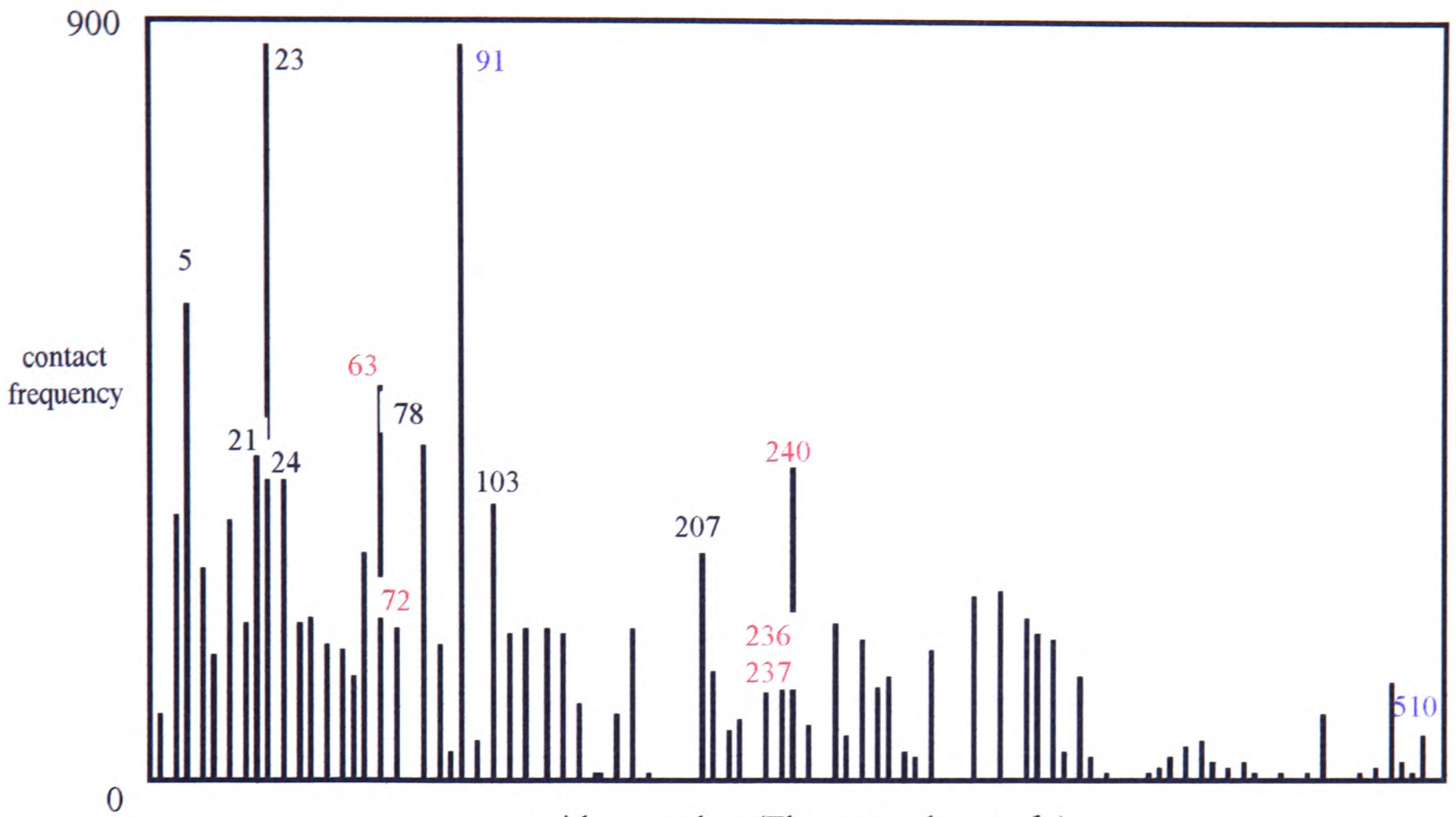

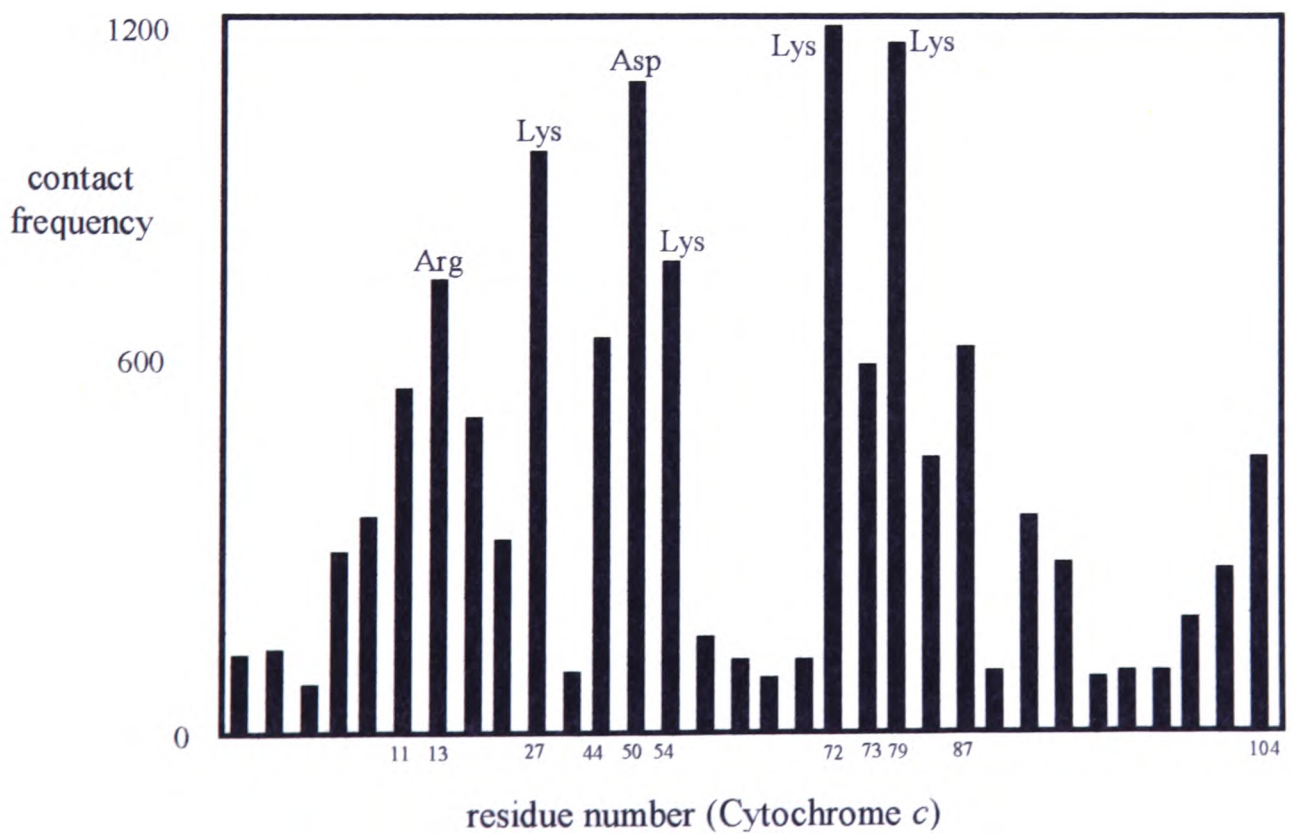

cytochrome domain is capped by the flavin domain, and so the cluster of binding sites for cytochrome *c* may be expected to be more diffuse. The formation of these encounter complexes also helps to explain why mutant-enzymes, with charge reversal of key residues for complex formation, can still produce reasonable rate of electron transfer.

The effect of ionic strength on the second order rate constant was analysed using the simplified Debye-Hückel equation (Figure **4.2.3**), and was applied simply to give a qualitative indication of the strength of the electrostatic interaction between the proteins. This does not strictly apply to protein-protein complexes as it treats the reacting molecules as uniformly charged spheres, and is restricted to ionic strengths below 0.1M to remove the dependence on the radii of the reactants. More complicated analyses of ionic interactions can be applied (Watkins *et al*, 1994; Van Leeuwan, 1983), but these would involve knowing the precise nature of the binding site and the interacting residues. Therefore, until more is known about the flavocytochrome b_2:cytochrome *c* complex they cannot be applied with confidence to this system. The second-order rate constant for the reaction between E63K:D72K and cytochrome *c* is less than that for the wild-type enzyme, and an increase in the ionic strength has less of an affect on the rate of the association of the two proteins. Therefore the simple conclusion from the ionic strength experiments is that there are fewer electrostatic interactions used in the molecular recognition and formation of the complex, therefore there is a decreased rate of association.

4.4 CONCLUSION

The flavocytochrome b_2 interaction with cytochrome *c* is controlled to some degree by electrostatics. The two residues found so far to affect the binding with cytochrome *c* are glutamate 63, and aspartate 72. These residues must provide the locus for the high affinity binding site for cytochrome *c* on flavocytochrome b_2. On the basis of these results, a proposed 'static' model of the interaction also predicted the involvement of residues glutamates 236, 237 and 240. The extent to which these residues affect complex formation has yet to be established.

References

Adam, G. & Delbrock, M. (1968) *"Structural Chemistry and Molecular Biology"* (Rich, A. & Davidson, N., eds.) Freeman, San Fransisco, USA.

Appleby, C.A. & Morton, R.K. (1954) *Nature* (London) **173** Pp. 749-752

Balme, A., Brunt, C.E., Pallister, R.L., Chapman, S.K., Reid, G.A. (1995) *Biochem. J.* **309** Pp.601-605.

Baudras, A..(1971) *Biochimie* **53** Pp. 929-933

Baudras, A., Krupa, M., Labeyrie, F. (1971) *Eur.J.Biochem.* **20** Pp.58-64

Baudras, A., Capeillere-Blandin, C., Iwatsubo, M., Labeyrie, F.(1972) *Structure and function of oxidation reduction enzymes* Pp. 273-290
Pergamon Press.

Baum, R.M. (1993) *Chemical and Engineering News* **71** Pp.20-23

Bell, C., Uhrinova, S., Barlow, P.N., Chapman, S.K., Reid, G.A. (1996) *12th International Symposium of Flavins and Flavoproteins*, Clagary, Alberta. In Press.

Beratan, D.N., Betts, J.N., Onuchic, J.N. (1991) *Science* **252** Pp. 1285-1288

Bernardi, P. & Azzone, G.F. (1981) *J. Biol. Chem.* **256** Pp. 7187-7192

Bjerrum, M.J., Casimiro, D.R., Chang, I-J., Bilio, A.J.D., Gray, H.B., Hill, M.G., Langen, R., Mines, G.A., Skov, L.K., Winkler, J.R., Wuttke, D.S. (1995) *J. Bioenerg. and Biomem.* 27 Pp. 295-302

Black, M.T., White, S.A., Reid, G.A., Chapman, S.K. (1989a) *Biochem. J.* **258** Pp. 255-259

Black, M.T., Gunn, F.J., Chapman, S.K., Reid, G.A. (1989b) *Biochem.J.* **263** Pp.973-976

Brunt, C.E., Cox, M.C., Thurgood, A.G.P., Moore, G.R., Reid, G.A., Chapman, S.K.(1992) *Biochem. J.* **283** 87-90.

Capeillere-Blandin, C., Iwatsubo, M., Testylier, G., Labeyrie, F..(1980) *6th international symposium on flavins and flavoproteins, Tokyo.* Pp. 617-630.

Capeillere-Blandin, C.(1975) *Eur.J.Biochem.* **56** Pp. 91-101

Capeillere-Blandin, C.(1982) *Eur.J.Biochem.* **128** Pp. 533-542

Capeillere-Blandin, C., Barber, M.J., Bray, R.C. (1986) *Biochem. J.* **238** Pp. 745-756

Capeillere-Blandin, C. & Albani, J. (1987) *Biochem. J.* **245** Pp. 159-165

Celerier, J., Risler, Y., Schwenke, J., Janot, J-M., Gervais, M. (1989) *Eur. J. Biochem.* **182** Pp. 67-75.

Chapman, S.K., White, S.A. & Reid, G.A. (1991) *Adv. Inorg. Chem.* **36** Pp. 257-301

Chapman, S.K., Reid, G.A., Daff, S., Sharp, R.E., White, P., Manson, F.D.C., Lederer, F. (1994) *Biochem. Soc. Trans.* **22** Pp. 713-717

Chapman, S.K. & Mount, A.R. (1995) *Natural Products Reports* **12** Pp. 93-100

Chapman, S.K., Reid, G.A., Bell, C., Short, D.M., Daff, S..(1996) *Biochem. Soc. Trans.* **24** Pp. 73-77.

Chen, L., Matthews, F.S., Davidson, V.L., Tegoni, M., Rivetti, C., Rossi, G.L. (1993) *Protein Science* **2** Pp. 147-154

Chen, L., Durley, R.C.E., Matthews, F.S., Davidson, V.L. (1994) *Science* **264** Pp. 86-90

Chothia,C. & Janin, J. (1975) *Nature (London)* **256** P.705-708

Curry, W.B., Grabe, M.D., Kurnikov, I.V., Skourtis, S.S., Beratan, D.N., Regan, J.J., Aquino, J.J., Beroza, P., Onuchic, J.N. (1995) *J. Bioenerg. and Biomem.* **27** Pp. 285-293

Daff, S., Manson, F.D.C., Reid, G.A., Chapman, S.K. (1994) *Biochem. J.* **301** Pp. 829-834

Daff, S., Sharp, R.E., Short, D.M., Bell, C., White, P., Manson, F.D.C., Reid, G.A., Chapman, S.K. (1996a) *Biochemistry* **35** Pp.6351-6357.

Daff, S., Ingledew, W.J., Reid, G.A., Chapman, S.K. (1996b) *Biochemistry* **35** Pp. 6345-6350

Dailey, H.A. & Strittmatter, P. (1979) *J. Mol. Biol.* **254** Pp. 5388-5396

Daum, G., Gasser, S.m., Schatz, G. (1982) *J. Biol. Chem.* **257** Pp. 13075-13080

Davidson, V.L. & Jones, L.H. (1995) *J. Biol. Chem.* **270** Pp. 23941-23943

Davidson, V.L. & Jones, L.H. (1996) *Biochemistry* **35** Pp. 8120-8125

Durham, B., Fairris, J.L., Mclean, M., Millet, F., Scott, J.R., Sligar, S.G., Willie, A. (1995) *J. Bioenerg. and Biomem.* **27** Pp. 331-340

Eley, C.G.S. & Moore, G.R. (1983) *Biochem. J.* **215** Pp.11-21

Gervais, M., Thomas, M.A., Labeyrie, F., Favaudon, V., Pochon, F..(1982) *Flavins and Flavoproteins.* **chptr137.**

Ghisla, S. (1982) *Flavins and Flavoproteins* (Massey, V. & Williams, C.H. eds.) Elsevier North Holland, Inc., Amsterdam. Pp. 133-142

Gibson, Q.H. & Hastings, S.W. (1962) *Biochem. J.* **83** P.368

Gray, K.A., Knaff, D.B., Husain, M., Davidson, V.L. (1986) *FEBS Lett.* **207** Pp. 239-242

Gray, K.A., Davidson, V.L., & Knaff, D.B. (1988) *J.Biol. Chem.* **263** Pp. 13987-13990

Guiard, B., Groudinsky, O., Lederer, F. (1974) *Proc.Nat.Acad.Sci. USA.* **71** (6) Pp.2539-2543

Gross, E.L. (1993) *Photosynth. Res.* **37** Pp.103-116

Guss, J.M. & Freeman, H.C. (1983) *J. Mol. Biol.* **169** Pp.521-563

Haument, P-Y., Thomas, M-A., Labeyerie, F. (1987) *Eur. J. Biochem.* **169** Pp. 539-546

Hazzard, J.T., Mclendon, G., Cusanovich, M.A., Tollin, G. (1988) *Biochem. and Biophys. Res. Comm.* **151** (1) Pp. 429-434

Hazzard, J.T., McDonough, C.A., Tollin, G. (1994) *Biochemistry* **33** Pp. 1345-13454

Husain, M. & Davidson, V.L. (1986) *J. Biol. Chem.* **261** Pp.8577-8580

Iwatsubo, M., Mevel-Ninio, M., Labeyerie, F. (1977) *Biochemistry* **16** (16) Pp. 3558-3566

Janot, J-M., Capeillere-Blandin, C., Labeyrie, F. (1990) *Biochim. Biophys. Acta.* **1016** Pp. 165-176

Jeng, M-F., Englander, S.W., Pardue, K., Rogalskyj, J.S., Mclendon, G. (1994) *Structural Biology* **1** Pp.234-238

Kay, C.J. & Lippay, E.W. (1993) *FASEB J.* **7** pA1170, Meetings abstract.

Koppenol, W.H., Margoliash, E. (1982) *J.Biol.Chem.* **257** Pp.4426-4437.

Kornblatt, J.A., Kornblatt, M.J., Hoa, G.H.B., Mauk, A.G. (1993) *Biophys. J.* **65** Pp.1059-1065

Kornblatt, J.A., Hoa, G.H.B., Eltis, L., Mauk, A.G. (1988) *J. Am. Chem. Soc.* **110** Pp. 5909-5911

Kunkel, T.A. (1985) *Proc. Natl. Acad. Sci. USA* **82** Pp. 488-492

Labeyrie, F., Boloeil, J.C., Thomas, M.A. (1988) *Biochem. Biophys. Acta.* **953** Pp.134-141

Lederer, F. (1974) *Eur. J. Biochem.* **46** Pp. 393-399

Lederer, F. (1978) *Eur. J. Biochem.* **88** Pp. 425-431

Lederer, F. & Matthews, F.S. (1987) *Flavins and Flavoproteins* (Edmonson, D.E., McCornick, D.B., Walter de Gryter & co., Berlin) Pp. 133-142

Lederer, F. (1991) *Chem. and Biochem. of Flavoenz.* (Franz Miller, ed., CRC press) Vol II Chpt 7. Pp.153-242

Lederer, F.. (1994) *Biochimie* **76** Pp.674-692

Lee, B.H., Hibino, T., Takabe, T., Weisbeek, P.J., Takabe, T. (1995) *J. Biochem.* **117** Pp. 1209-1217

Van Leeuwan, J.W., Mofers, F.J.M., Veerman, E.C.I. (1983) *Biochim. Biophys. Acta.* **743** Pp. 408-421

Linqvist, Y. & Branden, C-I. (1985) *Proc. Natl. Acad. Sci. USA.* **82** Pp.6855-6859

Linqvist, Y., Branden, C-I., Matthews, F.S., Lederer, F. (1991) *J. Biol. Chem.* **266** Pp. 3198-3207

Lijnzaad, P., Berendsen, H.J.C., Argos, P. (1996) *PROTEINS: Struct., Funct. & Gen.* **25** Pp. 389-397

Lloyd, E., Chapman, K., Chapman, S.K., Jia, Z-S., Lim, M-C., Tomkinson, N.P., Salmon, G.A., Sykes, A.G. (1994) *J. Chem. Soc. Dalton. Trans.* Pp.675-681

Marcus, R.A. (1956) *J. Chem. Phys.* **24** Pp. 966-978

Matsushima, A., Yoshimura, T., Aki, K. (1986) *J.Biochem.* **100** Pp.543-551

Mauk, M.R., Reid, L.S., Mauk, A.G. (1982) *Biochemistry* **21** Pp. 1843-1846

Mauk, A.G., Mauk, M.R., Moore, G.R., Northrup, S.H. (1995) *J. of Bioenerg. and Biomem.* **27** Pp. 311-330

McLendon, G. (1988) *Acc. Chem. Res.* **21** Pp. 160-167

McLendon, G. & Hake, R. (1992) *Chem. Rev.* **92** Pp. 481-490

Meyer, T.E., Rivera, M., Walker, F.A., Mauk, M.R., Mauk, A.G., Cusanovich, M.A., Tollin, G. (1993) *Biochemistry* **32** Pp. 622-627

Miles, C.S., Nathalie, R-F., Lederer, F., Matthews, F.S., Reid, G.A., Black, M.T., Chapman, S.K. (1992) *Biochem. J.* **284** Pp.187-192

Miller, M.A., Lui, R-Q., Hahm, S, Geren, L., Hibdon, S., Kraut, J., Durham, B., Millett, F. (1994) *Biochemistry* **33** Pp. 8686-8693

Miller, M.A., Geren,L., Han, G.W., Saunders, A., Beasley, J., Pielak, G.J., Durham, B., Millett, F., Kraut, J. (1996) *Biochemistry* **35** Pp. 667-673

Millett, F., Miller, M.A., Geren, L., Durham, B. (1995) *J. Bioenerg. and Biomem.* **27** Pp. 341-351

Moser, C.C., Keske, J.M., Warncke, K., Farid, R.S., Dutton, P.L. (1992) *Nature* **355** Pp. 796-802

Moser, C.C., Page, C.C., Farid, R., Dutton, P.L. (1995) *J. Bioenerg. and Biomem.* **27** Pp. 263-274

Mozhaev, V.V., Heremans, K., Frank, J., Masson, P., Balny, C. (1996) *PROTEINS: Struct., Funct., and Gen.* **24** Pp. 81-91

Ng, S., Smith, M.B., Smith, H.T., Millett, F. (1977) *Biochemistry* **16** Pp. 4975-4981

Nocek, J.M., Liang, N., Wallin, S.A., Mauk, A.G., Hoffman, B.M. (1990) *J. Am. Chem. Soc.* **112** Pp. 1623-1625

Northrup, S.H., Boles, J.O., Reynolds, J.C.L. (1988) *Science* **241** Pp. 67-70

Northrup, S.H. & Erickson, H.P. (1992) *Proc. Natl. Acad. Sci.* **89** Pp. 3338-3342

Northrup, S.H., Thomasson, K.A., Miller, C.M., Barker, P.D., Eltis, L.D., Guillemette, J.G., Inglis, S.C., Mauk, A.G. (1993) *Biochemistry* **32** Pp. 6613-6623

Onuchic, J.N., de Andrade, P.C.P., Beratan, D.N. (1991) *J.Chem.Phys.* **95** Pp. 1131-1138

Pajot, P. & Claisse, M.. (1974) *Eur. J. Biochem.* **49** Pp. 275-285

Pelletier, H. & Kraut, J. (1992) *Science* **258** Pp.1748-1755

Peerey, L.M. & Kostic, N.M. (1989) *Biochemistry* **28** Pp. 1861-1868

Poulos, T.L. & Kraut, J. (1980) *J. Biol. Chem.* **255** (21) Pp. 10322-10330

Poulos, T.L. & Mauk, A.G. (1983) *J. Biol. Chem.* **258** Pp. 7369-7373

Prats,M. (1977a) *Biochimie* **59** Pp.621-626

Prats, M.. (1977b) *Eur.J. Biochem.* **75** Pp.619-625.

Quin, L. & Kostic, N.M. (1993) *Biochemistry* **32** Pp. 6073-6080

Quin, L. & Kostic, N.M. (1996) *Biochemistry* **35** Pp. 3379-3386

Regan, J.J., Risser, S.M., Beratan, D.N., Onuchic, J.N. (1993) *J.Chem. Phys.* **97** Pp. 13083-13088

Reid, G,A., White, S.A., Black, M.T., Lederer, F., Matthews, F.S., Chapman, S.K. (1988) *Eur. J. Biochem.* **178** Pp. 329-333

Roberts, V.A., Freeman, H.C., Olson, A.J., Tainer, J.A., Getzoff, E.D. (1991) *J.Biol. Chem.* **266** Pp. 13431-13441.

Rodgers, K.K. & Sligar, S.G. (1991) *J. Mol. Biol.* **221** Pp. 1453-1460

Ross, P.D. & Subramian, S. (1981) *Biochemistry* **20** P.3096.

Salemme, F.R. (1976) *J.Mol. Biol.* **102** Pp. 563-568

Sharp, R.E., White, P., Chapman, S.K., Reid, G.A. (1994) *Biochemistry* **33** Pp. 5115-5120

Sharp, R.E., Chapman, S.K. & Reid, G.A. (1996) *Biochemistry* **35** pp. 891-899

Sigfridsson, K., Young, S. & Hansson, O. (1996) *Biochemistry* **35** Pp. 1249-1257

Silvestrini, M.C., Brunori, M., Tegoni, M., Gervais, M., Labeyrie, F..(1986) *Eur.J.Biochem.* **161** Pp. 465-472.

Storch, E.M. & Daggett, V. (1995) *Biochemistry* **34** Pp. 9682-9693

Tegoni, M., Mozzarelli, A., Rossi, G.L., Labeyrie, F.(1983) *J.Biol.Chem.* **258** Pp. 5424-5427

Tegoni, M., Labeyrie, F., Silvestrini, M.C., Brunori, M. (1984) *Flavins and Flavoproteins* Pp. 535-538

Tegoni, M., Janot, J-M., Labeyrie, F. (1990) *Eur. J. Biochem.* **190** Pp.329-342

Tegoni, M., White, S.A., Roussel, A., Matthews, F.S., Cambillau, C. (1993) *Proteins: Struct., Funct. & Gen.* **16** Pp.408-422

Thomas, M-A., Gervais, M., Favaudon, V., Valat, P.(1983) *Eur. J. Biochem.* **135** Pp.577-581

Ullmann, G.M. & Kostic, N.M. (1995) *J. Am. Chem. Soc.* (1995) **117** Pp. 4766-4774

Urban, P. & Lederer, F. (1985) *J. Biol. Chem.* **260** Pp. 11115-11122

Vanderkooi, J.M., Glatz, P., Casadei, J., Woodrow III, G.V..(1980) *Eur.J.Biochem.* **110** Pp.189-196

Vieira, J. & Messing, J. (1987) *Gene* **19** Pp. 259-268

Watkins, J.A., Cusanovich, M.A., Meyer, T.E., Tollin, G. (1994) *Protein Science* **3** Pp. 2104-2114

Wendoloski, J.J., Matthew, J.B., Weber, P.C., Salemme, F.R. (1987) *Science* **238** Pp. 794-797

White, S.A., Black, M.T., Reid, G.A., Chapman, S.K. (1989) *Biochem. J.* **263** Pp. 849-853

White, P., Manson, F.D.C., Brunt, C.E., Chapman, S.K., Reid, G.A. (1993) *Biochem. J.* **291** Pp.89-94

Williams, R.J.P. (1992) *Nature* **355** Pp.770

Witt, H., Zickermann, V., Ludwig, B. (1995) *Biochim. Biophys. Acta.* **1230** Pp. 74-76

Wuttke, D.S., Bjerrum, M.J., Winkler, J.R., Gray, H.B. (1992) *Science* **256** Pp. 1007-1009

Wuttke, D.S., Gray, H.B. (1993) *Current Opinion in Structural Biology* **3** Pp.555-563

Xia, Z-X., Shamala, N., Bethge, P.H., Lim, L.W., Bellamy, H.D., Xuong, N.H., Lederer, F., Matthews, F.S. (1987) *Proc. Natl. Acad. Sci.* USA. **84** Pp. 2629-2633

Xia, Z.-X. and Matthews, F.S. (1990) *J. Mol. Biol.* **212** Pp.837-863

Yi, Q., Erman, J.E., Satterlee, J.D. (1994) *Biochemistry* **33** Pp. 12032-12041

Yoshimura, T., Matsushima, A., Aki, K., Kakiuchi, K. (1977) *BBA* **492** Pp.331-339

Appendix 1
Courses and Conferences

Courses attended

Structure and function of proteins, 4th year Biochemistry.

Protein purification, 4th year Microbiology.

NMR post-graduate lectures, Chemistry.

Department of Chemistry Colloquia

Conferences

Scottish protein structure group meetings, Edinburgh (1993).

Biochemical Society Meetings, Cardiff (1994) & Dublin (1995).

7th International Conference on Bioinorganic Chemistry, Lubeck (1995).

12th International Symposium on Flavins and Flavoproteins, Calgary (1996).

Appendix 2
Publications

The following publications have resulted from work reported in this thesis :

Flavocytochrome b_2: An ideal model for studying protein-mediated electron transfer.

Chapman, S.K., Reid, G.A., Bell, C., Short, D., Daff, S. (1996)

Biochem. Soc. Trans., **24**, Pp.73-77.

Interaction of cytochrome *c* with flavocytochrome b_2

Daff, S., Sharp, R.E., Short, D.M., Bell, C., White, P., Manson, F.D.C., Reid, G.A. & Chapman, S.K. (1996) *Biochemistry*, **35** (20), Pp.6351-6357.

The cytochrome *c* binding site on flavocytochrome b_2

Short, D.M., Walkinshaw, M.D., Taylor, P., G.A.Reid, Chapman, S.K. (1996)

in *Flavins and Flavoproteins*, in press.

Reprints can be found at the back of this thesis.

Flavocytochrome b_2: an ideal model system for studying protein-mediated electron transfer

S. K. Chapman‡, G. A. Reid†, C. Bell*, D. Short* and S. Daff*

*Department of Chemistry, University of Edinburgh, West Mains Road, Edinburgh EH9 3JJ, Scotland, UK, and †Institute of Cell and Molecular Biology, University of Edinburgh, Mayfield Road, Edinburgh EH9 3JR, Scotland, UK

Introduction

Most of the recent intense scientific effort towards providing an understanding of electron transfer in proteins has focused on intraprotein electron transfer and on the pathway between the donor (D) and acceptor (A) redox centres. These centres are usually fixed within the protein matrix as in the case of the photosynthetic reaction centre [1], or involve attaching an artificial redox centre onto the surface of a protein at a fixed distance from the natural centre, e.g. in 'ruthenated' proteins [2]. Such studies usually reduce to an analysis of whether the electron travels from D to A directly through space (i.e. treating the intervening protein medium as homogeneous like an 'organic glass'), or whether it travels through a distinct σ-tunnelling pathway involving specific covalent bonds, hydrogen bonds, etc. (i.e., treating the protein medium as heterogeneous). As well as the distance between D and A, the rate of electron transfer is also influenced by the driving force of the reaction, $\Delta G°$, and the reorganization energy, λ [1].

In addition to intraprotein electron transfer, in which the redox centres are fixed within one protein, there is also intense interest in bimolecular reactions between proteins which result in interprotein electron transfer. Here, one must consider the dynamics of the interactions between the two proteins involved. Do the two proteins form one defined complex with a specific electron transfer path between redox centres? Are there a number of possible sites on the proteins where binding followed by electron transfer can occur? An interesting example is the complex between cytochrome *c* and cytochrome *c* peroxidase for which there is now a crystal structure [3]. Based on this structure a σ-tunnelling pathway linking the two haem groups has been proposed [3]. However an NMR study of the dynamics of the cytochrome *c*–cytochrome *c* peroxidase interaction indicates that the complex in solution is highly mobile and probably does not have a discrete architecture with one specific electron transfer pathway [4].

‡To whom correspondence should be addressed.

It is apparent then that to probe fully protein-mediated redox processes a model system is needed that can allow both the study of intraprotein electron transfer, between redox centres within the same protein, and interprotein electron transfer between centres in separate protein partners. Flavocytochrome b_2 is arguably the ideal model system for such studies for the following reasons: (i) it is soluble and easily obtained; (ii) the enzyme has been expressed at a high level in *Escherichia coli* [5] and a number of mutant enzymes have been generated [6–8]; (iii) crystal structures of the native and recombinant enzymes are available [9,10]; (iv) the crystal structure of the natural redox partner cytochrome *c* is also available [11]; (v) the structure of a hypothetical complex between flavocytochrome b_2 and cytochrome *c* has been proposed [12]; (vi) the redox potentials of all the prosthetic groups have been determined and there is a wealth of data on the mechanism of action of the enzyme [13,14].

Background to the flavocytochrome b_2 system

Flavocytochrome b_2 (L-lactate:cytochrome *c* oxidoreductase) from *Saccharomyces cerevisiae* is a homotetramer with subunit M_r of 57500. It is a soluble component of the mitochondrial intermembrane space, where it catalyses the transfer of electrons from L-lactate to cytochrome *c* [13]. We have cloned the DNA encoding the enzyme and expressed it at a high level in *E. coli*. (Note that the kinetic properties of flavocytochrome b_2 from yeast and the recombinant enzyme from *E. coli* are identical [5]). This has given us the ability to produce large amounts of fully active wild-type and mutant enzyme, which has facilitated our studies on the mechanism of action of the enzyme [6–8]. The X-ray crystal structures have been determined for the native enzyme from *S. cerevisiae* [9], and for the recombinant enzyme from *E. coli* [10]. These are isostructural and clearly show that each subunit is composed of two distinct domains as illustrated in Figure 1. One of these contains haem (the cytochrome domain) and the other flavin mononucleotide

(the flavin domain) [9]. The edge-to-edge distance between the flavin and haem groups is about 9.7 Å. The two domains are connected by a single segment of polypeptide chain, which constitutes an interdomain 'hinge'. This raises the question of whether or not mobility permitted by the hinge influences the interdomain electron transfer rate.

Although there is no X-ray structure available for the flavocytochrome b_2-cytochrome c complex there is now a hypothetical model for how these two proteins interact [12]. This model predicts that the b_2 and c haem groups are coplanar with an edge-to-edge distance of around 14 Å and with a possible σ-tunnelling electron-transfer pathway linking the two haems, involving residues 50–52 of flavocytochrome b_2 (Figure 2). The model also predicts a number of key electrostatic interactions between the two proteins, the most promiment of which is a salt bridge between Glu-91 of flavocytochrome b_2 and Arg-13 of cytochrome c [12].

We address in this paper two specific aspects of electron transfer in flavocytochrome b_2: (i) how can we probe the effect of domain mobility on interdomain electron transfer and (ii) is the published hypothetical complex between flavocytochrome b_2 and cytochrome c correct?

How can we probe the effect of interdomain mobility on electron transfer in flavocytochrome b_2?

In many cases, redox centres in proteins are rigidly locked in the protein matrix, an obvious example being the photosynthetic reaction centre [1]. In such cases it is relatively easy to measure the distance between donor and acceptor redox centres, since this distance will have a definite fixed value. However, what happens if the redox centres within a protein are not at a fixed distance, i.e. there is intraprotein fluxionality? A classic example would be where two domains in a protein (one containing D and the other A) are mobile with respect to each other. Is the rate of electron transfer in such a case regulated by the frequency of motion between the two domains?

Flavocytochrome b_2 is an ideal system to address this question since the cytochrome and flavin domains of the enzyme are connected by an interdomain 'hinge' (arrowed in Figure 1) that allows mobility of the domains with respect to each other. The occurrence of Interdomain mobility in flavocytochrome b_2 is supported by crystallographic [9] and NMR evidence [15] as follows. (1) Crystallographic evidence. The crystal structure of flavocytochrome b_2 shows two crystallographically distinguishable subunits in the asymmetric unit [9]. In subunit 1 the electron density map shows the presence of both

Figure 1

A single subunit of wild-type flavocytochrome b_2. The α-helices are shown as ribbons, β-sheets as arrows and the remaining α-carbon backbone as wire

The prosthetic groups are shown as ball and stick representations. The interdomain hinge is arrowed.

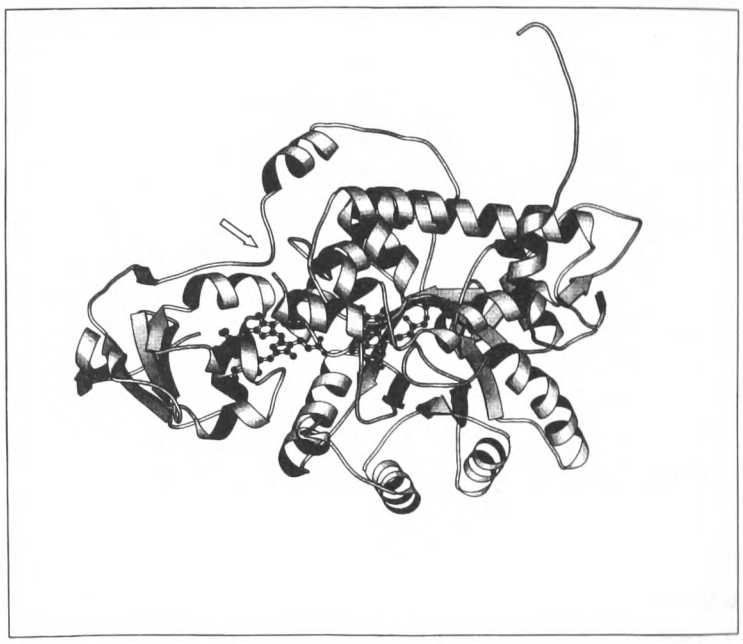

Figure 2

The proposed ρ-tunnelling pathway for electron transfer from the flavocytochrome b_2 haem to the cytochrome c haem, based on the hypothetical complex proposed by Tegoni et al. [12]

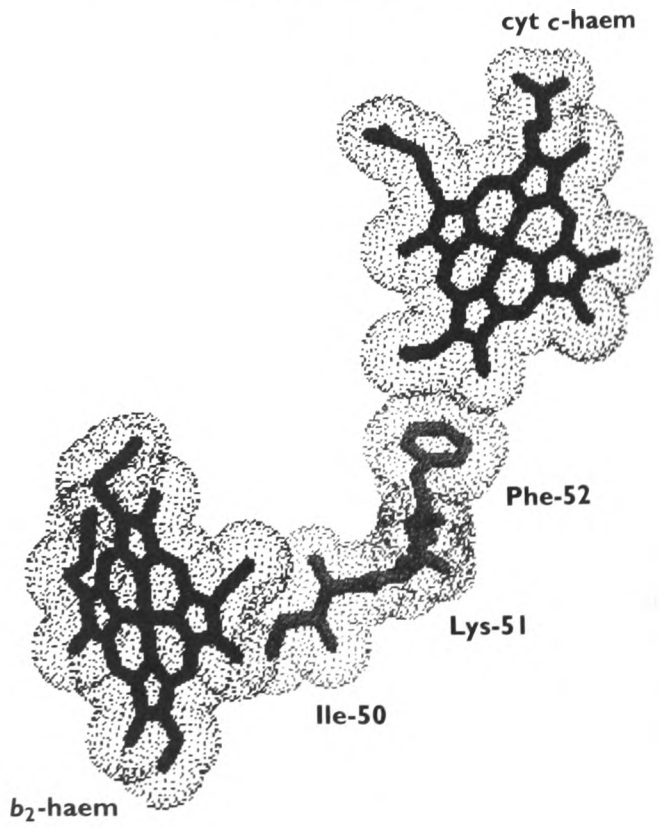

ytochrome and flavin domains. However in sub-nit 2, no electron density for the cytochrome lomain is resolved owing to positional disorder (Gly-100 is the first visible residue), indicating hat the haem domain can move with respect to he flavin domain. (2) NMR evidence. The line-widths of haem proton resonances in the intact enzyme are far sharper than would be expected if the cytochrome domain had no free motion rela-tive to the flavin domain [15]. This implies that the hinge region allows the cytochrome domain a considerable degree of mobility. From a number of studies on site-directed mutant forms of flavo-cytochrome b_2 with alterations in the hinge [7,8] and interface residues [6], it has now become clear that the rate of electron transfer from the fully reduced flavin to the haem is governed by the mobility of the two domains and the fre-quency of productive encounters between them.

To analyse further the effect of interdomain mobility on the rate of intramolecular electron transfer in flavocytochrome b_2 a methodology is needed that can be used to prevent interdomain mobility reversibly. For this reason we decided to introduce a disulphide bridge between the two domains to act as a 'reversible lock' on mobility. The power of this methodology has already been beautifully demonstrated in the case of some non-redox proteins. For example in the case of the sulphate-binding protein (SBP) from *E. coli* [16], two cysteines have been introduced into the protein to form a disulphide bond across the ligand binding site cleft that lies between two domains. This disulphide bond dramatically reduces domain flexibility in the protein [16]. Similarly, to regulate catalytic activity, a disulphide bond has been introduced across the active site cleft of T4 lysozyme. This disulphide link lowers mobility and completely removes catalytic activity [17]. Reductive cleavage of the disulphide link restores the enzyme to full activity, thus demonstrating the possibility of using an artificial disulphide bridge as a rever-sible lock.

In the case of flavocytochrome b_2, a suitable location needed to be identified to introduce cysteine residues that might form a disulphide bridge linking the domains and restricting mobility. Analysis of the three-dimensional struc-ture of the enzyme using molecular graphics allowed us to identify possible locations at the interface of the two domains where suitable disulphide linkages might be introduced. One such analysis indicated that a cysteine introduced at residue 67 (normally an alanine) in the cyto-chrome domain could form a disulphide bridge with an existing cysteine in the flavin domain at position 233. Using site-directed mutagenesis we have generated the Ala-67→Cys (A67C-b_2) mutant enzyme. Our preliminary studies on A67C-b_2 indicate that a disulphide bridge does indeed form in oxidizing conditions and that this bridge can be broken using reductants such as dithiothreitol. For example, Ellman assays on A67C-b_2 isolated from *E. coli* under oxidizing conditions revealed one fewer free cysteine than for wild-type enzyme, whereas Ellman assays on A67C-b_2 in the presence of reductants gave one more free cysteine. These results are exactly as would be expected if we had a reversible disulphide link as indicated schematically in Figure 3. We shall refer to the mutant enzyme with the disulphide bridge in place as the 'locked' form and in the absence of the bridge as the 'open' form.

Our preliminary kinetic studies on A67C-b_2 have produced some interesting results. Firstly, it is clear that in the presence of dithiothreitol, i.e. in the open form, the mutant enzyme has

Figure 3

Schematic representation of a flavocytochrome b_2 sub-unit showing the haem- and flavin-containing domains

The cysteine at position 67 was introduced by site-directed muta-genesis, whereas C233 is a naturally occurring cysteine residue. When there is no disulphide bridge, i.e. the open form, the haem domain is mobile with respect to the flavin domain. In the presence of a disulphide bridge, the locked form, domain mobility is restricted.

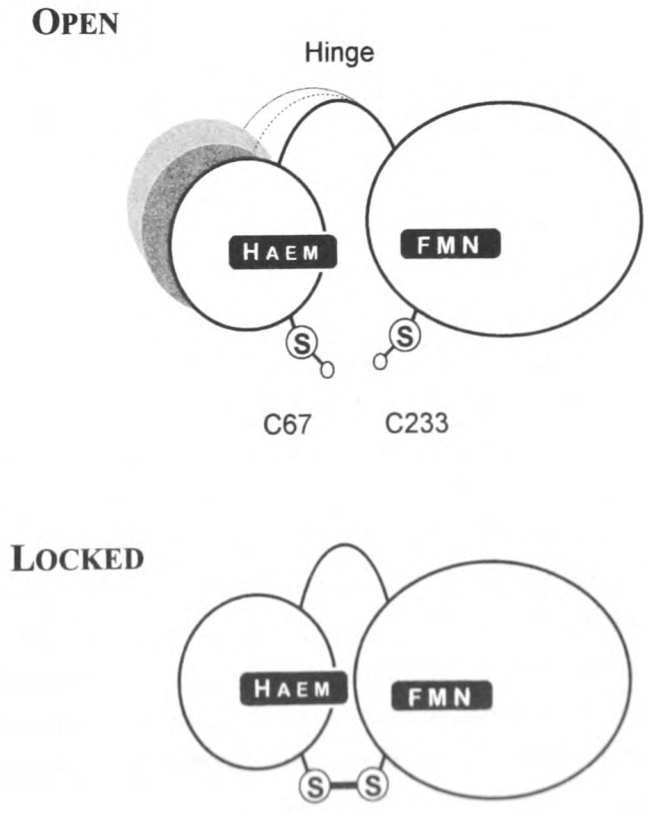

kinetic properties very similar to wild-type flavocytochrome b_2. For example, the rate constants for flavin and haem reduction measured under presteady-state conditions using stopped-flow spectrophotometry are the same within experimental error for both A67C-b_2 and wild-type enzyme. However, in the absence of dithiothreitol, in the locked form, the kinetic properties of A67C-b_2 are remarkably different from those of wild-type b_2. For A67C-b_2 in the locked form, the rate constant for haem reduction is some 10-fold lower than the value seen for the open form or for the wild-type enzyme. In contrast, the rate constant for flavin reduction in the locked form is only slightly affected. This is direct evidence that disulphide bridge formation has a major effect on flavin-to-haem electron transfer but not on the reduction of flavin by L-lactate. These preliminary data demonstrate the feasibility of placing a reversible lock on interdomain mobility in flavocytochrome b_2 and open up exciting possibilities for further analyses of intraprotein electron transfer in this system.

Is the published hypothetical complex between flavocytochrome b_2 and cytochrome c correct?

As mentioned above, a hypothetical model for the complex formed between a flavocytochrome b_2 tetramer and four cytochromes c has been proposed [12]. This model predicts a number of polar contacts between the two proteins, a notable example being that between Arg-13 of cytochrome c and Glu-91 of flavocytochrome b_2. In this case, the distance between the Arg and the Glu is suggested to be around 2.6 Å [12]. In order to test the importance of this electrostatic interaction for complex formation, we have used site-directed mutagenesis to replace Glu-91 with Lys to generate E91K-b_2. Such a change introduces a coulombic barrier, which should have a large effect on the kinetics of complex formation.

The model also indicates a possible σ-tunnelling pathway linking the b_2 and c haems that might act as the electron transfer route (Figure 2). From Figure 2 it is clear that the aromatic side chain of Phe-52 provides the link to the cytochrome c haem. To test the validity of this proposed pathway, we mutated Phe-52 to an Ala, generating F52A-b_2. This change will effectively interrupt the tunnelling pathway and would be expected to have a marked effect on the electron transfer rate from flavocytochrome b_2 to cytochrome c.

The two mutant enzymes, E91K-b_2 and F52A-b_2, have been characterized kinetically. The second-order rate constant for cytochrome c reduction by wild-type flavocytochrome b_2 has been found to be $35 \pm 1/\mu$M/s (at 25°C, pH 7.5, $I = 0.10$ M + 10 mM lactate) and the values for the two mutant enzymes are identical to this within experimental error. This rather surprising result indicates that the catalytically competent site on flavocytochrome b_2 at which cytochrome c binds is unlikely to be the one proposed from the published hypothetical complex. The results are also inconsistent with the proposed electron transfer pathway shown in Figure 2. It would appear then that the published hypothetical complex between the two proteins [12] does not represent a catalytically competent entity. We are now re-examining the structure of flavocytochrome b_2 to try and find alternative locations at which cytochrome c might bind in a catalytically competent way.

We are indebted to Professor F. S. Matthews, Dr F. Lederer, Dr M. Tegoni and Dr C. Cambillau for helpful discussions. This work was supported by the BBSRC through research grants. We are grateful to the EPSRC and BBSRC for postgraduate support for S.D. and D.S. and to the EU through the Human Capital and Mobility Programme (FLAPS Network contract no. ERBCHRXCT930166).

1 Moser, C. C., Keske, J. M., Warncke, K., Farid, R. S. and Dutton, P. L. (1992) Nature (London) **355**, 796–802
2 Lloyd, E., Chapman, K. E., Chapman, S. K., Jia, Z.-S., Lim, M.-C., Tomkinson, N. P., Salmon, G. A. and Sykes, A. G. (1994) J. Chem. Soc. Dalton. Trans. 675–681
3 Pelletier, H. and Kraut, J. (1992) Science **258**, 1748–1755
4 Jeng, M.-F., Englander, S. W., Pardue, K., Rogalskyj, J. S. and McLendon, G. (1994) Nature. Struct. Biol. **1**, 234–238
5 Black, M. T., White, S. A., Reid, G. A. and Chapman, S. K. (1989) Biochem. J. **258**, 255–259
6 Miles, C. S., Rouvière-Fourmy, N., Lederer, F., Mathews, F. S., Reid, G. A., Black, M. T. and Chapman, S. K. (1992) Biochem. J. **258**, 187–192
7 White, P., Manson, F. D. C., Brunt, C. E., Chapman, S. K. and Reid, G. A. (1993) Biochem. J. **291**, 89–94
8 Sharp, R. E., White, P., Chapman, S. K. and Reid, G. A. (1994) Biochemistry **33**, 5115–5120
9 Xia, Z.-X. and Mathews, F. S. (1990) J. Mol. Biol. **212**, 837–863
10 Tegoni, M. and Cambillau, C. (1994) Protein Sci.

3, 303–313
11 Louie, G. V., Brayer, G. D. (1990) J. Mol. Biol. **214**, 527–555
12 Tegoni, M., White, S. A., Roussel, A., Mathews, F. S. and Cambillau, C. (1993) Proteins **16**, 408–422
13 Chapman, S. K., White, S. A. and Reid, G. A. (1991). Adv. Inorg. Chem. **36**, 257–301
14 Lederer, F. (1991) in The Chemistry and Biochemistry of Flavoenzymes (Müller F., ed.) Vol. 2, pp. 154–242, CRC Press, Boca Raton
15 Labeyrie, F., Beloeil, J. C. and Thomas, M. A. (1988) Biochim. Biophys. Acta **953**, 131–141
16 Jacobson, B. L., He, J. J., Vererscb, P. S., Lemon, D. D. and Quiocho, F. A. (1991) J. Biol. Chem. **266**, 5220–5225
17 Matsumura, M. and Mathews, B. W. (1989) Science **243**, 792–794

Received 17 August 1995

The chemical mechanism of flavoprotein-catalysed α-hydroxy acid dehydrogenation: a mutational analysis

F. Lederer, A. Belmouden and M. Gondry
URA 1461, CNRS and Université Paris V, Hôpital Necker, 75743 Paris Cedex 15, France

The family of FMN-dependent L-2-hydroxy acid oxidizing enzymes

The oxidation of 2-hydroxy acids to keto acids is catalysed by both nicotinamide-linked and FMN-dependent enzymes. The two classes form distinct evolutionary families, which are believed to operate via different chemical mechanisms. Nicotinamide-dependent reactions are classically considered to proceed by transfer of a hydride ion, whereas the flavoenzymes are assumed to first abstract the substrate α-hydrogen as a proton, a step followed by flavin reduction (carbanion mechanism) [1].

The family of FMN-dependent α-hydroxy acid-oxidizing enzymes encompasses at present a dozen proteins with known sequences, including one open reading frame (ORF) in data banks [2–7]. The alignment, based on the comparison between the crystal structures of flavocytochrome b_2 from *Saccharomyces cerevisiae* (F1b_2) and spinach glycolate oxidase (GO) [2,8,9], indicates 31 totally invariant residues and 85 strongly conserved residues, out of about 350 positions aligned. The two structures [10–13] show a $\beta_8\alpha_8$ barrel fold for the flavodehydrogenase (FDH) domains with an rms difference of 0.93 Å for 311 superimposed Cα-atoms [8]. The most variable area between the two structures corresponds to β-barrel loop 4, which follows a different course in space over part of its length and for which, in both cases, a few residues cannot be located, owing to their mobility. In the overall sequence alignment, it is also the most variable region, including from about 45 to 75 residues with practically no similarity. This segment was assigned the role of membrane-binding anchor for mandelate dehydrogenase from *Pseudomonas putida* [3]. There is also indirect evidence concerning F1b_2 and long-chain α-hydroxy acid oxidase (HAO) ([9,14–16], A. Belmouden and F. Lederer, unpublished work) that loop 4 may modulate catalysis by interacting with the active site, even though the edges of the invisible segment lie some 15–20 Å away from it in the two known structures [10–12].

The F1b_2 structure afforded a picture of pyruvate, the reaction product, bound at the active site, where FMN is most likely under the semiquinone form. This led us to propose a binding mode for the substrate, lactate, and to assign to active site residues a role compatible with a carbanion mechanism [15,17,18], the validity of which rests on work carried out mainly with lactate mono-oxygenase from *Mycobacterium smegmatis* (LMO) [19] and F1b_2 [20]. Figure 1 shows the hypothetical substrate binding mode, which implies participation of R-376, Y-143 and Y-254. H-373 is the postulated catalytic general base, which removes the substrate α–H as a proton. Carbanion formation is assisted by the electrostatic interaction between the imidazolium ion and D-282. In the next step, electron transfer to FMN is facilitated by the K-349 positive charge which stabilizes the reduced flavin anionic form, irrespective of the exact mechanism of electron transfer [1,18]. All the side chains mentioned above are strictly conserved in all members of the family except for a substitution in HAO of F for Y-254 (Figure 1). Their good superposition in the crystal structures indicates a similar role for these side chains in GO and hence probably in all other family members. The observed shift between F1b_2 and GO in the flavin position relative to the

Figure 1

Proposed catalytic roles for active site side chains in flavocytochrome b_2

The substrate binding mode is deduced from that of pyruvate observed in the first Flb_2 crystal structure [10]. (A) Michaelis complex and abstraction of the substrate α proton by H-373. (B) Flavin reduction by the carbanion.

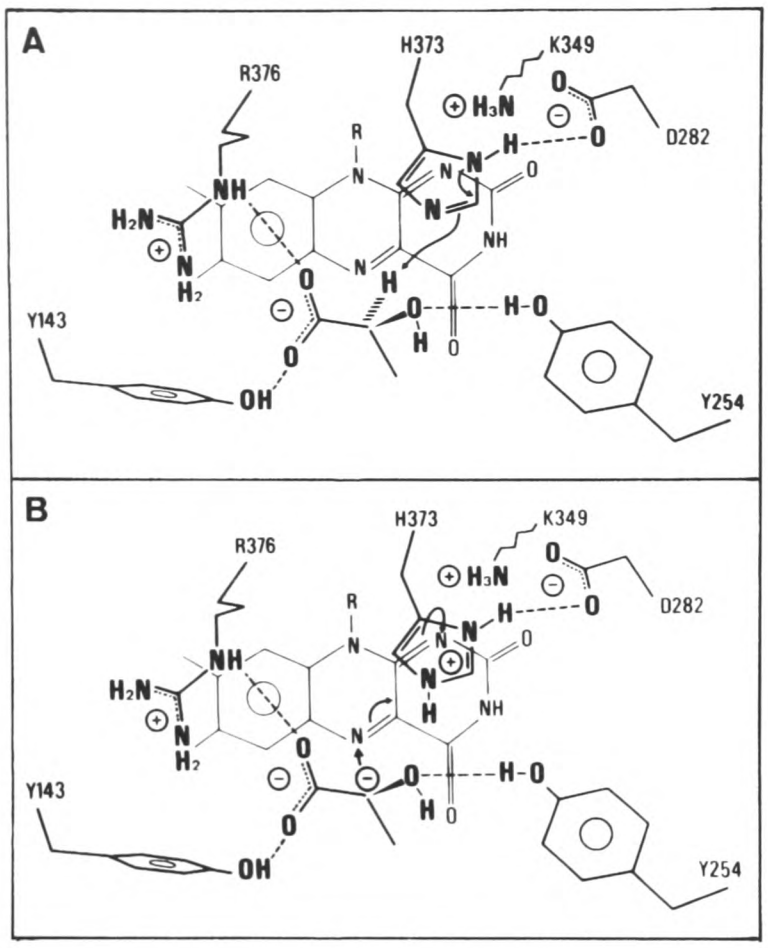

barrel backbone is possibly related to oxygen reactivity, and will not be discussed further here [8]. In the last few years, the study of site-directed mutant forms of Flb_2, GO, LMO and HAO, combined with modelling attempts, provided the means of probing the various aspects of catalysis mentioned above.

The active site histidine is the catalytic base

The critical role of H-373 (Figure 1) was demonstrated by mutating this residue and its LMO homologue H-290 to Q [21,22]. These two mutant enzymes had very low, if any, activity (Table 1). In Flb_2, the exact value of the intrinsic activity was obscured by the fact that the mutant enzyme preparations were contaminated by a trace of wild-type (WT) enzyme, presumed to arise from translational errors during biosynthesis. These results are compatible with a role of general base for H373 and its homologues. However it must be stressed that in a hydride transfer mechanism in which this residue would abstract the hydroxyl proton, a similar activity loss would be expected [30].

On the role of Y-254 and its homologues

The initial hypotheses predicted that Y-254 should form a hydrogen bond with the substrate in the Michaelis complex and that it could facilitate flavin reduction by acting as a second general base with respect to the substrate hydroxyl group at the carbanion stage [15,17–19]. Nevertheless, studies of the Y-254F and Y-254L variants of Flb_2 showed that it was α-proton abstraction that was slowed down [16,23,31]. The variations of k_{cat}/K_m values induced by the Y to F mutation indicated that the H-bond between substrate and tyrosine hydroxyl groups stabilizes the transition state (Table 1). It was suggested that this effect arises from the oritentation effect of the H-bond, leading to a correct positioning of the Cα-H-bond with respect to H-373 [23]. The Y to L mutation destabilizes the transition state even more (Table 1). For Y-152F LMO and Y-129F GO, the similarity in the energy level differences suggests that the effect of the mutation can be rationalized in the same way.

Contrary to expectations, mutations at position 254 and its homologues led either to no alteration of apparent affinities or even to a 10-fold increase in the case of LMO (Table 1). Should one then conclude that Y-254 does not contribute to Michaelis complex stabilization? The idea that lactate could have no other interactions in the enzyme–substrate (ES) complex than those with Y-143 and R-376 (Figure 1) is difficult to entertain in view of the fact that propionate behaves as a competitive inhibitor of lactate with $K_i = 28$ mM [32]. Modelling studies suggested that lactate could adopt a different conformation in the active site, but this would entail a switch to a hydride transfer mechanism, which was experimentally excluded for Y-254 Flb_2 [23]. Furthermore, an enzyme structural alteration possibly leading to a different lactate-binding mode was ruled out by crystal structure results for the Y-129F GO and Y-254F Flb_2 mutants [26,33]; these showed no protein structural change other than the loss of the tyrosine hydroxyl. A tentative explanation can be offered to rationalize these results. The apparent binding energy deduced from K_d values is the result of the replacing enzyme–solvent and substrate–solvent interactions by enzyme–substrate interactions. We may explain the lack of effect of the

Biochemistry

Interaction of Cytochrome *c* with Flavocytochrome b_2

Simon Daff, R. Eryl Sharp, Duncan M. Short, Cameron Bell, Patricia White, Forbes D. C. Manson, Graeme A. Reid, and Stephen K. Chapman

Department of Chemistry and Institute of Cell and Molecular Biology, Edinburgh Centre for Molecular Recognition, University of Edinburgh, West Mains Road, Edinburgh EH9 3JJ, Scotland, U.K., and Johnson Research Foundation, B501 Richards Building, Department of Biochemistry and Biophysics, University of Pennsylvania, 37th and Hamilton Walk, Philadelphia, Pennsylvania 19104

Reprinted from
BIOCHEMISTRY, Volume 35, Number 20, Pages 6351–6357

Interaction of Cytochrome *c* with Flavocytochrome b_2[†]

Simon Daff,[‡] R. Eryl Sharp,[§] Duncan M. Short,[‡] Cameron Bell,[‡] Patricia White,[‡] Forbes D. C. Manson,[∥] Graeme A. Reid,[∥] and Stephen K. Chapman*[,‡]

Department of Chemistry and Institute of Cell and Molecular Biology, Edinburgh Centre for Molecular Recognition, University of Edinburgh, West Mains Road, Edinburgh EH9 3JJ, Scotland, U.K., and Johnson Research Foundation, B501 Richards Building, Department of Biochemistry and Biophysics, University of Pennsylvania, 37th and Hamilton Walk, Philadelphia, Pennsylvania 19104

Received September 20, 1995; Revised Manuscript Received March 11, 1996[⊗]

ABSTRACT: Flavocytochrome b_2 from *Saccharomyces cerevisiae* couples L-lactate dehydrogenation to cytochrome *c* reduction. At 25 °C, 0.10 M ionic strength, and saturating L-lactate concentration, the turnover rate is 207 s^{-1} [per cytochrome *c* reduced; Miles, C. S., Rouviere, N., Lederer, F., Mathews, F. S., Reid, G. A., Black, M. T., & Chapman, S. K. (1992) *Biochem. J. 285*, 187−192]. The second-order rate constant for cytochrome *c* reduction in the pre-steady-state has been determined by stopped-flow spectrophotometry to be 34.8 (± 0.9) μM^{-1} s^{-1} in the presence of 10 mM L-lactate. This rate constant has been found to be dependent entirely on the rate of complex formation, the electron-transfer rate in the pre-formed complex being in excess of 1000 s^{-1}. Inhibition of the pre-steady-state reduction of cytochrome *c* by either zinc-substituted cytochrome *c* or ferrocytochrome *c* has led to the estimation of a K_d for the catalytically competent complex of 8 μM, and from this the dissociation rate constant of 280 s^{-1}, a value much less than the actual electron-transfer rate. The inhibition observed is only partial which indicates that electron transfer from the 1:1 complex to another cytochrome *c* can occur and that alternative electron transfer sites exist. The cytochrome *c* binding site proposed by Tegoni et al. [Tegoni, M., White, S. A., Roussel, A., Mathews, F. S., & Cambillau, C. (1993) *Proteins 16*, 408−422] has been tested using site-directed mutagenesis. Mutations designed to affect the complex stability and putative electron-transfer pathway had little effect, suggesting that the primary cytochrome *c* binding site on flavocytochrome b_2 lies elsewhere. The combination of tight binding and multiple electron-transfer sites gives flavocytochrome b_2 a low K_m and a high k_{cat}, maximizing its catalytic efficiency. In the steady-state, the turnover rate is therefore largely limited by other steps in the catalytic cycle, a conclusion which is discussed in the preceding paper in this issue [Daff, S., Ingledew, W. J., Reid, G. A., & Chapman, S. K. (1996) *Biochemistry 35*, 6345−6350].

Over recent years there has been a huge amount of research directed at understanding the rate and specificity of interprotein electron transfer (Marcus & Sutin, 1985; McLendon & Hake, 1992; Chapman & Mount, 1995; Moser et al., 1996). To date much of the work done to address this question has been based on the reactions of the promiscuous protein cytochrome *c*, with both its physiological (e.g., cytochrome *c* peroxidase) and nonphysiological (e.g., cytochrome b_5) redox partners. In this paper, we discuss the less well characterized interaction of cytochrome *c* with another of its physiological partners, flavocytochrome b_2.

Flavocytochrome b_2 (L-lactate:cytochrome *c* oxidoreductase, EC 1.1.2.3) from baker's yeast (*Saccharomyces cerevisiae*) is a homotetramer of subunit molecular weight 57 500 (Jacq & Lederer, 1974). It is a soluble component of the mitochondrial intermembrane space (Daum et al., 1982) where it catalyzes the oxidation of L-lactate to pyruvate with subsequent electron transfer to cytochrome *c* (Appleby & Morton, 1954). The crystal structure of flavocytochrome b_2 determined to 2.4 Å resolution (Xia & Mathews, 1990) shows that each subunit consists of two distinct domains: an N-terminal domain containing protoheme IX ("b_2-heme domain") and a C-terminal domain containing flavin mononucleotide ("flavin domain"). It has been shown that direct electron transfer from FMN to cytochrome *c* is insignificant (Forestier & Baudras, 1971; Iwatsubo et al., 1977; Balme et al., 1995), and that the role of the b_2-heme domain is to mediate this process. Therefore, the route of electron transfer in this system is L-lactate → FMN → b_2-heme → cytochrome *c*. The intraprotein FMN → heme electron transfer reactions of *S. cerevisiae* flavocytochrome b_2 have been extensively investigated (Capeillère-Blandin et al., 1975; Pompon et al., 1980; Miles et al., 1992; Walker & Tollin, 1991; Hazzard et al., 1994; White et al., 1993; Sharp et al., 1994; Chapman et al., 1994; Daff et al., 1996). However, the rather more intractable problem of investigating the interprotein electron transfer to cytochrome *c* has been performed with flavocytochrome b_2 from the yeast *Hansenula anomala* (Capeillère-Blandin, 1982), for which the crystal structure is not yet known.

Recently, in view of the unsuccessful attempts to obtain cocrystals of *S. cerevisiae* flavocytochrome b_2 and cyto-

[†] This work was funded by research grants from the Biotechnology and Biological Science Research Council (U.K.), which also provided studentships for R.E.S., and D.M.S., and by The European Commission (FLAPS Network) and the Engineering and Physical Sciences Research Council (U.K.), which provided a studentship for S.D.

* To whom correspondence should be addressed. Fax: (44)131 650 4743. E-mail: S.K.Chapman@ed.ac.uk.

[‡] Department of Chemistry, University of Edinburgh.

[§] University of Pennsylvania.

[∥] Institute of Cell and Molecular Biology, University of Edinburgh.

[⊗] Abstract published in *Advance ACS Abstracts,* May 1, 1996.

S0006-2960(95)02256-2 CCC: $12.00

chrome *c*, Tegoni et al. (1993) have proposed a hypothetical complex for the interaction between crystalline flavocytochrome b_2 and cytochrome *c*. The model binding site consists of an electrostatic interaction in which the positively charged side chains of cytochrome *c* (Arg13, Arg38, Lys54, and Lys79.) are positioned in the immediate vicinity of acidic flavocytochrome b_2 residues, and several hydrogen bonds are developed. Residue Glu91 of flavocytochrome b_2 is implicated in a number of these interactions and plays a key role in defining the model. As well as presenting a model binding site, Tegoni et al. (1993) suggest a possible pathway for electron transfer. This pathway proceeds from the b_2-heme through residues 50−51 and emerges on the enzyme surface at the side chain of Phe52.

In this paper we (i) report new solution studies on the flavocytochrome b_2-cytochrome *c* interaction and (ii) test the hypothetical complex using site-directed mutagenesis.

MATERIALS AND METHODS

DNA Manipulation, Strains, and Growth. Site-directed mutagenesis was performed by the Kunkel method of nonphenotypical selection (Kunkel, 1985) using the oligonucleotides G1194 (GTTATCAAGGCTAATGCCGG) and G1193b (ATGCCTCCTAAACTTGTCTG) to construct F52A and E91K, respectively (Oswel DNA Service, University of Edinburgh, Edinburgh, Scotland, U.K.). Standard methods for growth of *Escherichia coli*, plasmid purification, DNA manipulation, and transformation were performed as described in Sambrook et al. (1989). *E. coli* strains AR120 and TG1 were used for expression of mutant and wild-type flavocytochromes b_2, respectively.

Enzymes. Flavocytochrome b_2. Wild-type and mutant flavocytochromes b_2 expressed in *E. coli* were isolated from cells which had been stored at −20 °C. The purification procedure was essentially as described previously (Brunt et al., 1992; Black et al., 1989). Purified enzyme preparations were either stored in the reduced state under a nitrogen atmosphere at 4 °C as precipitates from 70% saturated $(NH_4)_2SO_4$ solution or as concentrated aliquots (approximately 100 μM) in the oxidized state, snap-frozen, and stored in liquid nitrogen. Under the former conditions, the enzymes retained full activity for several weeks and indefinitely when frozen in liquid nitrogen. Enzyme concentrations were calculated using previously published extinction coefficients (Pajot & Groudinsky, 1970).

Zinc-Substituted Cytochrome c. Porphyrin cytochrome *c* was prepared essentially as described by Vanderkooi and Erecinska (1975). Approximately 100 mg of freeze-dried horse-heart cytochrome *c* (Sigma) was placed in an open PTFE test tube and cooled in liquid nitrogen. HF gas was then condensed onto the cytochrome *c* while stirring with a PTFE rod. The HF was generated by bubbling nitrogen gas through a HF-saturated pyridine solution (Sigma) contained in a sealed PTFE vessel, the only exit from which led directly to the cytochrome *c* via a length of PTFE tubing. This apparatus was contained within a well ventilated fume hood. Once the cytochrome *c* was covered entirely by solid HF, the flow was stopped and reaction tube removed from liquid nitrogen. While stirring, the HF was evaporated in a steady stream of nitrogen gas. Purification was conducted as described by Vanderkooi and Erecinska (1975). The porphyrin cytochrome *c* was converted entirely to zinc-substituted cytochrome *c* as described by Vanderkooi et al. (1976). The Zn-cytochrome *c* was dialyzed into 10 mM Tris, HCl buffer, pH 7.5, *I* 0.10, and concentrated using Centricon tubes (Amicon) to approximately 250 μM. Aliquots were stored at −20 °C. Concentrations were calculated from previously reported extinction coefficients (Vanderkooi et al., 1976).

Kinetic Analysis. All kinetic experiments were carried out at 25 ± 0.1 °C in 10 mM Tris-HCl at pH 7.5, *I* 0.10. The buffer consisted of 10 mM HCl titrated against Tris solution to pH 7.5 and adjusted to *I* 0.10 by addition of NaCl. For experiments involving ionic strength effects, *I* was adjusted by addition of the appropriate amount of NaCl. Steady-state kinetic measurements involving the enzymatic oxidation of L-lactate were performed using a Shimadzu UV2101PC or a Beckman DU62 spectrophotometer. Horse-heart cytochrome *c* (type VI, Sigma) was used as the electron acceptor. Collection and analysis of the steady-state data was as previously described (Miles et al., 1992). The K_m and k_{cat} parameters were determined using nonlinear regression analysis.

Pre-steady-state kinetics were performed on an Applied Photophysics SF.17 MV stopped-flow spectrofluorimeter as previously described (Miles et al., 1992; Sharp et al., 1994). Cytochrome *c* reduction by prereduced flavocytochrome b_2 was monitored at 416.5 nm, a flavocytochrome b_2-heme isosbestic point. To ensure that the reduction occurred under pseudo-first-order conditions, flavocytochrome b_2 was always present in excess. Reduction was carried out over a range of flavocytochrome b_2 concentrations, typically 2−10 μM. The cytochrome *c* concentration was 1 μM after mixing. The traces were fitted to monophasic exponentials by nonlinear regression analysis. At least five runs were performed at each flavocytochrome b_2 concentration. Throughout each set of experiments involving ionic strength variation, L-lactate was added to the flavocytochrome b_2 solution to a concentration of 2 mM (before mixing), to fully reduce the enzyme. Over the time scale of the experiment (5 min) no autooxidation of the enzyme occurred and it remained fully reduced. For all other experiments the L-lactate concentration was 10 mM after mixing. For cytochrome *c* reduction by b_2-core, 0.1 μM wild-type flavocytochrome b_2 (a catalytic amount) was added to achieve full b_2-core reduction prior to mixing. Precautions were taken to prevent aerobic oxidation of b_2-core by handling all solutions under an N_2 atmosphere. Second-order-rate constants were determined by plotting k_{obs} for cytochrome *c* reduction against flavocytochrome b_2 concentration and fitting the data to a linear regression analysis.

Inhibition of pre-steady-state cytochrome *c* reduction by reduced or zinc-substituted cytochrome *c* was performed essentially as described above, except that the pre-reduced flavocytochrome b_2 was mixed with a known concentration of reduced or zinc-substituted cytochrome *c*. Flavocytochrome b_2 was kept at approximately 8 μM and inhibitor concentration was varied from 2 to 100 μM (after mixing). Cytochrome *c* reduction (2 μM after mixing) was monitored at 544.8 nm, a b_2-heme isosbestic point. The inhibition constant for cytochrome *c* reduction was determined by plotting the rate of cytochrome *c* reduction against the concentration of inhibiting cytochrome *c* and the data fitted to the equation shown in Chart 1.

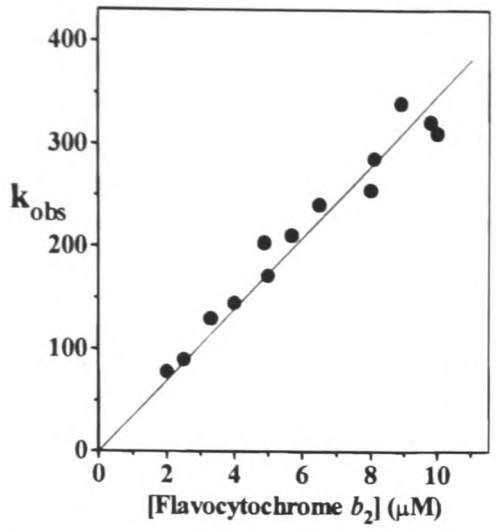

FIGURE 1: Determination of the second-order rate constant for cytochrome *c* reduction by pre-reduced wild-type flavocytochrome b_2 performed at 25 °C in 10 mM Tris−HCl buffer, pH 7.5, *I* 0.10, containing 10 mM L-lactate. k_{obs} is the pseudo-first-order rate constant for cytochrome *c* reduction derived from stopped-flow spectrophotometry at 416.5 nm (see Materials and Methods). The data are fitted by linear regression analysis. The gradient $k_2 = 34.8 \pm 0.9\ \mu M^{-1}\ s^{-1}$.

Scheme 1: Pre-Steady-State Reduction of Cytochrome *c* by Excess Flavocytochrome b_2 under Standard Conditions Follows a Single-Exponential Function[a]

(i) $F{:}H^{\bullet} + cytc \overset{\text{Fast}}{\rightleftharpoons} [F{:}H^{\bullet}\,cytc] \xrightarrow{\text{Slow}} [F{:}H\,cytc^{\bullet}]$

(ii) $F{:}H^{\bullet} + cytc \overset{\text{Slow}}{\rightleftharpoons} [F{:}H^{\bullet}\,cytc] \xrightarrow{\text{Fast}} [F{:}H\,cytc^{\bullet}]$

binding **electron transfer**

[a] This is only possible if one of the two schemes illustrated above is satisfied by the reaction mechanism. Therefore either (i) cytochrome *c* binding is fast and reversible and electron transfer slow by comparison, or (ii) cytochrome *c* association/ dissociation is slow and electron transfer is fast. F, flavin mononucleotide; H, b_2-heme; cytc, cytochrome *c*; ●, represents an electron thereby indicating redox state.

Reduction of wild-type flavocytochrome b_2-heme by L-lactate in the presence of zinc-substituted cytochrome *c* was monitored by stopped-flow spectrophotometry at 557 nm as described previously (Miles et al., 1992). The final concentrations were 5 μM flavocytochrome b_2, 10 mM L-lactate, and 0, 10, and 20 μM Zn-cytochrome *c*. Each trace shown in Figure 5 is an average of at least five different runs.

All data fitting was conducted by least-squares regression analysis using either Applied Photophysics software or Origin (Microcal).

RESULTS

Pre-Steady-State Reduction of Cytochrome c. Reduction of a substoichiometric amount of cytochrome *c* by reduced flavocytochrome b_2 was monitored by stopped-flow spectrophotometry as described in Materials and Methods. Figure 1 shows a plot of the observed rate constant against wild-type flavocytochrome b_2 concentration, which shows a linear dependency up to 10 μM, with the rate constant approaching 400 s^{-1}. Each of the generated traces fitted well to a single-exponential function (see Figure 3a), indicating that the reduction process is controlled by a single rate-determining step. The two possibilities for this mechanism are shown in Scheme 1. Either (i) complex formation is rapid and reversible, while electron transfer within the pre-formed complex is slow, or (ii) cytochrome *c* binding is slow while

Table 1: Second-Order Rate Constants for the Reduction of Cytochrome *c* by Pre-Reduced Wild-Type and Mutant Flavocytochromes b_2[a]

	second-order rate constant ($\mu M^{-1}\ s^{-1}$)
wild-type	34.8 ± 0.9
E91K	37.7 ± 1.2
F52A	34.3 ± 1.4
b_2-core	16.2 ± 0.3

[a] All experiments were performed at 25 °C in 10 mM Tris-HCl buffer, pH 7.5, *I* 0.10 containing 10 mM L-lactate. The second-order rate constants were determined as described in Materials and Methods and as illustrated in Figure 1. Errors represent standard deviations from least-squares fit.

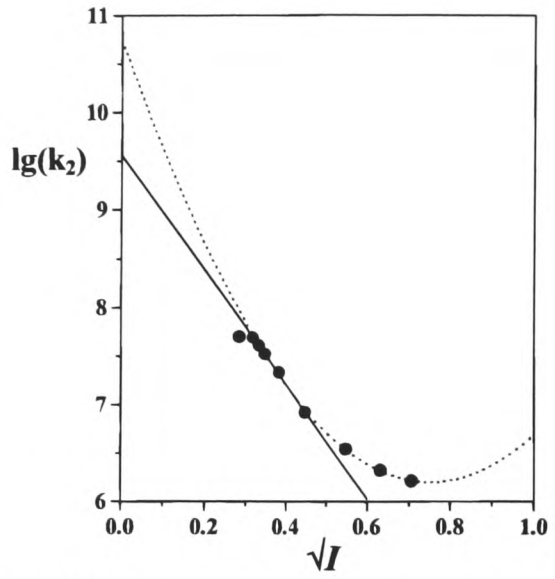

FIGURE 2: Log of the second-order rate constant (k_2) for cytochrome *c* reduction by wild-type flavocytochrome b_2 plotted against the square root of buffer ionic strength (10 mM Tris−HCl, pH 7.5 + NaCl + 1 mM L-lactate). (—) Fit to the Debye−Hückel equation ($\log k_2 = \log k_2^{\circ} + 2AZ_+Z_-\sqrt{I}$) gradient ($2AZ_+Z_-$) = −5.9 ± 0.1 (NB/Fit restricted to five data points *I* 0.10−0.20); (---) Fit to parabolic curve ($\log k_2 = \log k_2^{\circ} + 2AZ_+Z_-\sqrt{I} - BI$) gradient at *I* 0 ($2AZ_+Z_-$) = −12.1 ± 0.5. Errors represent standard deviations from a least-squares fit.

electron transfer is faster than both binding and dissociation. Model (i) would generally produce a hyperbolic curve saturating at the electron-transfer rate with $K_m = K_d$ for the bound complex. The linear region observed in Figure 1 would therefore have to occur at concentrations much less than the K_d for the bound complex. Model (ii) would generate a linear plot until the rate of binding approached the rate of electron transfer at which point single-exponential functions would no longer fit to the experimental traces. The second-order rate constant for cytochrome *c* reduction by wild-type flavocytochrome b_2 derived from Figure 1 is presented in Table 1 along with comparable values for the mutant enzymes E91K, F52A, and b_2-core (the separately expressed heme domain; Brunt et al., 1992). Neither point mutation has any effect on the rate of cytochrome *c* reduction, whereas the b_2-core mutant has a second-order rate constant less than half that of the wild-type value. Therefore residues E91 and F52 are unlikely to be important components of the cytochrome *c* binding site.

Variation of the Second-Order Rate Constant for Cytochrome c Reduction with Ionic Strength. The second-order rate constants for cytochrome *c* reduction by wild-type flavocytochrome b_2 at different ionic strengths are plotted in Figure 2. The straight line fit for log k_2 versus $\sqrt{I}$ according to the Debye−Hückel equation has a gradient $2AZ_+Z_- = -5.9 \pm 0.1$, indicating a positive/negative

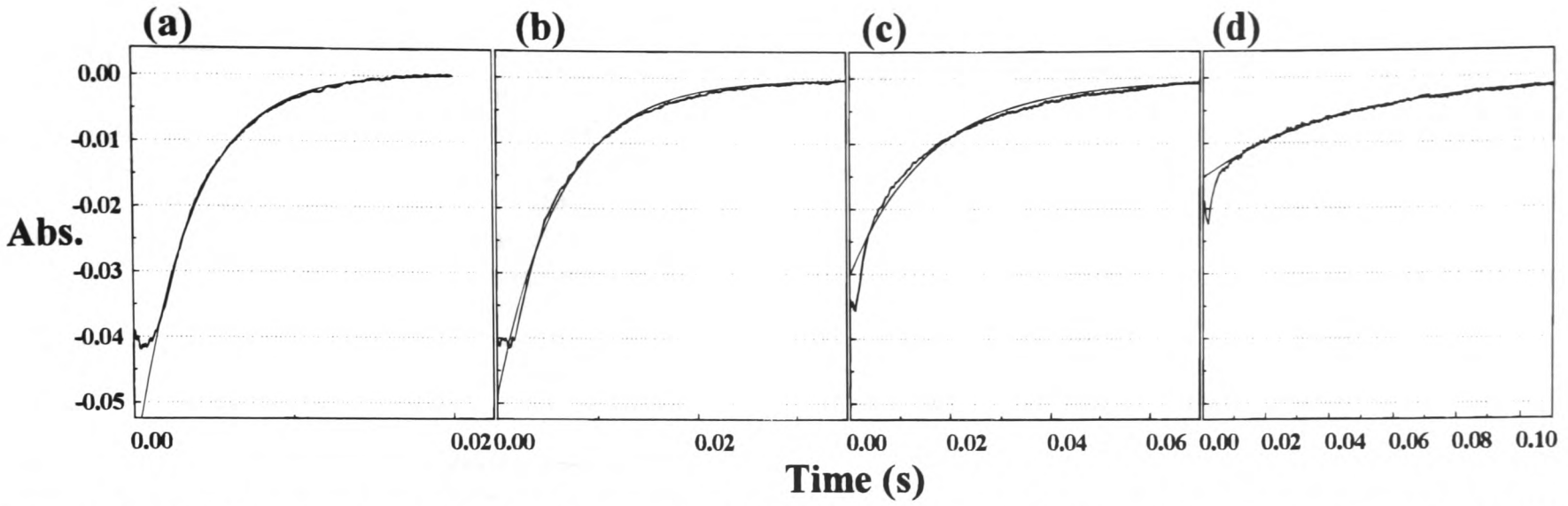

FIGURE 3: Stopped-flow traces showing pre-steady-state reduction of 1 μM cytochrome *c* by 8 μM reduced flavocytochrome b_2 at 25 °C, in 10 mM Tris-HCl buffer, pH 7.5, containing 1 mM L-lactate at four different ionic strengths (adjusted by addition of NaCl). Each trace is fitted by nonlinear least-squares regression analysis to a monophasic exponential function (shown) with rate constant *k* and amplitude *A*. (a) *I* 0.075, $k = 280\ s^{-1}$, $A = 0.060$; (b) *I* 0.050, $k = 171\ s^{-1}$, $A = 0.051$; (c) *I* 0.025, $k = 72\ s^{-1}$, $A = 0.031$; (d) *I* 0.010, $k = 24\ s^{-1}$, $A = 0.015$.

interaction at the cytochrome *c* binding site. However, it is clear from Figure 2 that the fit is far from satisfactory, deviating strongly at high ionic strength. This is not surprising in view of the well documented nonideal behavior exhibited during protein−protein interactions (Koppenol, 1980; Koppenol et al., 1978). Further, the ionic strength region studied (0.1−0.5) is well outside the range considered reasonable for an ideal solution (Robinson & Stokes, 1959). By introducing a term linearly dependent on ionic strength (with coefficient *B*) to the fitting function, a parabolic curve is generated. This fits better to the data and at $I = 0$ has a gradient of $2AZ_+Z_- = -12.1 \pm 0.5$, which again indicates a significant positive/negative interaction. The theoretical basis of this equation is also limited, as the coefficient *B* has no simple physical meaning (Perlmutter-Hayman, 1973). Its use in this case demonstrates the magnitude of uncertainty in the value of Z_+Z_- derived from Figure 2. Alternative more elaborate approaches use additional information to calculate the magnitude of charge−charge stabilization in a complex [e.g., Watkins et al. (1994)]. However, for the flavocytochrome b_2−cytochrome *c* complex the binding site location is unknown and such methods therefore inaccessible.

At lower ionic strength the stopped-flow method used to obtain second-order rate constants becomes unusable. The cytochrome *c* reduction traces no longer fit to single-exponential functions, suggesting that the reaction is now dependent on multiple rate-determining steps. Figure 3a−d shows four stopped-flow traces at different ionic strengths, each fitted to a single-exponential function. At lower ionic strength the amplitude of the observed reaction decreases and the apparent rate of reaction becomes slower, although the fit quality is poor. The decrease in amplitude indicates that a larger proportion of the reaction is occurring within the stopped-flow dead-time and is therefore happening too fast to be observed fully. This effect is to be expected if the trend of increasing second-order rate constant with decreasing ionic strength was continued as in Figure 2. The appearance of a slow phase indicates that not all the cytochrome *c* is reduced by this rapid step, but a proportion is delayed possibly by an inhibitory binding process. Such a deviation from pseudo-first-order behavior seriously limits the range of ionic strengths which can be used for the Debye−Hückel plot.

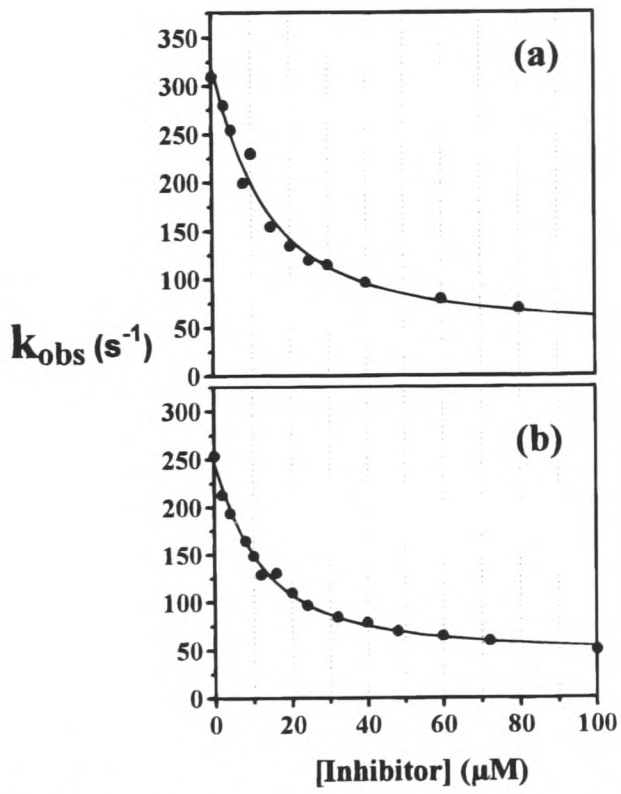

FIGURE 4: Rate constants observed (k_{obs}) for pre-steady-state reduction of ferricytochrome *c* (2 μM) by wild-type flavocytochrome b_2 are shown plotted against inhibitor concentration. (a) Inhibitor is ferrocytochrome *c* and concentration of flavocytochrome b_2 is 8.3 μM. (b) Inhibitor is zinc-substituted cytochrome *c* and concentration of flavocytochrome b_2 is 8.0 μM. Both data sets are fitted to the equation in Chart 1 by nonlinear least-squares regression analysis; (a) $K_i = 8.8 \pm 2.3$ μM (b) $K_i = 7.3 \pm 0.9$ μM.

Inhibition of Cytochrome c Reduction. Pre-steady-state cytochrome *c* reduction by wild-type flavocytochrome b_2 was inhibited by the addition of either zinc-substituted cytochrome *c* or ferrocytochrome *c* to the prereduced enzyme. The inhibition curves generated are plotted in Figure 4. The general similarity of the two data sets indicates that the use of the redox-inactive Zn−cytochrome *c* is unnecessary for this type of experiment. The electrode potential of cytochrome *c* (Loach, 1976) is some 270 mV more positive than that of the b_2-heme (White et al., 1993), and it is therefore unlikely that a significant reverse reaction would occur. Both systems appear to exhibit partial inhibition such that at high inhibitor concentration a significant rate constant is still observed (around 20% of the maximum value). This indicates that although the primary binding site is occupied rapidly by the inhibitor, cytochrome *c* reduction still occurs,

Chart 1[a]

$$k_{obs} = k_R E_T + \tfrac{1}{2}(k_2 - k_R)\left(E_T - I_T - K_i + \sqrt{(E_T - I_T - K_i)^2 + 4E_T K_i}\right)$$

- k_2 Second-order rate constant at $I_T = 0$.
- k_R Residual second-order rate constant (at $I_T = \infty$).
- E_T Total enzyme concentration.
- I_T Total inhibitor concentration.
- K_i Dissociation constant for inhibitor at primary binding site.

[a] Cytochrome *c* reacts at a single primary binding site per flavocytochrome b_2 subunit with second-order rate constant $k_2 - k_R$. It also reacts at alternative positions whether the primary site is occupied or not. The cumulative effect of these electron-transfer encounters is accounted for by introducing a residual second-order rate constant k_R. The potential binding properties of these alternative electron-transfer sites are ignored for simplicity. Inhibitor binds to the primary binding site with dissociation constant K_i and prevents further reaction at this position. Since I_T is not a lot greater than E_T, it is considered inappropriate to use a classical Michaelis−Menten function for the fitting process.

Table 2: Inhibition Constants (K_i) and Residual Second-Order Rate Constants (k_R) Calculated for Inhibition by either Zinc-Substituted Cytochrome *c* or Ferrocytochrome *c* of the Pre-Steady-State Reduction of Ferricytochrome *c* by Both Wild-Type and Mutant (E91K) Flavocytochromes b_2[a]

enzyme	inhibitor	K_i (μM)	k_R (μM^{-1} s^{-1})
wild-type	zinc-cytochrome *c*	7.3 ± 0.9	4.9 ± 0.6
wild-type	ferrocytochrome *c*	8.8 ± 2.3	4.5 ± 2.0
E91K	ferrocytochrome *c*	6.0 ± 2.0	7.5 ± 0.8

[a] Performed at 25 °C in 10 mM Tris-HCl buffer, pH 7.5 (*I* 0.10), containing 10 mM L-lactate. Rate constants generated by fitting stopped-flow data to monophasic exponential functions were plotted against inhibitor concentration, and fitted to the equation in Chart 1 by nonlinear regression analysis (as in Figure 4). Errors represent standard deviations from the least-squares fit.

albeit more slowly. K_i values for both curves in Figure 4 are presented in Table 2 along with the residual second-order rate constants (k_R). The model used to calculate these values assumes a single cytochrome *c* binding site per subunit of flavocytochrome b_2 and introduces a residual second-order rate constant k_R to account for the minimum rate constant observed. Both Zn−cytochrome *c* and ferrocytochrome *c* appear to cause partial inhibition with a dissociation constant of around 8 μM at the primary binding site. The additional data in Table 2 refer to the mutant E91K which shows no significantly different behavior with regard to inhibition by ferrocytochrome *c*, further supporting the view that this is not an important residue for binding cytochrome *c*.

Effect of Zinc-Substituted Cytochrome c Binding on b_2-Heme Reduction. Figure 5 shows three b_2-heme reduction traces for wild-type flavocytochrome b_2 generated by mixing with excess L-lactate in the presence of 0, 10, and 20 μM zinc-substituted cytochrome *c*. The Zn−cytochrome *c* is at high enough concentrations to ensure that a significant proportion of the binding sites are occupied (shown by the inhibition studies). The three traces overlay almost exactly, which indicates that there is no significant affect on either FMN to b_2-heme electron transfer or on the preceeding step, FMN reduction.

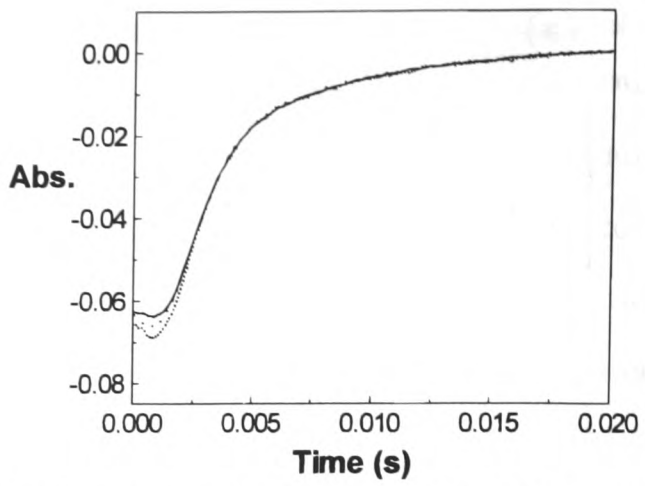

FIGURE 5: b_2-heme reduction traces for wild-type flavocytochrome b_2 (5 μM) on mixing with L-lactate (10 mM) in the presence of zinc-substituted cytochrome *c*: (—) 0 μM; (---) 10 μM; (•••) 20 μM. The traces were collected at 557 nm using stopped-flow spectrophotometry at 25 °C in 10 mM Tris−HCl buffer, pH 7.5, *I* 0.10.

DISCUSSION

There have been several attempts to characterize the complexation between flavocytochrome b_2 and cytochrome *c*; however, the lack of correlation between these studies has made interpretation difficult. For example, stoichiometries reported vary between one cytochrome *c* per flavocytochrome b_2 tetramer to one per subunit (Tegoni et al., 1993). Previous studies on the flavocytochrome b_2 from *H. anomala* (60% sequence identity with the *S. cerevisiae* enzyme; Black et al., 1989) have led to the conclusion that the cytochrome *c* binding site involves both flavin and b_2-heme domains (Thomas et al., 1983a,b; Capeillère-Blandin & Albani, 1987). A similar conclusion can be drawn for the *S. cerevisiae* enzyme since the isolated heme domain (b_2-core) has a second-order rate constant for cytochrome *c* reduction which is less than half the value for the intact enzyme (Table 1). In addition, Capeillère-Blandin (1982) reported that the catalytically competent *H. anomala* flavocytochrome b_2−cytochrome *c* complex is stabilized by electrostatic attraction. Similar conclusions hold for the *S. cerevisiae* enzyme (see Figure 2 and Results). In line with the above results, Tegoni et al. (1993) proposed a model for the complex between flavocytochrome b_2 and cytochrome *c* dominated by electrostatic interactions and involving both heme and flavin domains. They also imposed a stoichiometry of one cytochrome *c* per subunit. We have constructed mutants of flavocytochrome b_2 to test this model. E91K reverses the charge of a flavocytochrome b_2 residue postulated to be involved in an electrostatic interaction critical to cytochrome *c* binding, and F52A removes a phenyl ring suggested to be a crucial part of the electron transfer pathway between the two hemes. If the hypothetical model were correct, both mutations would be expected to have a profound effect on the cytochrome *c* reductase ability of the enzyme. The results in Table 1 show that this is not the case.

Since the Tegoni model is unlikely to be correct, we have analyzed the flavocytochrome b_2−cytochrome *c* interaction in more detail. For wild-type flavocytochrome b_2, the rate constant for electron transfer from b_2-heme to cytochrome *c* within the pre-formed complex has been estimated by photochemical excitation to be 200 (± 80) s^{-1} at 25 °C (McLendon et al., 1987). For the *H. anomala* enzyme, the rate constant has been determined from stopped-flow/ionic strength experiments to be 380 s^{-1} at 5 °C (Capeillère-Blandin, 1982). In our experiments on the *S. cerevisiae* enzyme (at 25 °C), cytochrome *c* reduction occurs at rates beyond the reliable range of the stopped-flow technique and must be in excess of 1000 s^{-1}. While the second value is not inconsistent with this (in view of the lower temperature

used and different enzyme form), it seems unlikely that the electron-transfer rate constant could be as low as 200 s^{-1} as determined by photochemical excitation. At low ionic strength biphasic kinetic behavior is observed (Figure 3), the slow phase of which is probably caused by the inhibitory binding of cytochrome *c* to low activity sites on flavocytochrome b_2, as weaker electrostatic forces become more significant. At *I* 0.01 the amplitude is greatly diminished as the fast phase can no longer be resolved. Using the Debye−Hückel equation to calculate a rate constant at this ionic strength (based on Figure 2), we can estimate that for a 8 μM enzyme solution $k_{obs} = 7500\ s^{-1}$. This would clearly not be observed in a stopped-flow experiment with a dead-time of 1 ms.

In order to resolve the confusion regarding cytochrome *c* binding to flavocytochrome b_2, kinetics can be used to discriminate for interactions at the catalytically active binding site. Vanderkooi et al. (1980) used iron free cytochrome *c* to inhibit the steady-state turnover of flavocytochrome b_2 and obtained a $K_i = 13\ \mu M$. The catalytic cycle for flavocytochrome b_2 is discussed in Daff et al. (1996), and it is clear from the model presented that competitive inhibition would only occur at low cytochrome *c* concentrations. To demonstrate this, we conducted several steady-state assays in which redox-inactive zinc-substituted cytochrome *c* was used as an inhibitor. Zn−cytochrome *c* has been widely used in place of ferrocytochrome *c* to study binding interactions and electron transfer [e.g., Thomas et al. (1983a,b), McLendon et al. (1987) and Alleyne et al. (1992)] and has been shown to be structurally identical to the native protein (Anni et al., 1995). At high concentrations of ferricytochrome *c* (>100 μM) assays containing an equimolar amount of Zn−cytochrome *c* retained at least 90% of the rate observed in the absence of Zn−cytochrome *c*. Inhibition by Zn−cytochrome *c* was also followed in the pre-steady-state to ensure that the inhibition constants were as close as possible to dissociation constants. Figure 4 panels a and b plot observed rate constants against ferrocytochrome *c* and Zn−cytochrome *c* concentrations, respectively, for the pre-steady-state reduction of ferricytochrome *c*. In both cases the K_i was found to be around 8 μM based on the use of the equation in Chart 1. The fact that this equation fits the data suggests that the stoichiometry is one cytochrome *c* per flavocytochrome b_2 subunit, for the main catalytically active binding site [in agreement with Vanderkooi et al. (1980)]. However, the need to introduce a residual second-order rate constant indicates that this is not the sole site for b_2-heme to cytochrome *c* electron transfer, and that cytochrome *c* reduction occurs even when the main binding site is occupied. The equation in Chart 1 does not, however, take account of the number or nature of these alternative reaction sites and so is flawed in this respect. Nevertheless, if these reaction sites are numerous and binding to them is weak, the equation can be applied over a limited range. Pre-steady-state cytochrome *c* reduction is a single step reaction, which is dependent entirely on cytochrome *c* binding. Therefore, the K_i determined is likely to be equivalent to the actual dissociation constant for ferrocytochrome *c*. Since the protein−protein interaction is expected to be similar in the ferricytochrome *c*−flavocytochrome b_2 complex, as a first approximation the K_d for the catalytically active complex would be expected to be the same. In view of this, it seems unlikely that model (i), Scheme 1 could represent the pre-steady-state reaction. As explained in Results, this model requires that $K_d \gg 10\ \mu M$. Model (ii), Scheme 1 can therefore be used to explain some of the effects already described. The rate constant for electron transfer has already been shown to be >1000 s^{-1}, which is consistent with this model. The rate constant for cytochrome *c* association would be equal to the second-order rate constant for cytochrome *c* reduction (i.e., 34.8 $\mu M^{-1}\ s^{-1}$). Finally, the dissociation rate must be less than the electron-transfer rate. By using the association rate constant and the inhibition constant, the dissociation rate constant can be estimated to be 280 s^{-1}. Although this value is significant when compared to the rate of enzyme turnover (207 s^{-1}) (Miles et al., 1992), the inhibition constant on which it is based is derived from partial inhibition. So although cytochrome *c* dissociation may be slow, the presence of alternative electron transfer sites means that at high concentration the turnover rate remains unaffected, whereas at low cytochrome *c* concentrations the binding affinity for cytochrome *c* remains high.

The possibility that inhibition by ferro-/Zn−cytochrome *c* in the steady-state may not be entirely competitive in nature was examined by monitoring flavocytochrome b_2 reduction by L-lactate in the presence of Zn−cytochrome *c*. Since b_2-heme reduction requires that both FMN reduction and FMN to b_2-heme intramolecular electron transfer take place, this was considered an appropriate experiment. Particular interest lies in the intramolecular electron transfer step which presumably depends on the relative orientation and position of the two domains. The traces displayed in Figure 5 overlay almost exactly suggesting either that the presence of bound Zn−cytochrome *c* has little affect on the enzyme's other catalytic processes or that the oxidized enzyme has a substantially lower Zn−cytochrome *c* binding affinity than the reduced form. Our current research is directed toward defining the precise location for cytochrome *c* reduction on flavocytochrome b_2.

ACKNOWLEDGMENT

We thank Prof. F. S. Mathews and Drs. F. Lederer, M. Tegoni, and C. Cambillau for helpful discussions.

REFERENCES

Alleyne, T. A., Wilson, M. T., Antonini, G., Malatesta, F., Vallone, B., Sarti, P., & Brunori, M. (1992) *Biochem. J. 287*, 951−956.

Anni, H., Vanderkooi, J. M., & Mayne, L. (1995) *Biochemistry 34*, 5744−5753.

Appleby, C. A., & Morton, R. K. (1954) *Nature 173*, 749−752.

Balme, A., Brunt, C. E., Pallister, R. L., Chapman, S. K., & Reid, G. A. (1995) *Biochem. J. 309*, 601−605.

Black, M. T., White, S. A., Reid, G. A., & Chapman, S. K. (1989) *Biochem. J. 258*, 255−259.

Brunt, C. E., Cox, M. C., Thurgood, A. G. P., Moore, G. R., Reid, G. A., & Chapman, S. K. (1992) *Biochem. J. 283*, 87−90.

Capeillère-Blandin, C. (1982) *Eur. J. Biochem. 128*, 533−542.

Capeillère-Blandin, C., & Albani, J. (1987) *Biochem. J. 245*, 159−165.

Capeillère-Blandin, C., Bray, R. C., Iwatsubo, M., & Labeyrie, F. (1975) *Eur. J. Biochem. 56*, 91−101.

Chapman, S. K., & Mount, A. R. (1995) *Nat. Prod. Rep. 12*, 93−100.

Chapman, S. K, Reid, G. A., Daff, S., Sharp, R. E., White, P. W., Manson, F. D. C., & Lederer, F. (1994) *Biochem. Soc. Trans. 22*, 713−718.

Daff, S., Ingledew, W. J., Reid, G. A., & Chapman, S. K. (1996) *Biochemistry* 35, 6345−6350.

Daum, G., Böhni, P. C., & Schatz, G. (1982) *J. Biol. Chem. 275*, 13028−13033.
Forestier, J-P., & Baudras, A. (1971) in *Flavins & Flavoproteins* (Kamin, H., Ed.) pp 599−605, University Park Press, Baltimore, MD.
Hazzard, J. T., McDonough, C. A., & Tollin, G. (1994) *Biochemistry 33*, 13445−13454.
Iwatsubo, M., Mével-Ninio, M., & Labeyrie, F. (1977) *Biochemistry 16*, 3558−3566.
Jacq, C., & Lederer, F. (1974) *Eur. J. Biochem. 41*, 311−320.
Koppenol, W. H. (1980) *Biophys. J. 29*, 493−508.
Koppenol, W. H., Vroonland, C. A. J., & Braams, R. (1978) *Biochim. Biophys. Acta 503*, 499−508.
Kunkel, T. A. (1985) *Proc. Natl. Acad. Sci. U.S.A. 82*, 488−492.
Loach, P. A. (1976) in *Handbook of Biochemistry & Molecular Biology (Physical & Chemical Data Vol. 1)* (Fasman, G. D., ed.), 3rd ed., pp 122−130, CRC Press Inc., Cleveland, OH.
Marcus, R. A., & Sutin, N. (1985) *Biochim. Biophys. Acta 811*, 265−322.
McLendon, G., & Hake, R. (1992) *Chem. Rev. 92*, 481−490.
McLendon, G., Pardue, K., & Bak, P. (1987) *J. Am. Chem. Soc. 109*, 7540−7541.
Miles, C. S., Rouviere, N., Lederer, F., Mathews, F. S., Reid, G. A., Black, M. T., & Chapman, S. K. (1992) *Biochem. J. 285*, 187−192.
Moser, C. C., Page, C. C., Farid, R., & Dutton, P. L. (1996) *J. Bioenerg. Biomembr.* (in press).
Pajot, P., & Groudinsky, O. (1970) *Eur. J. Biochem. 12*, 158−164.
Perlmutter-Hayman, B. (1973) in *Progress in Reaction Kinetics* (Jennings, K. R., & Cundall, R. B., Ed.) Vol. 6, pp 239−267, Pergamon Press Oxford.
Pompon, D., Iwatsubo, M., & Lederer, F. (1980) *Eur. J. Biochem. 104*, 479−488.
Robinson, R. A., & Stokes, R. H. (1959) *Electrolyte Solutions*, 2nd ed., pp 230−231, Butterworth & Co. Ltd., London.
Sambrook, J., Fritsch, E. F., & Maniatis, T. (1989) *Molecular Cloning: A Laboratory Manual*, 2nd ed., Cold Spring Harbor Laboratoy Press, Cold Spring Harbor, NY.
Sharp, R. E., White, P. W., Chapman, S. K., & Reid, G. A. (1994) *Biochemistry 33*, 5115−5120.
Tegoni, M., White, S. A., Roussel, A., Mathews, F. S., & Cambillau, C. (1993) *Proteins 16*, 408−422, and references therein.
Thomas, M. A., Favoudon, V., & Pochon, F. (1983a) *Eur. J. Biochem. 135*, 569−576.
Thomas, M. A., Gervais, M., Favaudon, V., & Valat, P. (1983b) *Eur. J. Biochem. 135*, 577−581.
Vanderkooi, J. M., & Erecinska, M. (1975) *Eur. J. Biochem. 60*, 199−207.
Vanderkooi, J. M., Adar, F., & Erecinska, M. (1976) *Eur. J. Biochem. 64*, 381−387.
Vanderkooi, J. M., Glatz, P., Casadei, J., & Woodrow, G. V. (1980) *Eur. J. Biochem. 110*, 189−196.
Walker, M. C., & Tollin, G. (1991) *Biochemistry 30*, 5546−5555.
Watkins, J. A., Cusanovich, M. A., Meyer, T. E., & Tollin, G. (1994) *Protein Sci. 3*, 2104−2114.
White, P., Manson, F. D. C., Brunt, C. E., Chapman, S. K., & Reid, G. A. (1993) *Biochem. J, 291*, 89−94
Witt, H., Zickermann, V., & Ludwig, B. (1995) *Biochim. Biophys. Acta 1230*, 74−76.
Xia, Z.-X., & Mathews, F. S. (1990) *J. Mol. Biol. 212*, 837−863.

BI9522561

The Cytochrome *c* Recognition Site on Flavocytochrome b_2

Duncan M. Short[1], Malcolm D. Walkinshaw[2], Paul Taylor[2], Graeme A. Reid[2], Stephen K. Chapman[1].

[1] The Department of Chemistry, [2] The Institute of Cell and Molecular Biology, [3]The Department of Biochemistry, King's Buildings, The University of Edinburgh, West Mains Road, Edinburgh, EH9 3JJ.

Flavocytochrome b_2 is a homotetrameric enzyme that catalyses the oxidation of lactate to pyruvate, and the reduction of cytochrome *c* in the mitochondrial inter-membrane space of yeast. Each subunit consists of two domains: A flavodehydrogenase domain, containing flavin mononucleotide; and a cytochrome domain, containing protohaem IX. These two domains are joined by a polypeptide linker. The first electron transfer steps from lactate to flavin, and from flavin to haem have been well studied (1). However, the terminal electron transfer step from the cytochrome domain to cytochrome *c* is not fully understood.

A hypothetical complex showing the interaction between flavocytochrome b_2 and cytochrome *c* was produced in 1993 by Tegoni *et al* (2). The authors considered several general areas on the flavocytochrome b_2 tetramer as plausible binding sites, but restricted themselves to examining the residues surrounding the interface between the two domains. Further restrictions placed on the model resulted in the discarding of binding sites that were not compatible with the crystal packing of the tetramer. This obviously provides a disclaimer for the authors, and reinforces the care needed when testing a hypothetical complex based on crystal structural data. The interaction area between the proteins is described as extensive, however a key point is that the interacting surfaces are not perfectly complementary, a fact noted by the authors. The stoichiometry is four cytochromes *c* per tetramer, and a proposed σ-tunnelling pathway from the flavocytochrome b_2 haem to the cytochrome *c* haem, looked convincing.

The model predicted that glutamate 91, on flavocytochrome b_2, would interact with lysine 13 on cytochrome *c*. To destroy this interaction, a coulombic barrier was

introduced by replacing this glutamate with a lysine residue. A second test of the model would be to cut the proposed σ-tunnelling pathway. The first mutation should decrease the rate of complex formation. The second mutation should decrease the efficiency of electron transfer. What is actually seen is that the second-order rate constant for cytochrome *c* reduction both mutant-enzymes (3) is equal to that of the wild-type. This shows that the kinetically relevant binding site is NOT the one proposed by Tegoni *et al*. In their paper (2), Tegoni *et al* state that the van der Waal's sphere of the pathway "touches" the haem of cytochrome *c*. From the co-ordinates, provided by the authors, we show in figure 1. that this is definitely NOT the case. In fact, there is a 10Å gap.

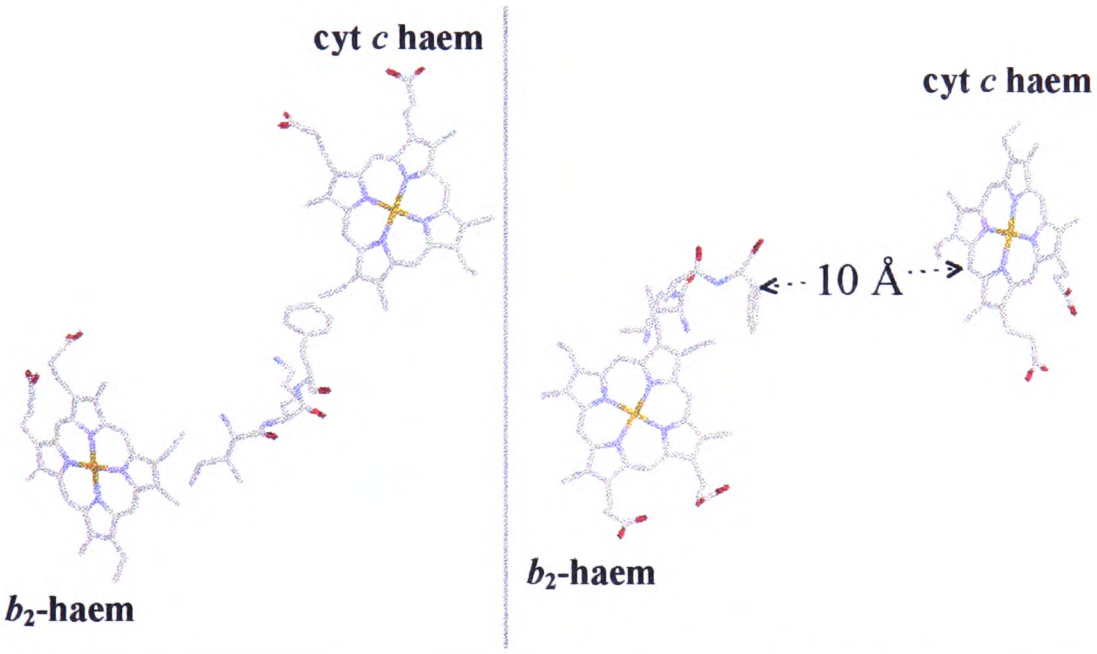

FIG.1. Two perspectives of the same σ-tunnelling pathway. Careful inspection of the model reveals a 10Å gap in the pathway.

The homology between the cytochrome b_2 core and cytochrome b_5 was used to predict a kinetically relevant binding site. Cytochrome b_5 has been intensively studied for some time (4), and analogy with the model derived by Guillemette *et al* (5), would show the cytochrome *c* binding site to bridge the interface between the flavin and haem domains in flavocytochrome b_2. This is in agreement with Tegoni's conclusions on the general location of the binding site. In considering the analogy with the cytochrome b_5:cytochrome *c* system and flavocytochrome b_2, several

residues on flavocytochrome b_2 that are conserved in cytochrome b_5 were looked at, using molecular graphics, in order to locate the most plausible binding site.

FIG.2. Rate constants for the reduction of cytochrome *c* plotted against flavocytochrome b_2 concentration. (*I* 0.1M, 25°C,pH 7.5).

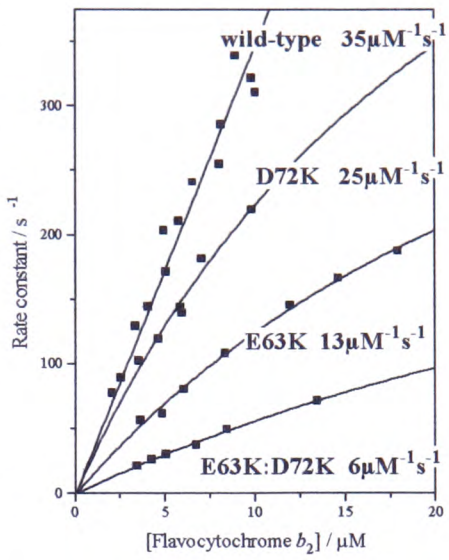

Two point-mutations were found to affect the second-order rate constant for cytochrome *c* reduction, Asp72→Lys and Glu63→Lys, and so must be involved in the molecular recognition and formation of the complex (fig.2). A double mutation was also engineered. This caused the greatest decrease in second order rate constant from $35\mu M^{-1}s^{-1}$ to $6\mu M^{-1}s^{-1}$. The haem midpoint electrode potentials measured for each of the mutant enzymes were within error of each other, but approximately 20mV greater than the wild-type. This however, should not significantly affect the electron transfer rate to cytochrome *c*, as the driving force is still around 250mV.

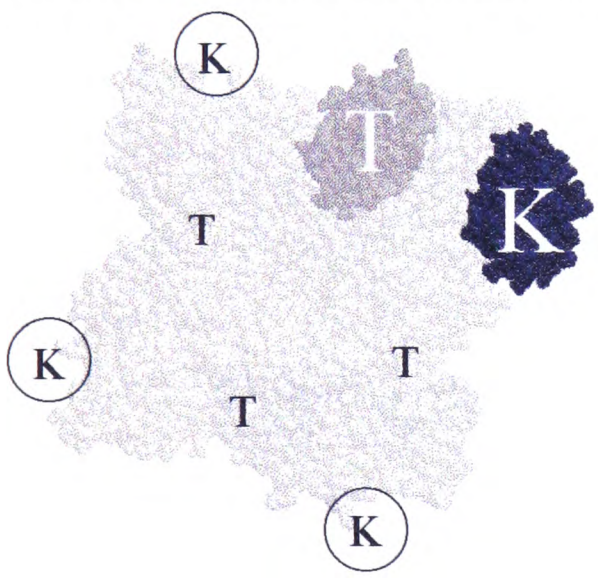

FIG.3. Cytochrome c binding locations on flavocytochrome b_2 for the present kinetically relevant model, K, and the previous Tegoni model, T.

From this data, a kinetically relevant solution complex can be produced that centres around residues 63 and 72.(fig.3). This has been done, and several important features can be highlighted. Unlike the Tegoni model, each cytochrome *c* contacts only one subunit of flavocytochrome b_2. Four cytochromes *c* can be accommodated on the tetramer and these cytochromes are positioned on the interdomain border. Residues from both the flavin and haem domains are involved in the stabilisation of the

complex. The residue that is implicated in stabilising the complex from the flavin domain is glutamate 237. The three residues form a triangular recognition site for cytochrome *c*. Asp72, Glu63 and Glu237 interact with Lys13, 27 and 79 respectively. Through the middle of this triangle runs a σ-tunnelling pathway (fig.4). This molecular wire spans residues 66 to 68, and starts with the flavocytochrome b_2 His66 axial ligand to the haem. This joins up with the backbone of Ala67 and ends with Pro68. The 'through space' jump is then 3Å to the cytochrome *c* haem. In total, the direct distance between His66 and the haem C3C pyrrole ring of cytochrome c is 13.1Å. This system would provide cytochrome *c* with 3 similar alternative binding sites to 'sample', without involving a separate electron transfer pathway. The rest of the interaction area, in agreement with other protein complexes, is made up of hydrophobic residues.

FIG.4. Complex formed at the interface between the two domains of flavocytochrome b_2 involving the σ-tunnelling pathway:

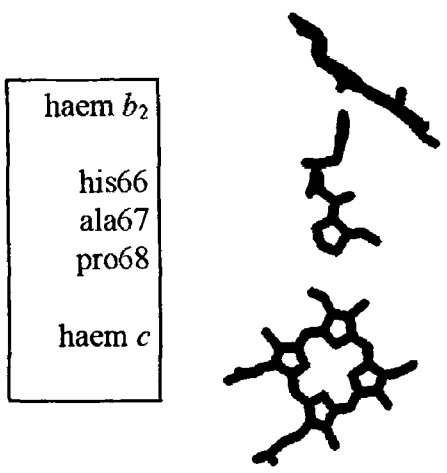

REFERENCES

1. Chapman, S.K., Reid, G.A., Daff, S., Sharp, R.E., White, P., Manson, F.C.D., Lederer, F.. 1994 Biochem. Soc. Trans.1994. **22**, 713.

2. Tegoni, M.,White, S.A., Roussel, A., Matthews, F.S., Cambillau, C.. Prot.:Struct.,Funct., and Gen.. 1993. **16**, 408.

3. Chapman, S.K., Reid, G.A., Bell, C., Short, D.M., Daff, S.. Biochem. Soc. Trans. 1996. **24**, 72.

4. Mauk, G.A., Mauk, R.M., Moore, G.R., Northrup, S.H.. J. of Bioen. and Biomem.. 1995. **27**,(3) 311.

5. Guillemette, J.G.,Barker, P.D., Eltis, L.D., Lo, T.P., Smith, M.,Brayer, G.D., Mauk, A.G., Biochemie. 1994. **76**, 592.